

https://dspace.org/

Assessing the efficacy of RNA polymerase II- and RNA polymerase III promoter-driven RNA interference effecter cassettes targeted to HBx

Dyer, Victoria Kate

2010-08-27
http://hdl.handle.net/10539/8567

Downloaded from a DSpace repository. https://dspace.org/

ASSESSING THE EFFICACY OF RNA POLYMERASE II- AND RNA POLYMERASE III PROMOTER-DRIVEN RNA INTERFERENCE EFFECTER CASSETTES TARGETED TO *HBx*

Victoria Kate Dyer

A dissertation submitted to the Faculty of Science, University of the Witwatersrand, Johannesburg, in fulfilment of the requirements for the degree of Master of Science

Johannesburg, 2010

DECLARATION

I, Victoria Kate Dyer (0211151E), am a student registered for the degree Master of Science, in the year 2010. On submittal of my dissertation, I do hereby declare the following:

- I confirm that this dissertation is my own unaided work except where I have explicitly indicated otherwise.
- I am submitting this work for the Degree of Master of Science in the University of the Witwatersrand, Johannesburg.
- I have followed the required conventions in referencing the thoughts and ideas of others.
- I have not submitted the work for any degree or examination at any other university.
- I understand that the University of the Witwatersrand may take disciplinary action against me if there is a belief that this is not my own unaided work or that I have failed to acknowledge the source of the ideas or words in my writing.

Victoria Kate Dyer Date

ABSTRACT

Globally, the status of chronic infection with hepatitis B virus (HBV) is increasing, with approximately twenty million new cases being reported each year. Chronically infected individuals are at risk of developing complications of cirrhosis and hepatocellular carcinomas. Currently, treatment of HBV entails a combination of therapeutics and successful treatment is limited to approximately 20% of patients. Efficient inhibition of HBV replication has been shown by harnessing the RNA interference (RNAi) pathway through the utilisation of U6 RNA Polymerase III (Pol III) promoter-driven short hairpin RNA (shRNA). The generation of a double stranded RNA (dsRNA) as a therapeutic tool is a realistic approach to treating HBV, however the expression of the dsRNA requires optimisation to prevent any toxic effects associated with off-targeting or saturation of the endogenous RNAi pathway. Two Pol III (H1 and $tRNA^{Lys3}$) promoter-driven shRNA expression cassettes and an Pol II (CMV) promoter-driven microRNA shuttle were generated and compared to the U6 shRNA constructs. Knockdown was assessed for five different target sites at varying concentrations of effecter to target ratios. The $tRNA^{Lys3}$ shRNA 5 caused significant inhibition of HBV, whilst the H1 and cytomegalovirus (CMV) promoter-driven effecter cassettes were only effective at high target to effecter ratios (1:10). *In vivo* analysis in a murine hydrodynamic injection model supported the data from cell culture analysis, and established U6 shRNA 5 and $tRNA^{Lys3}$ shRNA 5 as the most effective promoter-driven cassettes with which to silence HBV replication. Harnessing of the endogenous RNAi pathway to control the expression of HBV genes by target specific mRNA degradation is becoming an increasingly valuable approach in designing a therapeutic antiviral construct, particularly with a construct as effective as $tRNA^{Lys3}$ shRNA 5.

DEDICATION

I dedicate this dissertation to -

Andrea Rose Dyer

(30 November 1914 – 04 October 2007)

and

Dylan James Holm

(23 December 2007 -)

and

Alex Rhys Holm

(22 October 2009 -)

"Our doubts are traitors, and make us lose the good we oft might win, by fearing to attempt". Measure for Measure Act I, Scene IV.

William Shakespeare

ACKNOWLEDGEMENTS

I would like to extend my gratitude to my supervisor Prof. Patrick Arbuthnot and co-supervisor Dr. Marco Weinberg for their support, advice and proficient insight during the course of my research. I am eternally grateful for the oppurtunites I have had under their supervision, without which I would not have the grounding on which to further my scientific career.

I would like to thank Dr. Abdullah Ely for his unconditional support, willingness and patience in assisting me during my research, not only as a colleague but as an exceptional friend too. Furthermore, I would like to acknowldege all the members of the Antiviral Gene Therapy Research Unit (AGTRU), in particular, Kristie Bloom, for her assistance during the *in vivo* investigations.

I would like to acknowledge Dr. Lisa Scherer (Beckman Research Institute of the City of Hope) for generously providing the $tRNA^{Lys3}$ promoter encoding plasmid (p901-1).

Furthermore, I would like to extend my gratitude to my family and friends who have encouraged me during the times of failed research and who have celebrated with me when success was obtained. I will always treasure your support, genrosity and love.

I would like to acknowledge the following funding bodies for financial support: Poliomyelitis Research Foundation (PRF); Deutscher Akademischer Austausch Dienst (DAAD); University of the Witwatersrand Post Graduate Merit award (PMA) and the National Research Foundation (NRF).

Lastly, I would like to thank Our Saviour, the Lord Jesus Christ. You have picked me up the many times I have stumbled, quietened my soul during the times of struggle and pushed me to achieve all you had planned for me. I will continue to walk the extraordinary life path you have carved for me as I venture into new challenges.

CONTENTS

DECLARATION ..... **ii**

ABSTRACT ..... **iii**

DEDICATION ..... **iv**

ACKNOWLEDGEMENTS ..... **v**

LIST OF FIGURES ..... **xiii**

LIST OF TABLES ..... **xvi**

LIST OF SYMBOLS ..... **xvii**

LIST OF ABBREVIATIONS ..... **xviii**

1 INTRODUCTION **1**

1.1 Hepatitis B virus **1**

1.1.1 HBV genome structure **1**

1.1.2 Replication of HBV **4**

1.2 The endogenous RNA interference pathway **6**

1.2.1 Harnessing the RNAi pathway through exogenous RNA mimics **9**

1.2.1.1 Pri-miRNA mimics **9**

1.2.1.2 Pre-miRNA mimics **9**

1.2.1.3 miRNA Mimics **10**

1.2.1.4 Exploitation of the RNAi pathway to targeting HBV **10**

1.3 RNA polymerase promoters **12**

1.3.1 RNA polymerase II (Pol II) promoters **12**

1.3.2 RNA polymerase III (Pol III) promoters **12**

1.3.3 U6, H1 and $tRNA^{Lys3}$ RNA Pol III Promoters **14**

1.4 Utilising RNA Pol II and RNA Pol III promoters for RNAi 14

1.5 Export and processing 16

1.6 Aims of the investigation 17

2 MATERIALS AND METHODS 18

2.1 Construction of H1 shRNA Expression Cassettes 18

2.1.1 Generation of the H1 promoter **18**

2.1.2 Construction of H1 shRNA expression cassettes **19**

2.1.3 Cloning of H1 shRNA expression cassettes **21**

2.1.4 Orientation of H1 shRNA Expression Cassettes **23**

2.2 Generation of an H1 Mock Expression Cassette 23

2.3 tRNA^{Lys3} shRNA Expression Cassettes 24

2.3.1 Preparation of tRNA^{Lys3} shRNAs **24**

2.3.2 Directional cloning of tRNA^{Lys3} shRNA expression sequences **25**

2.3.3 Confirmation of tRNA^{Lys3} shRNA inserts **26**

2.4 Generation of tRNA+1 mock expression cassette 29

2.5 RNA Pol II-driven pri-miRNA-122 shuttles 29

2.5.1 Construction of the pri-miRNA-122/8 and -122/9 shuttles **29**

2.5.2 Cloning of the pri-miRNA-122 shuttles into pTZ57R/T **33**

2.5.3 Orientation of the pri-miRNA shuttles in pTZ57R/T **33**

2.5.4 Cloning of the pri-miRNA shuttles into pCI-neo **34**

2.5.5 Confirmation of pri-miRNA inserts in pCI-neo **35**

2.6 Target Vectors 37

2.6.1 psiCHECK-HBx **37**

2.6.2 pCH-9/3091 ..... **37**

2.7 Cell Culture 37

2.8 Transfection of Huh7 cells for Dual Luciferase Assay and HBsAg Assay 38

2.8.1 Assessing RNAi effecter knockdown efficacy of HBV targets..... **39**

2.9 Transfection of Huh7 cells using Lipofectamine2000™ for total, nuclear and cytoplasmic RNA extraction..... 39

2.10 Transfection of Huh7 cells using Calcium Chloride for total, nuclear and cytoplasmic RNA extraction..... 40

2.11 Total RNA Extraction for Northern Blot Hybridisation..... 41

2.12 Nuclear and Cytoplasmic Fractionation..... 41

2.13 DAPI Staining of Nucleic Acids 42

2.14 Northern Blot Hybridisation..... 43

2.15 *In vivo* Analysis of Effecter Sequences Targeted to *HBx* 44

2.15.1 HBsAg Assay using ELISA..... **44**

2.15.2 Nucleic Acid Isolation of HBV DNA from Mouse Serum **45**

2.15.3 Extraction of Genomic DNA (gDNA) from Homogenised Liver **45**

2.15.4 Quantitative Real-time PCR (qRT-PCR) for the detection of rcDNA and cccDNA **46**

2.16 Statistical Analysis..... 47

3 RESULTS..... 48

3.1 Design and Generation of H1 shRNA expression cassettes..... 48

3.2 Design and Generation of the tRNA^{Lys3} shRNA expression cassettes 49

3.3 Design and Generation of pri-miRNA-122/8 and pri-miRNA-122/9 shuttles... 50

3.4 GFP expression as a indicator of transfection efficacy..... 53

3.5. The efficacy of RNA Pol III and RNA Pol II transcribed effecter sequences to target *HB*x for knockdown..... 54

3.5.1 Effective *HBx* target knockdown by Pol II- and Pol III-driven effecter sequences 5 and 6 ..... **55**

3.5.2 Decreased *HBx* target knockdown by Pol II- and Pol III-driven effecter sequences 8, 9 and 10 ..... **59**

3.6. Effective inhibition of HBsAg secretion from cultured cells after transfection with by anti-HBV expression cassettes 64

3.7 Pol III- and Pol II- expression cassettes do not saturate the RNAi pathway.. 68

3.8 DAPI Stain 70

3.9 Expression and processing of anti-HBV effecter sequences in total, nuclear and cytoplasmic fractions 71

3.9.1 Processed anti-HBV guide strands detected in Total RNA **71**

3.9.2 Processed anti-HBV guide strands detected in Total and Cytoplasmic RNA **73**

3.9.3 Detection of processed anti-HBV guide strands in total, nuclear and cytoplasmic RNA **75**

3.10 Inhibition of HBV within an *In vivo* Mouse model 79

3.10.1 Kaplan-Meier survival curve of mice post hydrodynamic tail vein injection **79**

3.10.2 Inhibition of HBsAg secretion **81**

3.10.3 Detection of total HBV, cccDNA and rcDNA **83**

4 DISCUSSION 88

4.1 Efficacy of RNA Pol II and RNA Pol III promoter-driven effecter cassettes ... 89

4.2 Saturation and off-targeting 90

4.3 Processing of shRNA and pri-miRNA expression cassettes 90

4.4 *In vivo* Efficacy 91

5 CONCLUSIONS 93

6 REFERENCES 95

APPENDIX A 115

A.1 Preparation of Agarose Gels 104

A.1.1 50× TAE Buffer **104**

A.2 Extraction of DNA - Qiagen MinElute™ Gel Extraction 104

A.3 Preparation of Chemically Competent DH5-α *E.coli* Cells 105

A.3.1 Luria-Bertani Broth (LB Broth) **106**

A.3.2 1000× Ampicillin **106**

A.3.3 Transformation Buffer **106**

A.4 LB Amp Agar Plates 106

A.5 X-gal (5-bromo-4-chloro-3-indolyl-beta-D-galactopyranoside) 106

A.6 IPTG (isopropyl thiogalactoside) 106

A.7 Blue-white Screening 107

A.8 Extraction of pDNA - Roche High Pure Plasmid Isolation 107

A.9 Automated Cycle Sequencing 108

A.9.1 ABI Big Dye Terminator Cycle Sequencing Kit **108**

A.10 Isolation of Plasmid DNA by standard Alkaline Lysis 108

A.11 Promega Dual Luciferase™ Assay 109

A.12 HBsAg Detection - MONOLISA® Ag HBs PLUS Kit 110

A.13 Calcium chloride (2.5 M) 110

A.14 2 × HEPES Buffer 110

A.15 Cellular Fractionation Method 1 110

A.16 Cellular Fractionation Method 2 111

A.17 Cellular Fractionation Method 3..... 111

A.18 Extraction of RNA from nuclear and cytoplasmic fractions - PARIS™ Kit.. 112

A.19 Preparation of Polyacrylamide Gel 112

A.19.1 10 × TBE Buffer **..... 113**

A.20 Radioactive labelling of Oligonucleotide Probes 113

A.21 20 × SSC Buffer..... 113

A.22 Quantitative Real Time PCR – LightCycler® FastStart DNA Master^{PLUS} SYBR Green I Kit..... 113

APPENDIX B - Animal Ethics Clearance 116

APPENDIX C - Supplementary Data 117

LIST OF FIGURES

Figure 1.1: Map of hepatitis B virus genome. 3

Figure 1.2: HBV replication cycle. 5

Figure 1.3: The endogenous RNAi pathway. 8

Figure 1.4: Exploitation of the RNAi pathway. 11

Figure 1.5: Gene structure of the U6, H1 and tRNA. 13

Figure 2.1: Generation of the H1 shRNA expression cassettes. 22

Figure 2.2: Insertion of shRNA encoding sequences into p901-1. 28

Figure 2.3: Construction of the pri-miRNA shuttles in pTZ57R/T. 32

Figure 2.4: Ligation of the pri-miRNA shuttle sequence into pCI-neo. 36

Figure 3.1: H1 shRNA expression cassette structure. 48

Figure 3.2: Schematic representation of the $tRNA^{Lys3}$ shRNA expression cassettes 50

Figure 3.3: Design of pri-miRNA-122/8 and pri-miRNA-122/9 shuttles. 51

Figure 3.4: M-fold predictions of pri-miRNA-122/8 and pri-miRNA-122/9 shuttles 52

Figure 3.5: A representation of GFP expression in Huh7 cells as a measure of transfection efficacy. 53

Figure 3.6: *HBx* knockdown by Pol III-shRNA 5 and miRNA-122/5. 57

Figure 3.7: *HBx* knockdown by Pol III-shRNA 6 and miRNA-122/6. 58

Figure 3.8: *HBx* knockdown by Pol III-shRNA 8 and miRNA-122/8. 61

Figure 3.9: *HBx* knockdown by Pol III-shRNA 9 and miRNA-122/9. 62

Figure 3.10: *HBx* knockdown by Pol III-shRNA10 and miRNA-122/10. 63

Figure 3.11: Inhibition of HBsAg by U6 and H1 promoter-driven shRNA expression cassettes. 66

Figure 3.12: Inhibition of HBsAg by $tRNA^{Lys3}$ and CMV promoter-driven shRNA expression cassettes. 67

Figure 3.13: Saturation assay of miR-16. 69

Figure 3.14: Presence of nucleic acids within fractionated lysates at 10 x Magnification. 70

Figure 3.15: Northern blot hybridisation of processed anti-HBV effecter sequences of a total RNA lysate. 72

Figure 3.16: Northern blot hybridisation of the processed anti-HBV effecter sequence (guide 5) within total lysate and cytoplasmic RNA fraction 74

Figure 3.17: Northern blot hybridisation of U6 and H1 processed anti-HBV effecter sequences of total, cytoplasmic and nuclear RNA. 76

Figure 3.18: Northern blot hybridisation of processed $tRNA^{Lys3}$ and pri-miRNA-122/5 anti-HBV effecter sequences of total, nuclear and cytoplasmic RNA. 78

Figure 3.19: Kaplan-Meier survival curves of the hydrodynamically injected mice. 80

Figure 3.20: Decrease of serum HBsAg in mice following HDI treatment. 82

Figure 3.21: Quantification of total HBV DNA isolated from livers of mice subjected to HDI. 85

Figure 3.22: Quantification of U6 and H1 total HBV, cccDNA and rcDNA isolated from livers of mice subjected to HDI. 86

Figure 3.23: Quantification of $tRNA^{Lys3}$ and CMV total HBV, cccDNA and rcDNA isolated from livers of mice subjected to HDI. 87

Figure C.1: Verification of the generation of the H1 shRNA expression cassettes. 117

Figure C.2: DNA sequence of H1 shRNA 5. 118

Figure C.3: DNA sequence of H1 shRNA 6. 119

Figure C.4: DNA sequence of H1 shRNA 8. 120

Figure C.5: DNA sequence of H1 shRNA 9. 121

Figure C.6: Predicted structure of $tRNA^{Lys3}$ shRNA expression cassettes. 122

Figure C.7: Sequence analysis of $tRNA^{Lys3}$ shRNA 5. 123

Figure C.8: Sequence analysis of $tRNA^{Lys3}$ shRNA 6. 123

Figure C.9: Sequence analysis of $tRNA^{Lys3}$ shRNA 8. 124

Figure C.10: Sequence analysis of $tRNA^{Lys3}$ shRNA 9. 124

Figure C.11: Sequence analysis of $tRNA^{Lys3}$ shRNA 10. 125

Figure C.12: Analysis of RNA integrity extracted from Total, nuclear and cytoplasmic fractions. 126

Figure C.13: Analysis of integrity of RNA extracted using the PARIS™ Kit. 127

Figure C.14: RNA anaylysis of total, nuclear and cytoplasmic fractions. 128

Figure C.15: Delivery efficiency of anti-HBV effecter sequences to the liver. 129

LIST OF TABLES

Table 2.1: The reverse primers designed for the construction of H1 shRNA expression cassettes using two-step PCR 20

Table 2.2: Oligonucleotides for the generation of $tRNA^{Lys3}$ shRNA expression cassettes 27

Table 2.3: The forward and reverse primers for the initial primer extension reaction required for the construction of pri-miRNA-122/8 and pri-miRNA-122/9 31

Table 2.4: Sequences of probes used in Northern Blot Hybridisation 44

Table 2.5: Primer sets used in real-time quantitative PCR 46

Table 6.1: Quantitative Real Time LightCycler® PCR Protocol 115

Table C.1: P values for shRNA 5 and pri-miRNA-122/5 *HBx* Dual Luciferase Assay 130

Table C.2: P values for shRNA 6 and pri-miRNA-122/6 *HBx* Dual Luciferase Assay 130

Table C.3: P values for shRNA 8 and pri-miRNA-122/8 *HBx* Dual Luciferase Assay 131

Table C.4: P values for shRNA 9 and pri-miRNA-122/9 *HBx* Dual Luciferase Assay 131

Table C.5: P values for shRNA 10 and pri-miRNA-122/10 *HBx* Dual Luciferase Assay 132

Table C.6: Statistical analysis of *in vitro* HBsAg (P values) 132

Table C.7: Statistical analysis of *in vitro* HBsAg (P values) 133

LIST OF SYMBOLS

1. α - Alpha
2. β - Beta
3. µ - Micro

LIST OF ABBREVIATIONS

1.	**AAV**	-	Adenoassociated virus
2.	**Ago2**	-	Argonaut 2
3.	**ATP**	-	Adenosine triphosphate
4.	**bp**	-	Base pair
5.	**Bq**	-	Becquerel
6.	**ccc**	-	Covalently closed circular
7.	**Ci**	-	Curie
8.	**CIP**	-	Calf intestinal phostphatase
9.	**CMV**	-	Cytomegalovirus
10.	**DGCR8**	-	Digeorge syndrome critical region 8
11.	**DMEM**	-	Dulbecco's Modified Eagles Medium
12.	**DNA**	-	Deoxyribonucleic acid
13.	**ds**	-	Double stranded
14.	**DSE**	-	Distal sequence element
15.	**FCS**	-	Foetal calf serum
16.	**GFP**	-	Green fluorescent protein
17.	**kb**	-	Kilobase
18.	**HBcAg**	-	Hepatitis B core antigen
19.	**HBsAg**	-	Hepatitis B surface antigen
20.	**HBV**	-	Hepatitis B virus
21.	**HBx**	-	Hepatitis B X
22.	**HCC**	-	Hepatocellular carcinoma
23.	**HDI**	-	Hydrodynamic injection
24.	**Huh**	-	Human hepatoma cells
25.	**IPTG**	-	sopropyl thiogalactoside

26.	**L**	-	Large
27.	**M**	-	Medium
28.	**MCS**	-	Multiple cloning site
29.	**mRNA**	-	Messenger RNA
30.	**miRNA**	-	MicroRNA
31.	**nt**	-	Nucleotide
32.	**NPC**	-	Nuclear pore complex
33.	**ORF**	-	Open reading frame
34.	**PAGE**	-	Polyacrylamide gel electrophoresis
35.	**PBS**	-	Phosphate buffered saline
36.	**PCR**	-	Polymerase Chain Reaction
37.	**pds**	-	Partially double stranded
38.	**PNK**	-	Polynucleotide kinase
39.	**Pol**	-	Polymerase
40.	**Pre-miRNA**	-	Precursor microRNA
41.	**Pri-miRNA**	-	Primary microRNA
42.	**PSE**	-	Proximal sequence element
43.	**rc**	-	Relaxed circular
44.	**RISC**	-	RNA Induced Silencing Complex
45.	**RNA**	-	Ribonucleic acid
46.	**RNAi**	-	RNA interference
47.	**rRNA**	-	Ribosomal RNA
48.	**S**	-	Small
49.	**SDS**	-	Sodium dodecyl sulphate
50.	**shRNA**	-	Short hairpin RNA
51.	**siRNA**	-	Small interfering RNA

52. **SSC** - Saline-sodium citrate
53. **snRNA** - Small nuclear RNA
54. **TAE** - Tris-acetate-EDTA
55. **TBE** - Tris-borate-EDTA
56. **tRNA** - Transfer RNA
57. **TRBP** - TAR RNA binding protein
58. **X-gal** - 5-bromo-4-chloro-3-indolyl-beta-D-galactopyranoside

1 INTRODUCTION

1.1 Hepatitis B virus

Globally, chronic infection with the hepatitis B virus (HBV) is estimated to affect 400 million people, with between 10 and 20 million new infections occurring every year. HBV-related complications, including hepatocellular carcinoma (HCC) and cirrhosis, are responsible for an annual mortality rate of approximately one million individuals (26, 47, 56). Currently, there are three classes of therapeutic agents available to treat HBV, which comprise immunomodulators, nucleotide and nucleoside analogues. The existing treatment of chronically infected individuals entails a combinatorial approach. Therapeutics administered are an immunomodulator (interferon-α) with either and a nucleotide analogue (adefovir) or a nucleoside analogue (lamuvidine). However the success of the combination therapy is limited to approximately 20% of patients and the response is rarely durable after withdrawal of therapy (5, 26, 47, 56). Alternative approaches to targeting HBV are being investigated, with particular emphasis being placed on antiviral gene therapy.

1.1.1 HBV genome structure

HBV is a member of the *Hepadnaviridae* family of hepatotropic viruses. The family consists of two genera, namely the *Orthohepadnaviruses* and the *Avihepadnaviruses*. *Orthahepdnaviruses* infect squirrels and woodchucks from the *Sciuridae* family and a variety of primates, including *Homo sapiens,* from the *Lorisidae* family, whilst *Avihepadnaviruses* infect ducks, herons and geese.

The viral genome is enclosed within the nucleocapsid and comprises a 3.2 kilobase (kb) partially double stranded (pds) relaxed circular (rc) deoxyribonucleic acid (DNA), which is

converted into covalently closed circular (ccc) DNA during active infection (4, 23) and four partially overlapping open reading frames (ORFs) (Figure 1.1).

The *X* ORF encodes for the 0.9 kb *Hepatitis B X* (*HBx)* viral transcript. The functioning of the X protein is not clearly understood, however it is known to be required for active infection and is a possible mediatior involved in the debilitating hepatocarcinomas associated with chronic HBV infection (59). In 2010, Bouchard and colleagues (17) demonstrated the involvement of *HBx* in the regulation of cell proliferation and HBV replication.

The *polymerase* ORF encodes for viral polymerase, which has reverse transcriptase activity required for the replication of the virus.

The *precore/core* ORF contains two in phase transcriptional start codons, generating two viral transcripts of ~3.5 kb. The *precore* region of the *precore/core* gene encodes an additional 29 nucleotides (nt) at the N-terminal domain of the protein (12). The viral transcripts encode the viral capsid protein or hepatitis B core antigen (HBcAg), which assemble into the viral core particle.

The fourth ORF contains three in phase transcriptional start codons, which generate the glycoproteins of the viral envelope. The smallest surface protein, which is 226 amino acids in length, is encoded by the *surface* domain of the ORF. The *Pre-S2* and *surface* region of the ORF together code for the middle (M) protein. The large (L) surface protein (389 amino acids) is encoded for by the *Pre-S1*, *Pre-S2* and *surface* domains of the ORF. A comprehensive review of the viral transcripts has been previously discussed (12, 47).

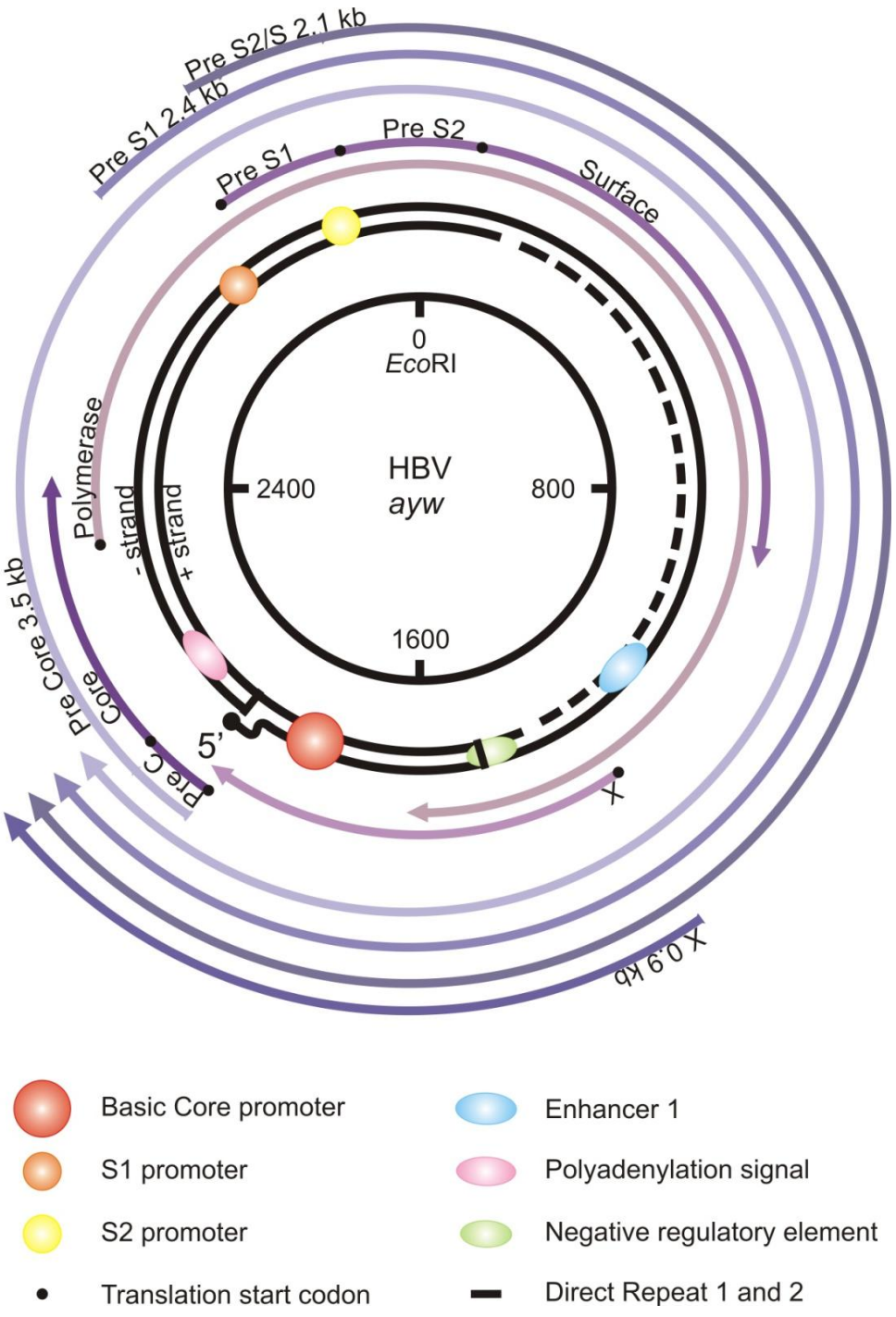


Figure 1.1: Map of hepatitis B virus genome.

The inner four arrows represent the four ORFs which encode the viral proteins of HBV. The viral transcripts are represented by the four outer arrows and terminate at a unique site on the 3' end. The figure was adapted from previously published work (5).

1.1.2 Replication of HBV

The inability of the virus to infect cells *in vitro* and the lack of convenient animal models that are infectable by the virus has limited analysis of early events in the life cycle of HBV. As a consequence although it is known that hepatocytes are the primary site of infection the precise mechanism and receptor the virus uses to attach and enter the cells remains unknown. Nevertheless, investigations have defined two epitope regions within the HBsAg involved in attaching the virion to the hepatocyte. The first epitope occurs within the Pre-S1 region between amino acids 21 to 47 (40, 41) and the second region occur within the small HBsAg and is predicted to enhance the attachment of the virion to the cell (43).

Post virion adherence to the hepatocyte, the pds rcDNA viral genome, which is comprised of the long minus strand (- strand) and short plus strand (+ strand) (Figure 1.1) is transported to the nucleus. The genome is transcribed into cccDNA, which acts as the template for the transcription of viral mRNAs (12, 47). The pre-genomic RNA (pgRNA) transcript is 3.5 kb in length, which is longer than genome and forms the basis for synthesis of the (-) strand by reverse transcription. Synthesis of a small primer sequence is initialised by the viral Pol promoter at the 5' end. The primer-polymerase complex translocates to a homolgous region at the 3' end of the pgRNA and begins reverse transcribing the viral transcript generating the (-) strand (Figure 1.2). The primer-polymerase complex again translocates to the 5' end of the synthesised (-) strand and begins synthesising the (+) strand. (12).

The synthesis of the viral genome from an RNA intermediate (i.e. the pgRNA) allows viral replication to be directly targeted by RNAi. In contrast established cccDNA may not be susceptible to RNAi-mediated silencing and as a consequence limit efficacy of RNAi-

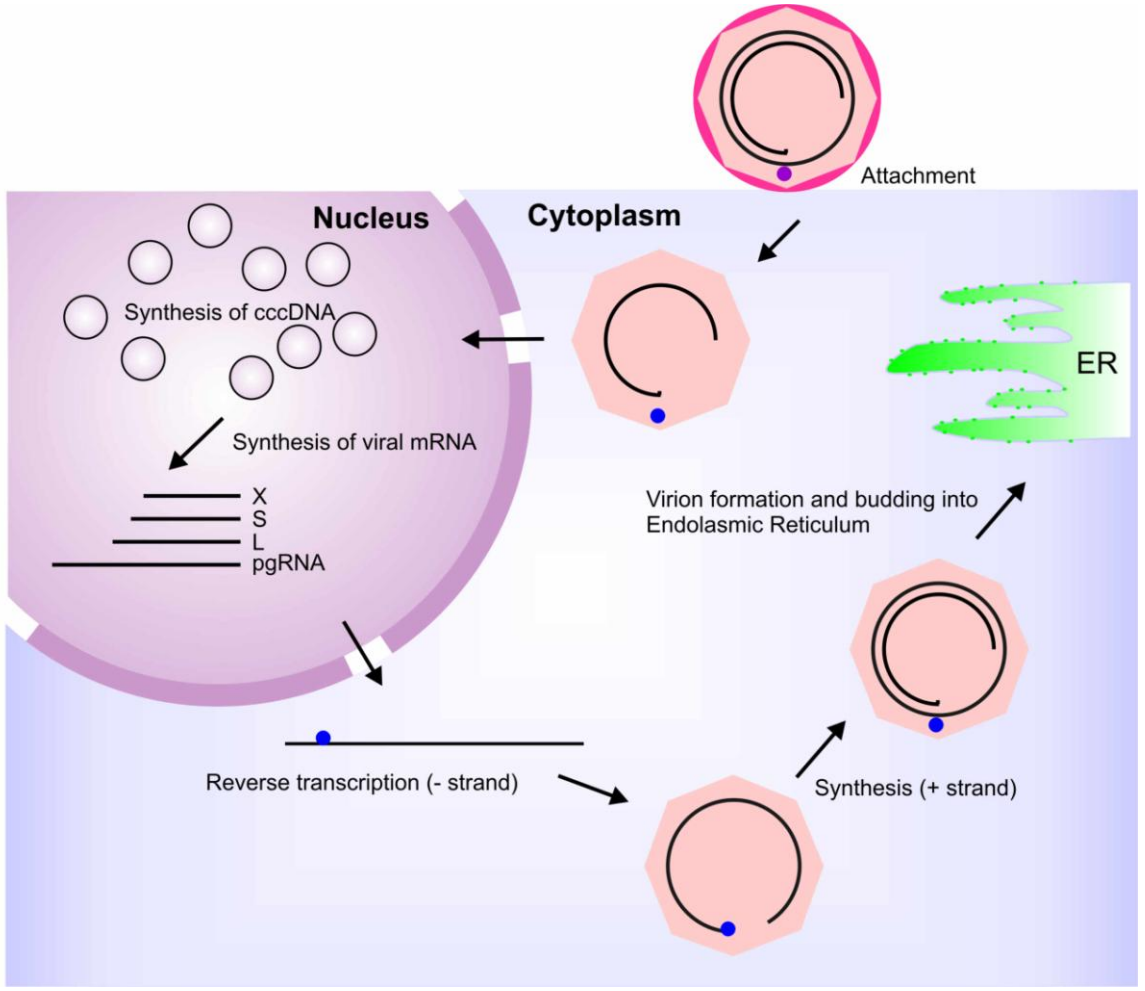


Figure 1.2: HBV replication cycle.

The virion attaches to the hepatocyte and is internalised into the cytoplasm of the cell. The viral genome is transloacated to the nucleus and synthesised into cccDNA. The pgRNA viral transcript is synthesised to form the (-) strand and following translocation of the polymerase primer complex, the (+) strand is synthesised. The virion is formed and buds out through the endoplasmic reticulum.

based therapeutics (49). The overlapping nature of the HBV genome also makes it a perfect target for RNAi therapeutics as there is little chance for the occurrence of mutations within the genome. Furthermore, because the viral transcripts overlap, the targeting of a single site within an overlapping region silences multiple viral transcripts.

1.2 The endogenous RNA interference pathway

The RNA interference pathway is an evolutionary conserved cellular pathway involved in post-transcriptional gene silencing. In 1998, Fire *et al* (16) coined the term RNA interference (RNAi) to describe the silencing of genes by dsRNA. The mechanism of RNAi, however, had been observed in plants almost a decade earlier by two different groups attempting to increase the hue in petunias by introducing a transgene (38, 50). Notably, the genetically altered petunias were either variegated purple and white or complete white. There was no forthcoming explanation for this phenomenon, until the discovery of RNAi in *Caenorhabitis elegans* (16).

In 2001, Tuschl *et al* (13) demonstrated the suppression of target Luciferase using 21 nt small interfering RNAs (siRNAs). Evidentially, this was the principal investigation that showed RNAi-mediated gene silencing in mammalian cell culture. The endogenous RNAi pathway (Figure 1.3) begins with the transcription of long principal transcripts termed primary miRNAs (pri-miRNAs) by RNA Polymerase II (Pol II). The pri-miRNAs are recognised and stabilised by Digeorge syndrome critical region 8 (DGCR8) (55). DGCR8 directs the cleavage of the pri-miRNAs into ~70 nt pre-cursor miRNAs (pre-miRNAs) with a 2 nt overhang at the 3' end, by RNaseIII Drosha (32, 55). The pre-miRNAs are exported from the nucleus into the cytoplasm by Exportin-5 (31). The PAZ domain of the RNaseIII enzyme Dicer recognizes the 2 nt overhang of the pre-miRNAs which are subsequently processed into ~22 nt mature miRNAs by Dicer/TAR RNA binding protein (TRBP) (33).

The mature miRNAs are incorporated into the RNA-induced silencing complex (RISC) and are unwound by an adenosine triphosphate (ATP)-dependent helicase into two independent strands (anti-guide and guide), which are known as siRNAs. Argonaut 2 (Ago 2) selects the strand complementary to the messenger RNA (mRNA) target, subsequently binding the strand to the target. Complete binding of the guide strand to the mRNA target through Watson-Crick base pairing causes translational repression and silencing of the target gene. Alternatively, incomplete binding of a guide strand due to mismatched base pairs between the guide strand and mRNA target results in degradation of the target (36, 57). It has since been shown that miRNAs play an important role in various biological processes, including differentiation and proliferation of the cell (10, 24, 54).

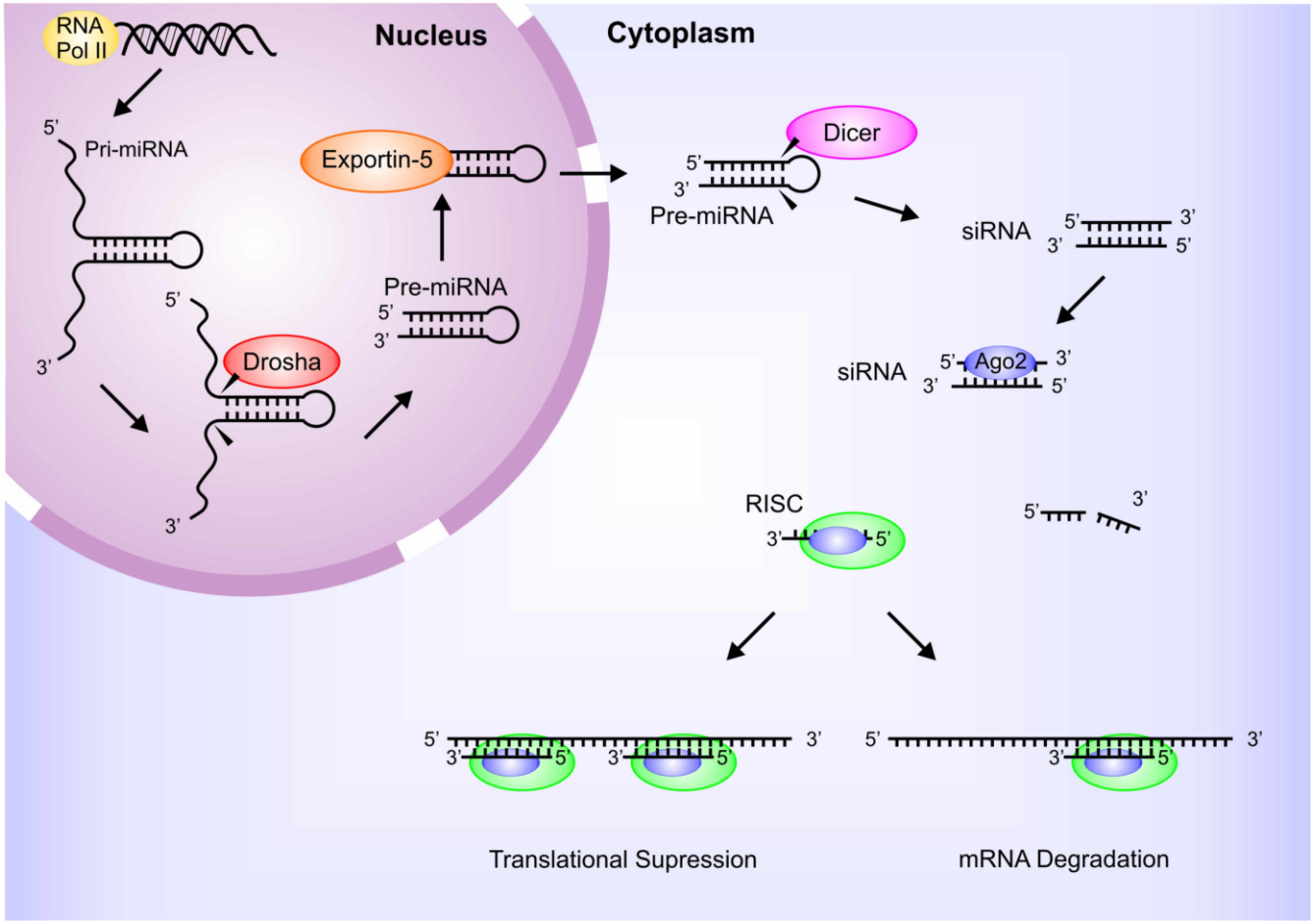


Figure 1.3: The endogenous RNAi pathway.

Pri-miRNAs are transcribed from DNA by Pol II, anchored by DGCR8 and cleaved by Drosha into a pre-miRNA. The pre-miRNAs are exported out of the nucleus and into the cytoplams by exportin-5. Cleavage of the pre-miRNA by Dicer generates a 22 nt siRNA duplex. An ATP-dependent helicase unwinds the duplex, and Ago2 incorporates the guide strand into RISC. Complete complementarity of the guide strand to the mRNA target causes degradation of the target gene, whereas incomplete complementarity causes translational suppression of the target gene.

1.2.1 Harnessing the RNAi pathway through exogenous RNA mimics

The endogenous RNAi pathway may be harnessed as a novel approach for antiviral gene therapy and research based therapeutics, due to the target specificity of dsRNAs (~19-25 nt). There are three different approaches involved in exploiting the endogenous RNAi pathway through the introduction of exogenous RNAi intermediates, which mimic either the pri-miRNA, pre-miRNA or mature miRNA components of the endogenous pathway (Figure 1.4).

1.2.1.1 Pri-miRNA mimics

Pri-miRNA mimics are designed to incorporate the effecter sequence within the pre-miRNA stem region (~22 nt). The structural design of the pre-miRNA is critical when generating a mimic because the secondary folding of the pre-miRNA mimic should be maintained as to be as identical as possible to that of the pre-miRNA. Pol II transcribes natural endogenous pri-miRNAs within the nucleus of a cell before entering the RNAi pathway. Pri-miRNA mimics are inserted downstream of a Pol II promoter contained within an expression vector. Post transportation of the vector into the nucleus of the cell, the pri-miRNA mimics are transcribed and processed by the endogenous microprocessor complex (Drosha and DGCR8) and exported via the RNAi pathway.

1.2.1.2 Pre-miRNA mimics

Exogenous pre-miRNA mimics are generally referred to as short hairpin RNAs (shRNAs). These mimics represent ‘processed pri-miRNAs’ and are comprised of only the effecter sequence complementary to the mRNA target incorporated into the 5’ stem region and a loop and have no flanking sequences. As with expressed pri-miRNA mimics, expressed shRNAs require DNA-dependent RNA polymerase to drive transcription. RNA Pol III promoters are generally chosen to drive the expression of shRNAs as these promoters

initiate transcription at a definitive start site, adjacent to which the shRNAs are located. Transcribed shRNAs enter the RNAi pathway by being exported out of the nucleus and into the cytoplasm for Dicer processing.

1.2.1.3 miRNA Mimics

The final way in which to exploit the endogenous RNAi pathway is through the introduction of siRNAs. Comprised of only the effecter and complementary sequence, these small dsRNAs can be transduced directly into the cytoplasm of the cell. Selection of the guide strand by Ago2 and incorporation into the RISC complex proves a simple and effective approach in exploiting the RNAi pathway.

1.2.1.4 Exploitation of the RNAi pathway to targeting HBV

Exploitation of the RNAi pathway as a tool for powerful and specific gene silencing has initiated investigations into the utilisation of expressed or synthetic effecter sequences for therapeutic purposes. The compact genome and limited mutability of HBV has established the virus as an excellent candidate for RNAi-based therapy. Previous studies have indicated that gene therapy approaches (eg ribozyme therapy (44, 52, 53)) may be effective as an HBV therapeutic. RNAi offers a powerful to for specifically silencing viral replication. Subsequent development of a potent RNAi construct may in time lead to therapeutics effective in managing chronic HBV infection (5, 37).

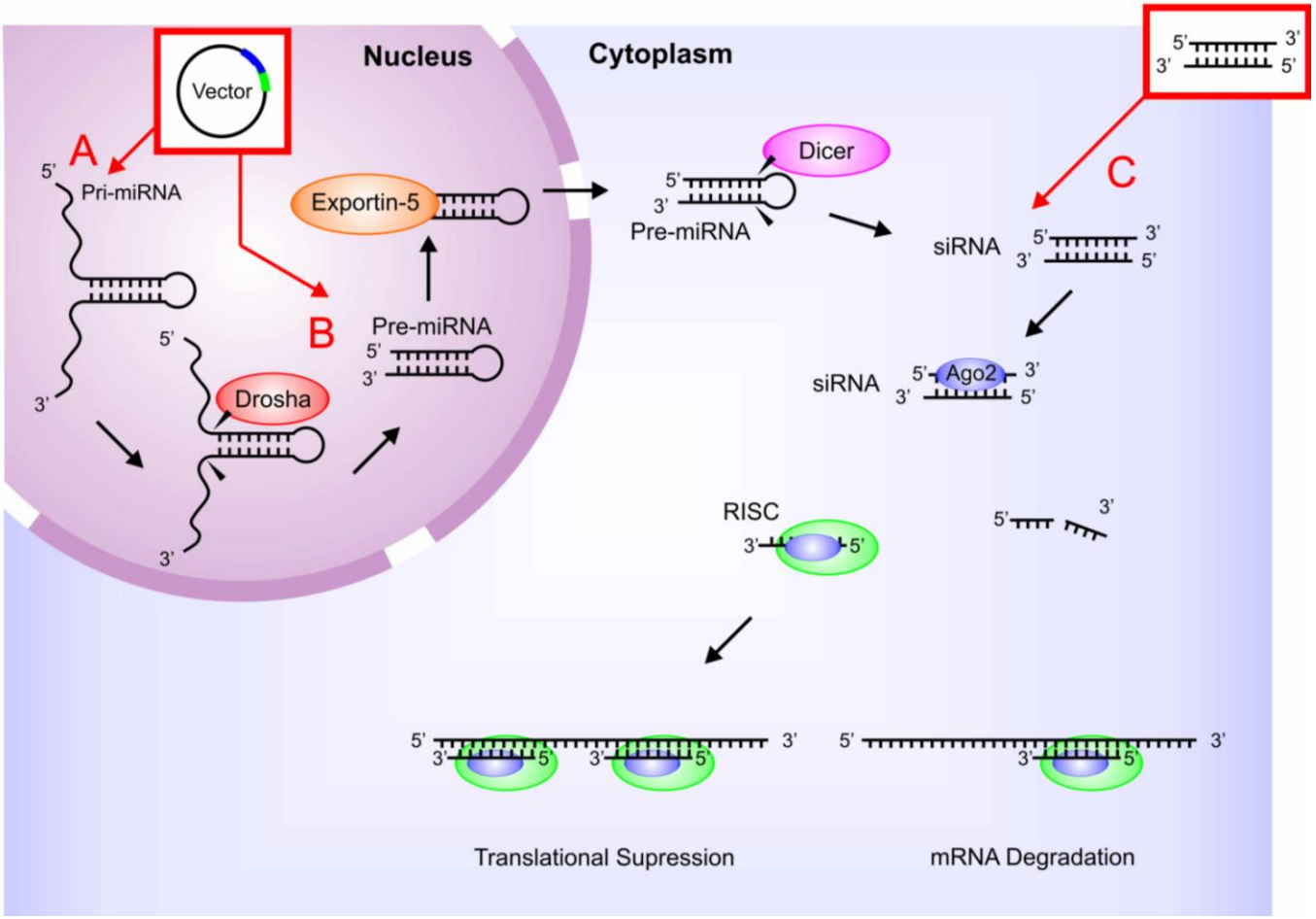


Figure 1.4: Exploitation of the RNAi pathway.

(A) Pri-miRNA mimics are transcribed within the nucleus and are processed in the same manner as endogenous pri-miRNAs. **(B)** pre-miRNA mimics are transcribed within the nucleus and exported into the cytoplasm by exportin-5. **(C)**. Synthetic miRNAs can be transduced directly into the cytoplasm as a siRNA duplex. Complete complementarity of the mimic guide strand to the mRNA target causes degradation of the target gene, whereas incomplete complementarity causes translational suppression of the target gene.

1.3 RNA polymerase promoters

Eukaryotes maintain transcriptional control of genes within the nuclei through the functioning of three different types of DNA-dependent RNA polymerases namely Pol I, Pol II and Pol III (7). Gene transcription by Pol I is limited to the synthesis of large ribosomal RNA (rRNA). Pol III synthesises 5S RNA and transfer RNA (tRNA). Pol II, however, is capable of transcribing an extensive selection of genes as it is responsible for the synthesis of mRNA.

1.3.1 RNA polymerase II (Pol II) promoters

RNA Pol II is known to transcribe a vast range of mRNAs within the cell. Initial hypotheses speculated Pol III promoters to drive synthesis of miRNA genes, however in 2004, Lee *et al* (33) identified the regulatory elements to be Pol II promoters. Investigations have since demonstrated that RNA Pol II promoters can direct gene silencing to a particular cell or tissue, whereas Pol III promoters lack cell or tissue specificity (58).

1.3.2 RNA polymerase III (Pol III) promoters

Pol III promoters are robust transcriptional activators, which are divided into three classes based upon their structural arrangements. Class I Pol III and class II Pol III promoters contain internal control regions (promoter elements) situated downstream of the transcripton start site. Class III Pol III promoters differ from those of class I and class II in that the genes do not contain internal promoter elements, but do contain three promoter elements situated upstream of a defined transcriptional start site (8, 35, 45, 46). The promoter elements, namely the distal sequence element (DSE), proximal sequence element (PSE) and TATA box are required for gene expression, and the structural layout of the class III Pol III promoter closely resembles that of Pol I and Pol II promoters (Figure 1.5).

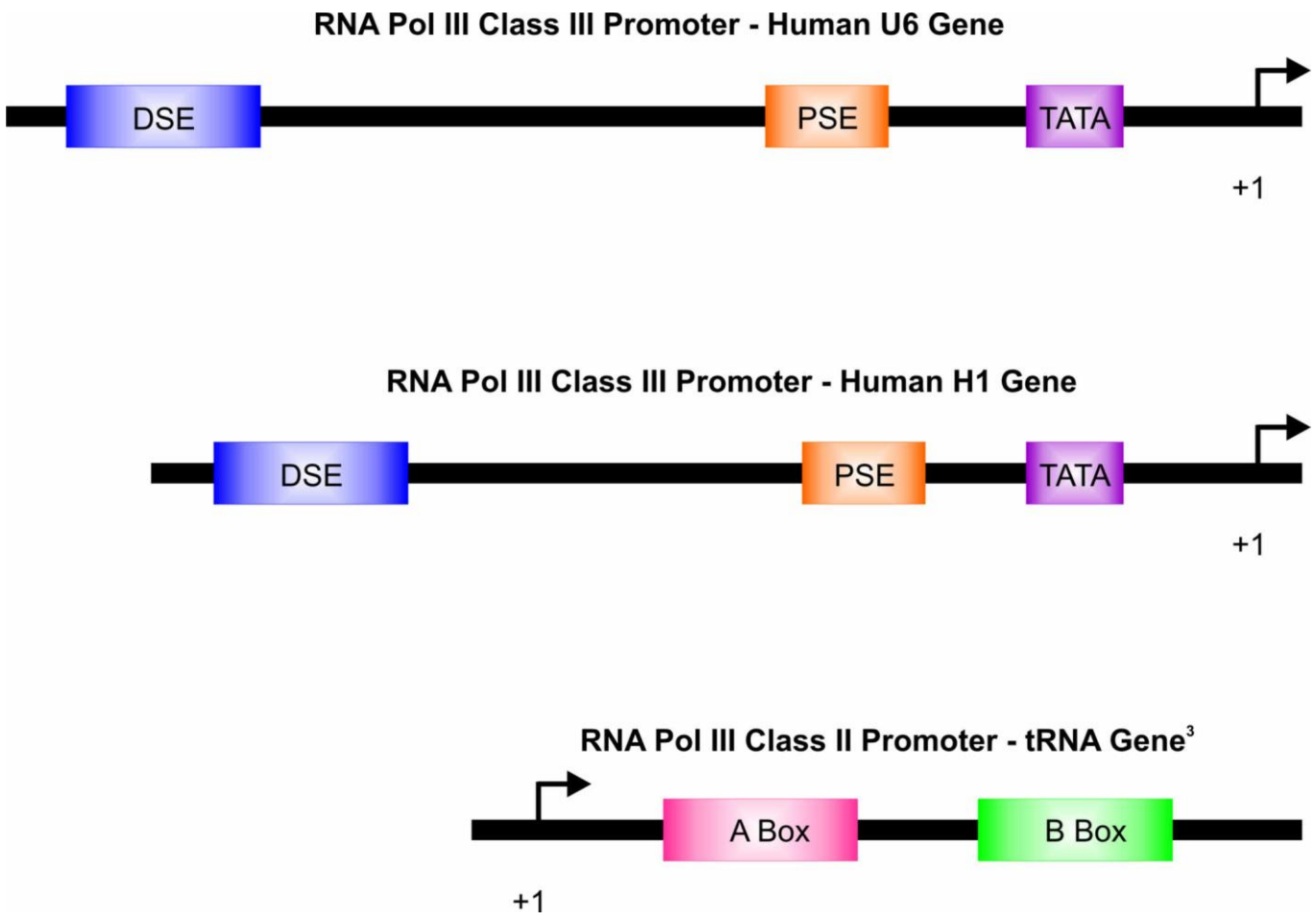


Figure 1.5: Gene structure of the U6, H1 and tRNA.

(A and B) U6 and H1 are class III Pol III promoters and share a similar gene structure, although H1 is smaller. The distal sequence element (DSE)and proximal sequence element (PSE) are found downstream of the TATA box, which initiates transcription at a definative start site (+1). **(C)** The tRNA gene is a class II Pol III promoter. Transcription begins within the structural genes of the tRNA, trascribing precursor tRNAs.

1.3.3 U6, H1 and $tRNA^{Lys3}$ RNA Pol III Promoters

The gene encoding U6 small nuclear RNA (snRNA) has a characteristically different structure in comparison to the remaining eleven snRNAs found within the U series. In 1986, several of the structural differences within the U6 snRNA prompted Pederson *et al* (29) to hypothesise that U6 snRNA was not sythesised by Pol II, but by an alternate polymerase. The investigation demonstrated that Pol III was responsible for the transcription of U6 snRNA. This initial finding was further supported by the identification that transcription of U6 snRNA was terminated by a series of thymine nucleotides (poly-T tail) at the 3' end. This particular nature of transcriptional termination was initially identified for 5S rRNA, which is known to be under the transcriptional control of a Pol III promoter (3).

In 1989, Baer *et al* (1) assessed the structure and transcription of H1 RNA. Structurally H1 was found to be compact and the promoter elements required for transcription located upstream of the transcription start site (Figure 1.3). As discovered within U6 snRNA, the structural genes of H1 RNA were characteristic of both Pol II and Pol III transcripts, but transcription was synthesised by Pol III (1).

tRNA genes are grouped within class I of Pol III promoters. The transcriptional start site of the promoter occurs within the structural gene of tRNAs and are smaller when compared to class III RNA Pol III promoters (43).

1.4 Utilising RNA Pol II and RNA Pol III promoters for RNAi

Pol III promoters are capable of rapidly synthesising shRNAs, which is advantageous in directing rapid gene silencing (58). Specific Pol III promoters, however, are more effective at transcribing RNA than other promoters within the same class. This is particularly evident

between U6 and H1, where H1 transcribes at a lower rate when compared to U6. Although expressing high levels of RNAs, Pol III promoters lack the ability to successfully transcribe RNAs of greater nucleotide length whereas Pol II is perfectly capable. Furthermore, Pol II promoters are capable of spatial and temporal control of gene expression at a localised tissue or cell, which is important in site-directed antiviral gene therapy (33, 58).

There are three important requirements to consider when generating effecter cassettes for antiviral gene therapy. Firstly, dsRNA, should be potent in its ability to actively silence the target mRNA. Secondly, the level of expression of the dsRNA is important, as the concentration of the effecter cassette should be low but optimally expressed. Finally, there should be no off-target or toxic effects associated with the delivery and expression of an effecter cassette. This is of particular importance based on the initial findings in which Grimm *et al* (22) assessed the effects associated with the long-term expression of shRNAs in mice. Briefly, adeno-associated viral (AAV) vectors that express anti-HBV shRNAs were administered to mice. Dose-dependent liver injury was noted in 73% of the mice, of which 63% died. It was determined that the exogenous shRNAs were competing with endogenous pre-miRNAs for the cellular factors required for processing and exporting of RNAs, subsequently saturating the endogenous miRNA pathway within the hepatocytes.

Previous investigations have demonstrated that efficacy of U6 promoters to transcribe effecter sequences at higher levels when compared to H1, silencing a variety of different targets, *in vitro* and *in vivo,* through RNAi (8). Furthermore, $tRNA^{Val}$, $tRNA^{Lys3}$ and U6 promoter-driven shRNA expression cassettes have demonstrated a comparable efficacy of target knockdown between the promoters (27, 45, 46). These preliminary investigations have initiated suggestions that lower level transcription has a particular importance in RNAi as the targets are optimally silenced and no off-target or toxic effects (28, 46).

Recently, Kay *et al* (18) demonstrated that a shRNA expression cassette driven by a liver specific Pol II promoter functions optimally in silencing HBV *in vitro* and *in vivo.*

1.5 Export and processing

The export of transcribed tRNAs, rRNAs and mRNAs from the nucleus to the cytoplasm occurs through the nuclear pore complexes (NPC) (34). The shuttling of components is mediated by the transport receptors importin and exportin, which differ depending upon the macromolecule being transported (30, 34).

Pre-miRNAs, which are processed from pri-miRNAs by the RNAse III enzyme Drosha are transported out of the nucleus and into the cytoplasm via the transport receptor exportin-5. The cleavage by Drosha produces a characteristic short 3' overhang, which is recognised by exportin 5 (48). Export of the pre-miRNAs into the cytoplasm precedes Dicer processing and incorporation of duplexes into RISC.

Exportin-t and RanGTP, which bind to tRNA to form a trimeric complex, assist in the shuttling of the $tRNA^{Lys3}$ from the nucleus to the cytoplasm. After transportation from the nucleus, the complex is disassembled within the cytoplasm (30, 34). Prior to the export, precursor tRNAs (pre-tRNAs) undergo particular post-transcriptional modifications to become functionally active tRNAs. The modifications, which include trimming of the 3' and 5' ends, nucleoside alterations and the addition of a 3'CCA (34) are carried out to stabilise the conformation of the clover-leaf secondary structures and to assist in the activities performed by tRNAs (8, 25). The precise mechanism involved in processing $tRNA^{Lys3}$-shRNA is remains unclear, however Scherer *et al* (45) have proposed that the 3' tRNase (tRNase Z^{L}) is responsible for cleaving $tRNA^{Lys3}$-shRNA.

1.6 Aims of the investigation

The primary aim of the investigation was to assess whether four different promoters could successfully transcribe anti-HBV effecter sequences capable of rapidly and effectively inhibiting HBV. The RNA Pol III (U6, H1 and $tRNA^{Lys3}$) and RNA Pol II (CMV) promoters were used to drive the expression of five different RNAi effecter sequences. Furthermore, the project aimed to analyse whether expression from the H1, $tRNA^{Lys3}$ and CMV promoters is less than that from U6 promoter expression, whilst maintaining the same degree of knockdown.

The efficacy of these shRNAs expression cassettes and pri-miRNA shuttles to knockdown their targets at varying concentrations would provide an insight into establishing the lowest possible dosage at which the shRNA or miRNA could optimally function, which is of importance in creating a therapeutic tool to actively target HBV.

In conclusion, the project aims to provide an insight into the functioning of shRNA and miRNA expression cassettes driven by Pol II and Pol III promoters and the targeting of HBx at different sites, without causing any resultant off targeting or saturation effects. Ultimately, the findings of the investigation would assist in aiding research into developing treatment of HBV utilising antiviral therapeutics through RNA interference.

.

2 MATERIALS AND METHODS

2.1 Construction of H1 shRNA Expression Cassettes

2.1.1. Generation of the H1 promoter

The full H1 promoter described by Chen and colleagues (11) was engineered to incorporate an *Eco*RI and a *Spe*I restriction site at the 5' end. The H1 forward (5'-GAT CGA ATT CAC TAG TGA ACG CTG ACG TCA TCA A-3') and primers (5'-GGA TCC GTG GTC TCA TAC AGA ACT TAT AAG ATT CCC AAA TC-3') were synthesised using standard phosphoramidite chemistry (IDT, IA, USA). The lyophilised oligonucleotides were resuspended as 100 µM stocks and 15 µM working stocks were prepared. The H1 promoter was amplified by polymerase chain reaction (PCR) in a final reaction volume of 25 µl containing 100 ng H1 human genomic DNA; 15 pmol H1 forward primer; 15 pmol H1 reverse primer; 2.5 mM dNTP mix; 0.25 U TripleM™ Taq polymerase and was carried out in 1× high fidelity buffer using the TripleM™ High Fidelity PCR Kit (Eppendorf, Germany). The PCR was programmed to run with an initial denaturation at 94°C for 5 minutes with ten cycles of touchdown PCR (denaturation at 94°C for 10 seconds; annealing at 67°C for 10 seconds and elongation at 72°C for 10 seconds, with the annealing temperature decreasing by 1 degree with every cycle). Thereafter fourteen cycles of standard PCR (denaturation at 94°C for 20 seconds; annealing at 57°C for 20 seconds and elongation at 72°C for 45 seconds) and a final elongation step at 72°C for two minutes and thirty seconds followed (Eppendorf Mastercycle Gradient, Germany). The size of the DNA fragment amplified by PCR was verified using agarose gel electrophoresis (Appendix A.1). The desired band was excised from the gel and then purified using the MinElute™ Gel Extraction Kit (Qiagen, Germany) according to the manufacturer's instructions (Appendix A.2). The purified H1 promoter DNA was used as the template for generating the H1 shRNA expression cassettes.

2.1.2 Construction of H1 shRNA expression cassettes

Primers (Table 2.1) were designed to generate H1 shRNA expression cassettes equivalent to the previously described U6 shRNA cassette (5).The shRNA expression cassettes were constructed using a two-step PCR reaction (Figure 2.1) (6). Reverse primers for the first round of PCR were designed to incorporate the sense strand, loop and four nucleotides of the antisense strand for shRNA 5, shRNA 6, shRNA 8, shRNA 9 and shRNA 10 (5). The expressed shRNA sequences were designed to target nucleotides 1575-1599, 1580-1604, 1678-1692, 1774-1788 and 1863-1877 of HBV (Genbank Accession Number J02203.1). Base wobbles were inserted into the sense strand to prevent errors from occurring during PCR, subsequently aiding in cloning. The oligonucleotides were synthesised using standard phosphoramidite chemistry (IDT, IA, USA) and prepared as previously described (Section 2.1.1). Reverse primers for the second round of PCR were designed to incorporate the remaining sequence of the antisense strand as well as the termination signal to the amplicon from the first round PCR. The H1 forward primer (5'-GAT CGA ATT CAC TAG TGA ACG CTG ACG TCA TCA A-3') was used in both rounds of the two-step PCR reaction. The first round PCR was prepared in a final reaction volume of 25 µl containing 100 ng H1 promoter template DNA; 15 pmol H1 forward primer; 15 pmol shRNA N.1 (where N denotes the hairpin i.e. 5, 6, 8, 9, or 10) round one reverse primer; 4 mM dNTP mix; 0.75 U GoTaq® Polymerase; 1 mM $MgCl_2$ and was carried out in 1× GoTaq® Flexi Buffer using the GoTaq® Flexi DNA Polymerase Kit (Promega, WI, USA). The PCR cycle was carried out as previously described (Section 2.1.1) and the sizes of the amplified DNA fragments verified using agarose gel electrophoresis. The desired DNA bands were

Table 2.1: The reverse primers designed for the construction of H1 shRNA expression cassettes using two-step PCR

shRNA	Round	Sequence
H1 shRNA 5	1	5′**TCTGTGACAGGAAGCAGAG**GCGAAGCAAAGCGCACACG*ACGGATCCGAGTGGTCTCATAC* 3′
	2	5′CCCAGATCTACGCGTAAAAAACCGTGTGCACTTCGCTTCACC**TCTGTGACAGGAAGCAGAG** 3′
H1 shRNA 6	1	5′**ACGTTGACAGGAAGATGTG**TAGAGGTGAAGCGAGGTGTA*CGGATCCGAGTGGTCTCATAC* 3′
	2	5′CCCAGATCTACGCGTAAAAAATGCACTTCGCTTCACCTCTGC**ACGTTGACAGGAAGATGTG** 3′
H1 shRNA 8	1	5′**AGGCTGACAGGAAGGCTTC**AAGGTTGGTTGTTGACGTTG*CGGATCCGAGTGGTCTCATAC* 3′
	2	5′CCCAGATCTACGCGTAAAAAACAATGTCAACGACCGACCTTG**AGGCTGACAGGAAGGCTTC** 3′
H1 shRNA 9	1	5′**TGGTTGACAGGAAGACTAA**TTTGTGCCTACAGCTTCTTA*CGGATCCGAGTGGTCTCATAC* 3′
	2	5′CCCAGATCTACGCGTAAAAAATAGGAGGCTGTAGGCATAAAT**TGGTTGACAGGAAGACTAA** 3′
H1 shRNA10	1	5′**TTGGTGACAGGAAGCCAAAG**CACAACTCGGAGGCTCGAA*CGGATCCGAGTGGTCTCATAC* 3′
	2	5′CCCAGATCTACGCGTAAAAAATTCAAGCCTCCAAGCTGTGCC**TTGGTGACAGGAAGCCAAG** 3′

The H1 promoter binding sequences are italicised, with primer overlapping sequences in bold. The hairpin loop encoding sequence is underlined and the base wobbles within the sense strand are double underlined

excised from the gel and purified using the MinElute™ Gel Extraction Kit. The purified first round PCR product was used as template in the second round of PCR for the generation of the complete H1 shRNA cassettes.

The second round PCR was prepared in a final reaction volume of 50 µl containing 100 ng first round PCR product DNA; 15 pmol H1 forward primer; 15 pmol H1 shRNA N.2 round two reverse primer; 10 mM dNTP mix; 0.25 U TripleM™ Taq polymerase and was carried out in 1× High Fidelity buffer using the TripleM™ High Fidelity PCR Kit. The PCR cycle was programmed as previously described (Section 2.1.1) and the size of the amplicons verified by agarose gel electrophoresis. The desired DNA bands were excised and purified using the MinElute™ Gel Extraction Kit.

2.1.3 Cloning of H1 shRNA expression cassettes

The H1 shRNA expression cassettes were inserted into the PCR cloning vector pTZ57R/T (InsT/Aclone™ Fermentas, MD, USA). Ligation reactions were prepared in a final reaction volume of 20 µl containing 300 ng H1 shRNA PCR product; 0.165 µg pTZ57R/T; 7.5 U T4 DNA ligase and was carried out in 1× ligation buffer (Fermentas, MD, USA) and incubated overnight at room temperature. The ligation mixtures were used to transform chemically competent *Escherichia coli (E. coli)* DH5-α cells (Invitrogen, CA, USA) (Appendix A.3). Transformed bacteria were plated onto Luria-Bertani (LB) agar plates (Appendix A.4) containing 5-bromo-4-chloro-3-indolyl-beta-D-galactopyranoside (X-gal) (Appendix A.5) and isopropyl thiogalactoside (IPTG) (Appendix A.6) and incubated overnight at 37°C. Bacteria transformed with the pTZ57R/H1 shRNA plasmids were identified using blue/white screening (Appendix A.7). Five clones of each H1 shRNA were picked, inoculated in 4 ml LB and incubated at 37°C overnight in a shaking incubator. The H1 shRNA plasmid DNA (pDNA) was purified from

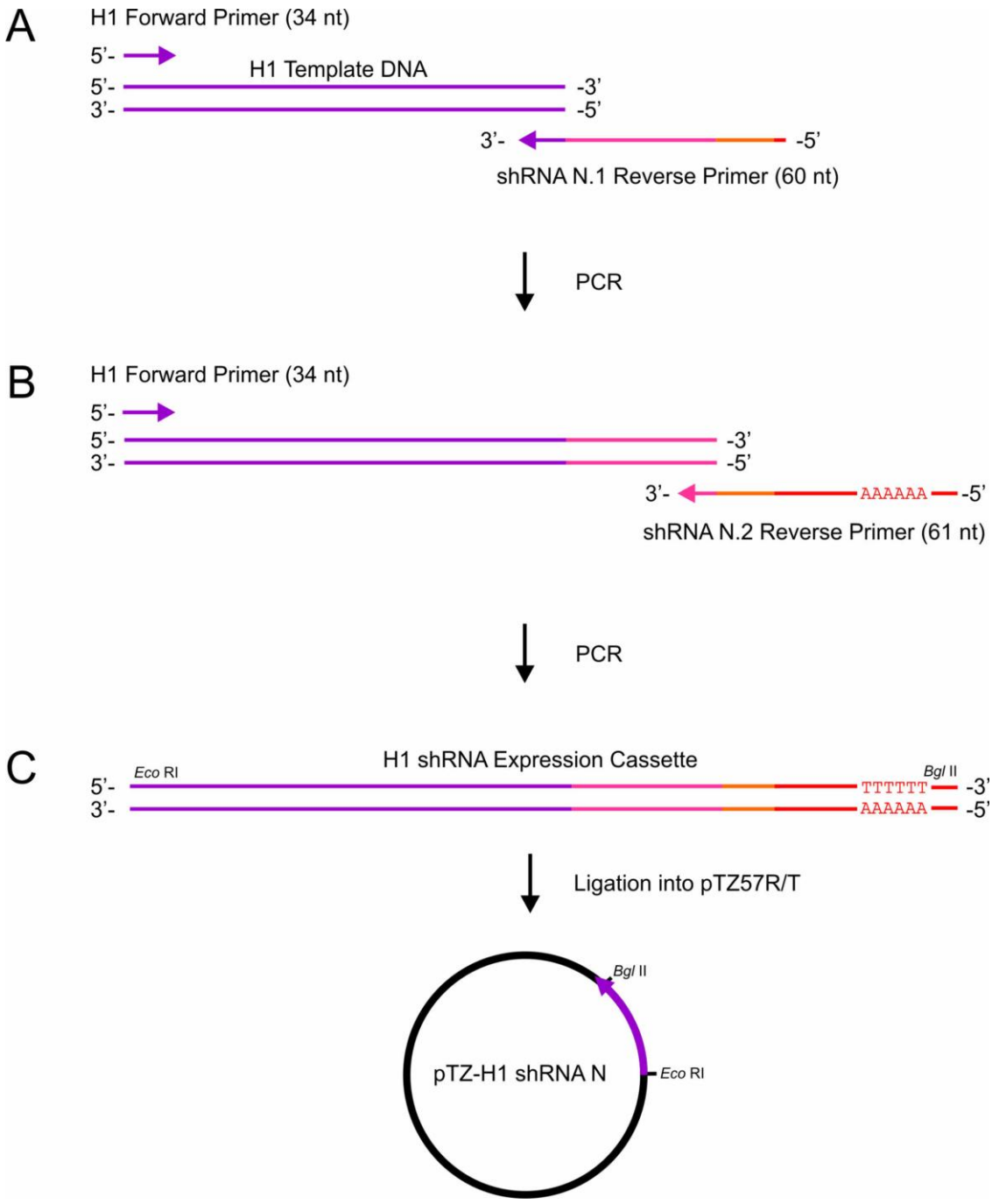


Figure 2.1: Generation of the H1 shRNA expression cassettes.

The H1 shRNA expression cassettes were constructed in a two-step PCR and ligated into the cloning vector pTZ57R/T. **(A)** The first round amplified the H1 promoter (purple), the sense strand (pink) the loop (orange) and 4 nucleotides of the antisense strand (red). **(B)** The second round of PCR amplified the first round product and completed the amplification of the antisense strand and poly-T termination site. **(C)** The H1 shRNA expression cassette was ligated into pTZ57R/T between the *Eco*RI and *Bgl*II restriction sites.

the bacterial cultures using the High Pure Plasmid Isolation Kit (Roche, Germany) according to the manufacturer's instructions (Appendix A.8).

2.1.4 Orientation of H1 shRNA Expression Cassettes

The orientation of the individual H1 shRNA cassettes inserted into the multiple cloning site (MCS) of pTZ57R/T was determined using an *Eco*RI (Fermentas, MD, USA) restriction digestion in a final reaction volume of 20 µl containing 10 U *Eco*RI; 1700 ng pTZ57R/H1 shRNA and was carried out in 1× *Eco*RI buffer. The restriction digest reactions were incubated for one hour at 37°C. The DNA fragments from the digested clones were subjected to agarose gel electrophoresis. The clones were sequenced using automated cycle sequencing using the universal M13 forward (5'-GTA AAA CGA CGG CCA G-3') and reverse (5'-CAG GAA ACA GCT ATG AC-3') primers (Inqaba, Pretoria, RSA) (Appendix A.9). The chromatograms were analysed using FinchTV™ version 1.4.0 (Geospiza Inc. WA, USA).

2.2 Generation of an H1 Mock Expression Cassette

An H1 Mock expression cassette was designed as a control against the H1 shRNA expression cassettes. The H1 Mock reverse primer (5'-GAT CAA AAA ACG GAT CCG AGT GGT-3') was designed to contain only the termination signal. The oligonucleotide was synthesised using standard phosphoramidite chemistry (Inqaba, Pretoria, RSA) and prepared as previously described (Section 2.1.1). The PCR was prepared in a final reaction volume of 20 µl containing 500 ng H1 promoter template DNA; 15 pmol H1 forward primer; 15 pmol H1 Mock reverse primer and 2.5 µl MasterMix™ (Promega, WI, USA). The PCR cycle was performed as previously described (Section 2.1.1) and the size of the amplified DNA fragment verified using agarose gel electrophoresis. The DNA band was excised from the gel and purified using the MinElute™ Gel Extraction Kit. The H1

Mock expression cassette was inserted into the PCR cloning vector pTZ57R/T as described in Section 2.1.3. The successful insertion of the H1 Mock expression cassette into pTZ57/T was assessed by colony PCR. Briefly, ten colonies were selected and resuspended in 10 µl sterile water. The PCR was prepared in a final reaction volume of 20 µl containing 5 µl of the resuspended clone; 10 pmol M13 forward primer; 10 pmol H1 reverse primer and 12.5 µl MasterMix™ (Promega, WI, USA). The PCR was programmed to run with an initial denaturation at 94°C for 5 minutes with thirty cycles of standard PCR (denaturation at 94°C for 20 seconds; annealing at 57°C for 20 seconds and elongation at 72°C for 45 seconds) and a final elongation step at 72°C for two minutes and thirty seconds followed (Eppendorf Mastercycle Gradient, Germany). The size of the clones was verified by agarose gel electrophoresis. The selected clone was inoculated in 4 ml LB and incubated at 37°C overnight in a shaking incubator and the pDNA was purified from the bacterial cultures using a standard alkaline lysis plasmid isolation protocol (Appendix A.10).

2.3 tRNA^{Lys3} shRNA Expression Cassettes

2.3.1 Preparation of tRNA^{Lys3} shRNAs

The generation of the p901-1 plasmid has been previously described (45) Briefly, the tRNA^{Lys3}-*Nru*I promoter sequence was generated by PCR and cloned into pBluescript as a *Sal*I/*Hin*dIII fragment. The p901-1 tRNA^{Lys3} vector provides a backbone for the direct insertion of annealed shRNA encoding oligonucleotides between the *Nru*I restriction site within the tRNA^{Lys3} promoter sequence and the *Pst*I restriction site of pBluescript. The tRNA^{Lys3} shRNA oligonucleotides (Table 2.2) were designed to be complementary to each other and anneal as dsDNA with a 5' blunt end and a 3' overhang compatible with a *Pst*I created sticky end. Oligonucleotides were synthesised using standard phosphoramidite chemistry (IDT, IA, USA). Lyophilised oligonucleotides were resuspended to 100 µM

stocks and individually phosphorylated in a final reaction volume of 20 µl containing 200 pmol oligonucleotide; 1 mM ATP; 5 U T4 polynucleotide kinase (PNK) (Promega, WI, USA) and was carried out in 1× PNK buffer for one hour at 37°C. The complementary phosphorylated oligonucleotides were mixed to a final concentration of 5 µM and the PNK heat inactivated at 75°C for ten minutes. The heating block was removed from the chamber and cooled slowly allowing the oligonucleotides to anneal. The annealed oligonucleotides were diluted 25-fold (200 nM) and stored at -20°C until required.

2.3.2 Directional cloning of tRNA^{Lys3} shRNA expression sequences

The tRNA^{Lys3} shRNA sequences were inserted into p901-1 by directional cloning (Figure 2.2). The sequence of the p901-1 backbone was confirmed by a double restriction digest with *Dra*I and *Sal*I (Fermentas, MD, USA) in a final reaction volume of 20 µl containing 10 U *Dra*I; 10 U *Sal*I; ~1000 ng p901-1 and was carried out in 1× Buffer Tango for one hour at 37°C.

To clone the tRNA^{Lys3} shRNA sequences into the p901-1 vector, the vector was subjected to a double restriction digest with *Nru*I and *Pst*I (Fermentas, MD, USA) in a final reaction volume of 30 µl containing 10 U *Nru*I; 10 U *Pst*I; 2000 ng p901-1 and was carried out in 1× Buffer R at 37°C for two hours. The *Nru*I/*Pst*I digested plasmid was dephosphorylated using calf intestinal phosphatase (CIP) (New England Biolabs, UK) in a total reaction volume of 40 µl containing 10 U CIP and was carried out in 1× CIP buffer at 37°C for one hour. The reaction mix was incubated at 75°C in a dry heating block for ten minutes. The dephosphorylated p901-1 plasmid fragment was subjected agarose gel electrophoresis, excised and purified using the MinElute™ Gel Extraction Kit. The purity of the dephosphorylated p901-1 vector DNA was verified using agarose gel electrophoresis. The

DNA concentration (ng/µl) of dephosphorylated p901-1 was measured at 260 nm (NanoDrop ND-1000 Spectrophotometer, DE, USA).

The dephosphorylated backbone and annealed dsDNAs were ligated in a final reaction volume of 20 µl containing 50 ng dephosphorylated p901-1; 0.5 nM dsDNA ($tRNA^{Lys3}$ shRNA 5, 6, 8, 9 or 10); 7.5 U T4 DNA ligase and was carried out in 1× ligation buffer (Fermentas, MD, USA) at 16°C for 24 hours. Ligation mixtures were used to transform chemically competent *E. coli* (DH5-α cells). Transformed bacteria were plated onto LB agar plates containing ampicillin and incubated overnight at 37°C. Three colonies from each $tRNA^{Lys3}$ shRNA plate were picked, inoculated in 4 ml LB and incubated at 37°C overnight in a shaking incubator. The pDNA was purified from the bacterial cultures using the High Pure Plasmid Isolation Kit.

2.3.3 Confirmation of $tRNA^{Lys3}$ shRNA inserts

The p901-1 $tRNA^{Lys3}$ shRNA clones were subjected to a double restriction digest with *Bam*HI and *Xho*I (Fermentas, MD, USA) in a final reaction volume of 20 µl containing 10 U *Bam*HI; 10 U *Xho*I; ~1000 ng $tRNA^{Lys3}$ shRNA clones and was carried out in 1× Buffer O at 37°C for one hour. The insertion of the shRNA encoding sequences was detected using agarose gel electrophoresis. The clones were sequenced using automated cycle sequencing. The chromatograms were analysed using FinchTV™ version 1.4.0 and the sequences aligned using VectorNTI™ version 10.1.1 AlignX™ application.

Table 2.2: Oligonucleotides for the generation of tRNA^{Lys3} shRNA expression cassettes

shRNA	Primer	Sequence
tRNA^{Lys3}	F	5′ *GGCG*TCGTGTGCGCTTTGCTTCGCCTTTGTGTAG**GGTGAAGCGAAGTGCACACGG**TTTTTTGCA 3′
shRNA 5	R	5′ AAAAACCGTGTGCACTTCGCTTCACCCTACACAAAGGCGAAGCAAAGCGCACACGA*CGCC* 3′
tRNA^{Lys3}	F	5′ *GGCG*TACACCTCGCTTCACCTCTACTTTGTGTAG**GCAGAGGTGAAGCGAAGTGCA**TTTTTTGCA 3′
shRNA 6	R	5′ AAAAATGCACTTCGCTTCACCTCTGCCTACACAAAGTAGAGGTGAAGCGAGGTGTA*CGCC* 3′
tRNA^{Lys3}	F	5′ *GGCG*CAACGTCAACAACCAACCTTGTTTGTGTAG**CAAGGTCGGTCGTTGACATTG**TTTTTTGCA 3′
shRNA 8	R	5′ AAAAACAATGTCAACGACCGACCTTGCTACACAAACAAGGTTGGTTGTTGACGTTG*CGCC* 3′
tRNA^{Lys3}	F	5′ *GGCG*TAAGAAGCTGTAGGCACAAAT*A*TTGTGTAG**ATTTATGCCTACAGCCTCCTA**TTTTTTGCA 3′
shRNA 9	R	5′ AAAAATAGGAGGCTGTAGGCATAAATCTACACAA*T*ATTTGTGCCTACAGCTTCTTA*CGCC* 3′
tRNA^{Lys3}	F	5′ *GGCG*TTCGAGCCTCCGAGTTGTGCT*A*TTGTGTAG**GGCACAGCTTGGAGGCTTGAA**TTTTTTGCA 3′
shRNA 10	R	5′ AAAAATTCAAGCCTCCAAGCTGTGCCCTACACAA*T*AGCACAACTCGGAGGCTCGAA*CGCC* 3′

The sequence encoding the tRNA^{Lys3} acceptor arm sequence is italicised and the base wobbles within the sense strand are double-underlined. The loop is underlined and the A → T base change in shRNA 9 and shRNA 10 are underlined and italicised. The sequence encoding the antisense strand is indicated bold. (F) Forward; (R) Reverse.

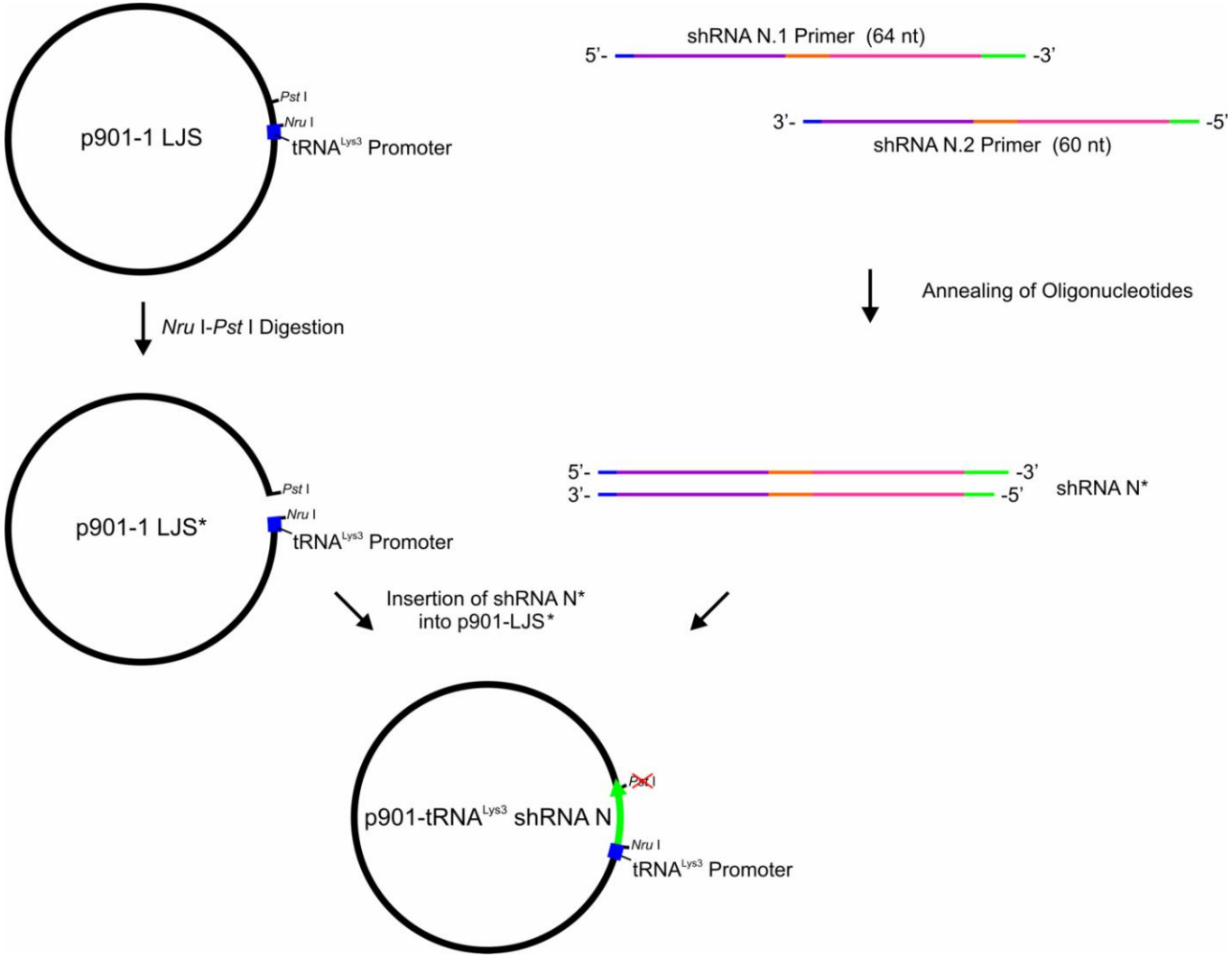


Figure 2.2: Insertion of shRNA encoding sequences into p901-1.

Two complementary oligonucleotides were annealed to create the shRNA encoding sequence, which was subsequently ligated into the digested p901-1 between the *Pst*I and *Nru*I restriction sites.

2.4 Generation of tRNA+1 mock expression cassette

The $tRNA^{Lys3}$ Mock expression cassette was designed to incorporate only the termination signal. The $tRNA^{Lys3}$ Mock forward (5'-GGC GTT TTT TCT GCA GCC CGG GGG ATC CAC TAG TTC TAG AGC-3') and $tRNA^{Lys3}$ Mock reverse (5'-GGC CGC TCT AGA ACT AGT GGA TCC CCC GGG CTG CAG AAA AAA CGC C-3') oligonucleotides were designed to be complementary to each other and anneal as dsDNA with a 5' blunt end and a 3' overhang compatible with a *Pst*I created sticky end. Oligonucleotides were synthesised using standard phosphoramidite chemistry (Inqaba, Pretoria, RSA) and prepared as described in Section 2.3.1. The $tRNA^{Lys3}$ Mock sequences were cloned into the p901-1 vector as previously described (Section 2.3.2). Ligation mixtures were used to transform chemically competent *E. coli* (DH5-α cells). Transformed bacteria were plated onto LB agar plates containing ampicillin and incubated overnight at 37°C. Four clones were inoculated in 4 ml LB and incubated at 37°C overnight in a shaking incubator and the pDNA was purified from the bacterial cultures using a standard alkaline lysis plasmid isolation protocol (Appendix A.10).

2.5 RNA Pol II-driven pri-miRNA-122 shuttles

The method employed for the generation of RNA Pol II-driven pri-miRNA-122/5, -122/6 and -122/10 has been previously described (15) and a description of the generation of pri-miRNA-122/8 and -122/9 shuttles is given below.

2.5.1 Construction of the pri-miRNA-122/8 and -122/9 shuttles

Primer sets (Table 2.3) were designed for the generation first of pre-miRNA sequences by primer extension followed by PCR amplification of these templates with additional primer sets to create the complete pri-miRNA shuttle sequences (Figure 2.3). The

oligonucleotides were synthesised by standard phosphoramidite chemistry (IDT, IA, USA) and prepared as previously described (Section 2.1.1). The forward and reverse primers for the second round of PCR were designed to anneal to the pre-miRNA shuttles at the site of the stem sequence, subsequently completing the construction of the pri-miRNA shuttles.

Primer extension was performed as a PCR in a final reaction volume of 25 µl containing 100 pmol pre-miRNA forward primer; 100 pmol pre-miRNA reverse primer; 4 mM dNTP mix; 0.75 U GoTaq® Polymerase; 0.5 nM $MgCl_2$ and was carried out in 1× GoTaq® Flexi Buffer using the GoTaq® Flexi DNA Polymerase Kit. The PCR thermal cycler was programmed to run with an initial denaturation at 94°C for 5 minutes, 24 cycles of standard PCR (denaturation at 94°C for 20 seconds; annealing at 57°C for 20 seconds and elongation at 72°C for 45 seconds) and a final elongation step at 72°C for 2 minutes and 30 seconds. The amplified DNA fragments were subjected to agarose gel electrophoresis, excised and purified using the MinElute™ Gel Extraction Kit. The purified primer extended product was used as the DNA template for the subsequent PCR reaction, to generate the complete pri-miRNA shuttles.

Table 2.3: The forward and reverse primers for the initial primer extension reaction required for the construction of pri-miRNA-122/8 and pri-miRNA-122/9

miRNA	Primer	Sequence
pre-miR-122/8	F	5′GAGTTTCCTTAGCAGAGCTGCTCAAGGTCGGTCGTTG**ACATTGGTCTAAACATAAATGT** 3′
	R	5′*GGATTGCCTAGCAGTAGCTA*CGAAAGGTCGTTCGTTG**ACATTTATGTTTAGACCAATGT** 3′
pre-miR-122/9	F	5′GAGTTTCCTTAGCAGAGCTGCAATTTATGCCTACAGC**CTCCTAGTCTAAACAAAAGGAG** 3′
	R	5′*GGATTGCCTAGCAGTAGCTA*CGGTTTATGCTTACAGC**CTCCTTTTGTTTAGACTAGGAG** 3′
pri-miR-122	F	5′GACTGCTAGCTGGAGGTGAAGTTAACACCTTCGTGGCTACAGAGTTTCCTTAGCAGAGCTG 3′
	R	5′GATCACTAGTAAAAAAGCAAACGATGCCAAGACATTTATCGAGGGAA*GGATTGCCTAGCAGTAGCTA* 3′

The complementary sequences of the pre-miRNA oligonucleotides for primer extension are underlined and in bold. The binding regions of pri-miRNA forward primer are underlined and are italicised for the reverse primer. (F) Forward; (R) Reverse.

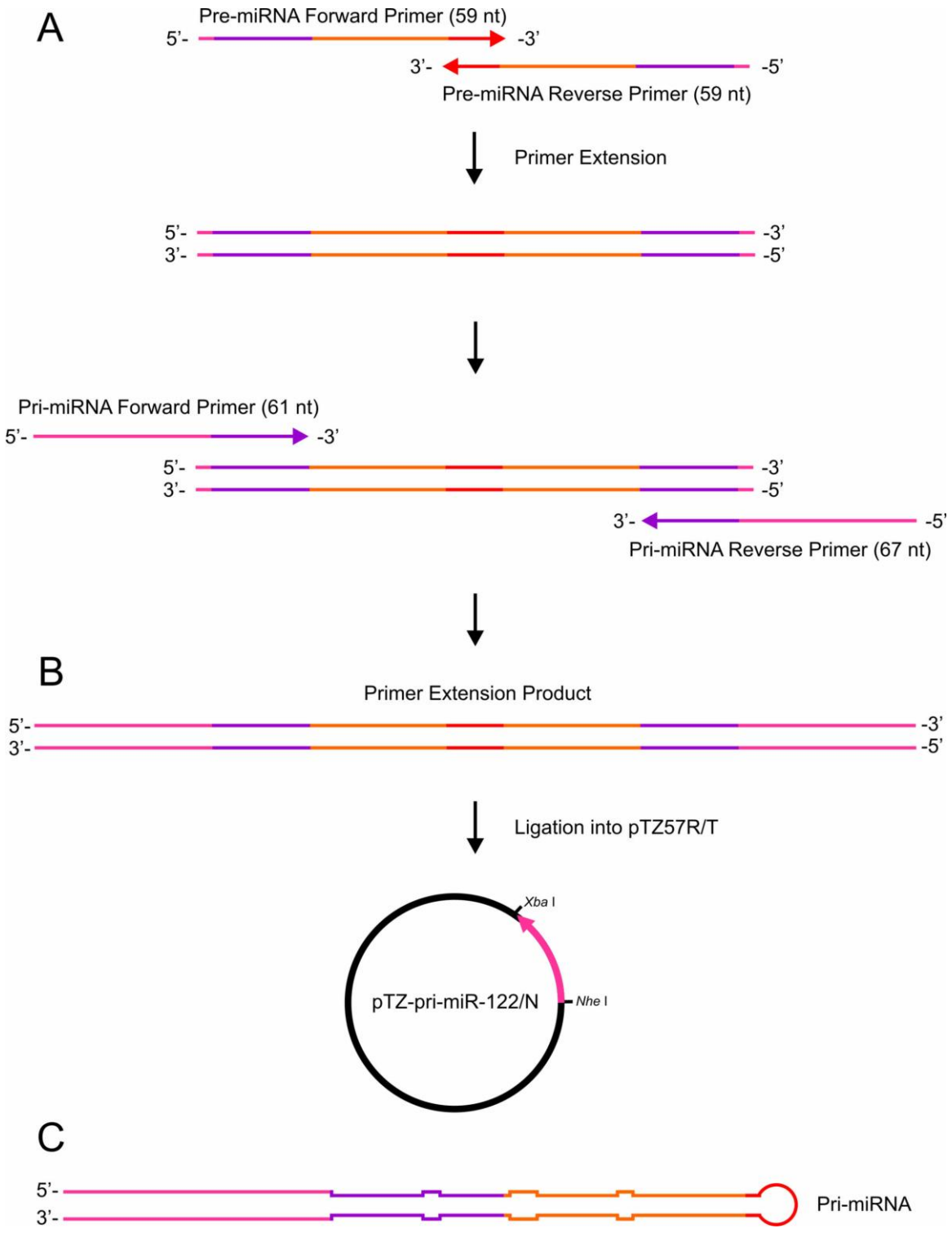


Figure 2.3: Construction of the pri-miRNA shuttles in pTZ57R/T.

(A) The pre-miRNAs were generated by primer extension PCR. **(B)** The pre-miRNAs were amplified, generating the pri-miRNAs. **(C)** The pri-miRNA primer extension was ligated into the cloning vector pTZ57R/T.

The PCR components were prepared in a final reaction volume of 25 µl containing 100 ng primer extended product; 10 pmol universal pri-miRNA-122 forward primer; 10 pmol universal pri-miRNA-122 reverse primer; 10 mM dNTP mix; 0.75 U GoTaq® Polymerase; 0.5 nM $MgCl_2$ and was carried out in 1× GoTaq® Flexi Buffer using the GoTaq® Flexi DNA Polymerase Kit. The thermal cycler was programmed as described above and putative bands corresponding to the completed pri-miRNA shuttle sequences were identified using agarose gel electrophoresis, excised and purified using the MinElute™ Gel Extraction Kit.

2.5.2 Cloning of the pri-miRNA-122 shuttles into pTZ57R/T

The pri-miRNA-122 shuttle sequences were inserted into the InsT/Aclone™ PCR cloning vector pTZ57R/T. Ligation reactions were prepared in a final reaction volume of 20 µl containing 300 ng pri-miRNA-122/8 or -122/9 PCR product; 0.165 µg pTZ57R/T; 7.5 U T4 DNA ligase and was carried out in 1× ligation buffer and ligated overnight at 16°C. The ligation mixtures were used to transform chemically competent *E. coli* (DH5-α cells). Transformed bacteria were plated onto LB agar plates containing ampicillin, X-gal and IPTG and incubated overnight at 37°C. Bacterial colonies containing the pTZ-pri-miRNA-122 plasmids were identified using blue/white screening. Five clones of each miRNA-122 shuttle were picked, inoculated in 4 ml LB and grown overnight in a shaking incubator. The pDNA was purified from the bacterial cultures using the High Pure Plasmid Isolation Kit.

2.5.3 Orientation of the pri-miRNA shuttles in pTZ57R/T

The orientation of the individual pri-miRNA shuttles inserted into the MCS of pTZ57R was determined by a double restriction digest with *Spe*I and *Nhe*I (Fermentas, MD, USA) in a final 20 µl reaction volume containing 5 U *Spe*I; 5 U *Nhe*I; 100 ng pTZ57R/miRNA-122/8

or -122/9 and was carried out in 1× Buffer Tango. The restriction digestions were incubated for one hour at 37°C. DNA fragments from the digested clones were subjected to agarose gel electrophoresis. Four pri-miRNA-122/8 clones and five pri-miRNA-122/9 clones were prepared for automated cycle sequencing using the ABI Big Dye Terminator Cycle Sequencing Kit (Applied Biosystems, CA, USA) according to the manufacturer's instructions (Appendix A.9.1). The chromatograms were analysed as previously described (Section 2.1.4).

2.5.4 Cloning of the pri-miRNA shuttles into pCI-neo

Sequences encoding the pri-miRNA shuttles were inserted into the mammalian expression vector pCI-neo (Promega, WI, USA) using directional cloning (Figure 2.4). The pCI-neo and the pTZ-pri-miRNA vectors were subjected to a double restriction digest with *Nhe*I and *Xba*I (Fermentas, MD, USA) in a final reaction volume of 30 µl containing 10 U *Nhe*I; 10 U *Xba*I; ~ 4000 ng pTZ-pri-miRNA or ~ 3000 ng pCI-neo and was carried out in 1× Buffer Tango at 37°C for two hours. The *Nhe*I/*Xba*I digested pCI-neo backbone was dephosphorylated by CIP in a total reaction volume of 40 µl containing 10 U CIP and was carried out in 1× CIP buffer at 37°C for one hour. The digestion reaction was incubated at 75°C in a dry heating block for ten minutes. The dephosphorylated pCI-neo backbone was subjected to agarose gel electrophoresis, the required bands excised and purified using the MinElute™ Gel Extraction Kit. The purity of the dephosphorylated pCI-neo vector DNA was verified using agarose gel electrophoresis. The DNA concentration (ng/µl) of dephosphorylated pCI-neo was measured at 260 nm.

The dephosphorylated backbone and pri-miRNA shuttles were ligated in a final reaction volume of 20 µl containing ~1000 ng dephosphorylated pCI-neo; 3000 ng pri-miRNA shuttle fragment; 7.5 U T4 DNA ligase and was carried out in 1× ligation buffer at 16°C for

24 hours. Ligation mixtures were used to transform chemically competent *E. coli* (XL1-Blue cells). Transformed bacteria were plated onto LB agar plates containing 100 µg/ml ampicillin and incubated overnight at 37°C. Colonies from each plate were picked, inoculated in 4 ml LB and incubated at 37°C overnight in a shaking incubator. The pCI-pri-miR-122/8 and -122/9 DNA was purified from the bacterial cultures using a standard alkaline lysis plasmid isolation protocol (Appendix A.10).

2.5.5 Confirmation of pri-miRNA inserts in pCI-neo

The pCI-neo-miRNA-122/8 and -122/9 clones were subjected to a double restriction digest with *Nhe*I and *Hin*dIII (Fermentas, MD, USA) in a final reaction volume of 20 µl containing 5 U *Nhe*I; 10 U *Hin*dIII; ~150 ng pCI-pri-miR-122/8 or -122/9 clones and was carried out in 1× Buffer Tango at 37°C for one hour. Insertion of the pri-miRNA shuttles was verified using agarose gel electrophoresis.

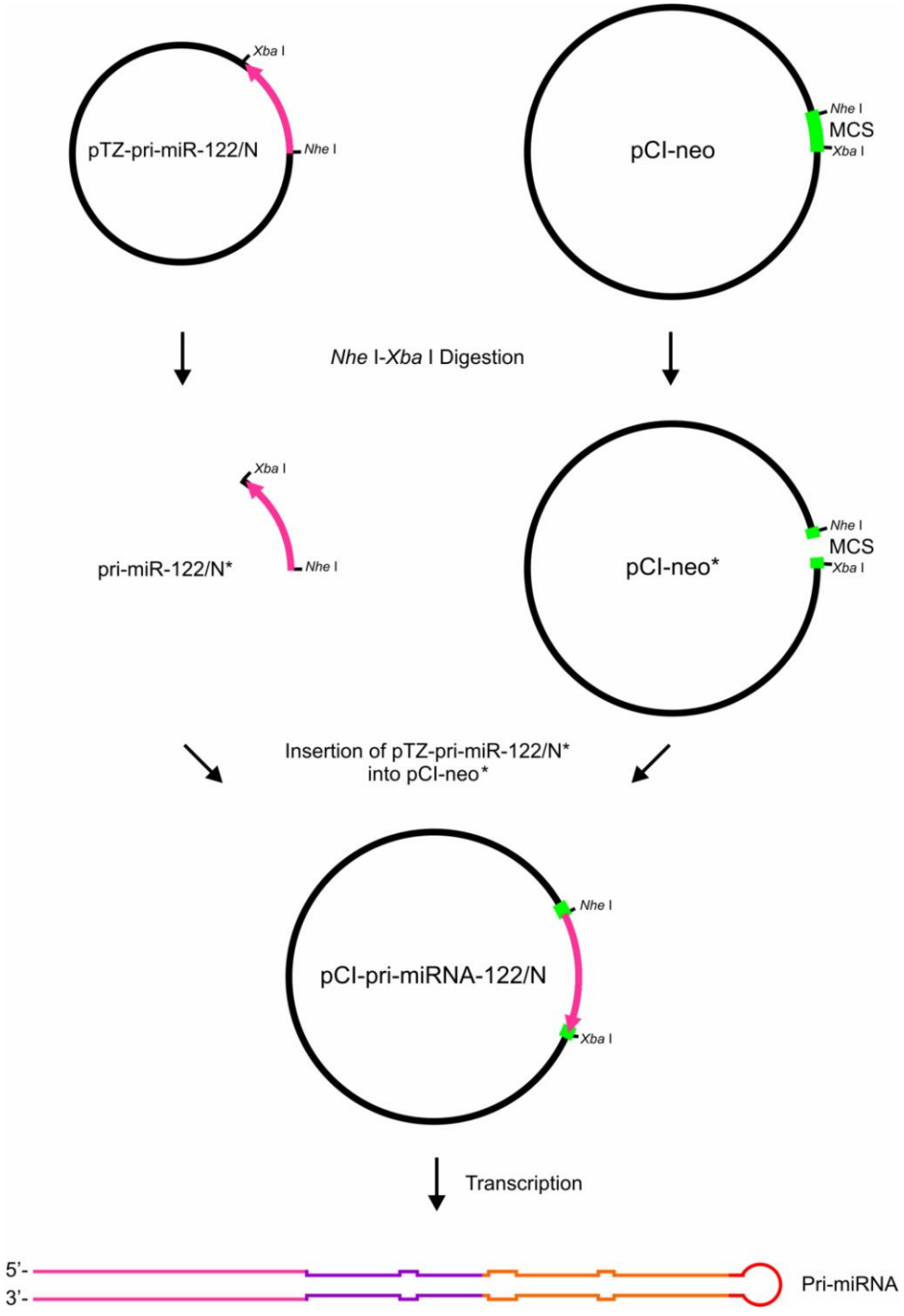


Figure 2.4: Ligation of the pri-miRNA shuttle sequence into pCI-neo.

pTZ-pri-miR-122/N and pCI-neo were digested separately with an NheI-XbaI double digest. The pri-miR-122/N* fragment was ligated into the MCS of pCI-neo* at the analogous restriction sites. The complete pri-miRNA shuttle sequences were generated following transcription.

2.6 Target Vectors

2.6.1 psiCHECK-HBx

psiCHECK-HBx (51) is a 6806 bp dual luciferase reporter plasmid with the *HBx* ORF inserted downstream of the Renilla *luciferase* ORF (Promega, WI, USA). *Renilla* luciferase expression is driven by the SV40 promoter. Additionally the plasmid also contains the *Firefly luciferase* gene, which is driven by an HSV-TK promoter. *Renilla* luciferase activity is therefore an indication of HBx expression and Firefly luciferase activity is an indicator of transfection efficiency. The ratio of *Renilla* to Firefly luciferase is measured to assess the efficacy of RNAi effecters targeting the *HBx* sequence.

2.6.2 pCH-9/3091

The generation of pCH-9/3091 has been previously described (39). pCH-9/3091 contains a greater than genome length HBV sequence under the transcriptional control of the CMV immediate early promoter-enhancer. This structure functionally mimics the circular nature of the HBV genome by allowing a greater than genome length pregenomic RNA and subsequently cccDNA to be generated thereby simulating HBV replication. pCH-9/3091 is useful in observing the inhibition of HBV replication by RNAi effecters *in vitro* and *in vivo*.

2.7 Cell Culture

Human hepatoma cells (Huh7) were maintained in Dulbecco's Modified Eagles Medium (DMEM) (BioWhittaker, MD, USA) supplemented with 10% foetal calf serum (FCS) (Invitrogen, CA, USA), penicillin (1000 U/ml), streptomycin (100 µg/ml) (Gibco BRL, United Kingdom) and ciprobay (100 µg/ml) (Highveld Biologicals, Johannesburg, RSA) in a humidified incubator at 37°C and 5% CO_2.

2.8 Transfection of Huh7 cells for Dual Luciferase Assay and HBsAg Assay

Prior to the day of transfection Huh7 cells were seeded at 40% confluency in Costar® 24-well plates (Corning, NY, USA) in DMEM supplemented with 10% FCS, which was replaced on the day of transfection. Transfections were carried out on cells at a confluency of ~70% with Lipofectamine 2000™ (Invitrogen, CA, USA) according to the manufacturer's instructions. Briefly, cells were transfected with 1 µg of total DNA constituted by combining 90 ng of a target vector (psiCHECK-HBx or pCH-9/3091), 0.9 to 900 ng of an effecter vector (U6 shRNA, H1 shRNA, $tRNA^{Lys3}$ shRNA or pri-miRNA-122 shuttle vectors), 10 ng of the green fluorescent protein (GFP) expression plasmid pCMV-GFP (44) and an empty vector (pTZ57R). The initial DNA concentrations (ng/µl) of the vectors were measured at 260 nm and the vectors required for the transfection were prepared in quadruplicate at the correct amounts. The plasmids were transferred to sterile 1.5 ml microcentrifuge tubes and mixed before adding Opti-MEM (Gibco BRL, United Kingdom) to a final volume of 50 µl. The DNA/Opti-MEM mixtures were mixed and incubated at room temperature for five minutes. The volume of Lipofectamine 2000™ (Invitrogen, CA, USA) required for the transfection was aliquoted and mixed with the required volume of Opti-MEM and incubated at room temperature for five minutes. Fifty microlitres of the Lipofectamine 2000™/Opti-MEM mix was added to 50 µl of the DNA/Opti-MEM mixes. The mixtures were incubated for 20 minutes at room temperature and 100 µl added per well in triplicate. The media was removed the following day and replaced with 500 µl of fresh DMEM supplemented with 10% FCS, penicillin (1000 U/ml), streptomycin (100 µg/ml) and ciprobay (100 µg/ml). Forty-eight hours post transfection the cells were viewed using at 456 nm using a confocal fluorescence microscope (Zeiss Axiovision 100, Germany) and assessed for GFP expression.

2.8.1 Assessing RNAi effecter knockdown efficacy of HBV targets

The ability of shRNAs and pri-miRNA shuttle sequences to inhibit the expression of target plasmid was assessed by transfecting Huh7 cells with 1 µg of total DNA with varying concentrations of RNAi effecter plasmid. Forty-eight hours post-transfection the cells were analysed for knockdown efficiency. Cells transfected with psiCHECK-HBx were analysed for luciferase activity using the Dual Luciferase Assay System (Promega, WI, USA) (Appendix A.11) and the Veritas™ Microplate Luminometer (Turner BioSystems, CA, USA). Growth medium from cells transfected with pCH-9/3091 was harvested and subjected to HBsAg ELISA using the MONOLISA® Ag HBs PLUS Kit (Bio-Rad, CA, USA) according to the manufacturer's instructions (Appendix A.12).

2.9 Transfection of Huh7 cells using Lipofectamine2000™ for total, nuclear and cytoplasmic RNA extraction

Prior to the day of transfection Huh7 cells were seeded at 40% confluency to 10 cm plates (TPP®, Switzerland) in DMEM supplemented with 10% FCS, which was replaced on the day of transfection. Transfections were carried out on cells at a confluency of ~80% with Lipofectamine 2000™ according to the manufacturer's instructions. Briefly, cells were transfected with 16 µg of total DNA constituted by 15 µg of either a Mock (pTZ57R) or an effecter vector (U6 shRNA, H1 shRNA, $tRNA^{Lys3}$ shRNA or pri-miRNA-122 shuttle vectors) and 1 µg pCMV-GFP. The initial DNA concentrations (ng/µl) of the vectors were measured at 260 nm. The plasmids were aliquoted into sterile 1.5 ml microcentrifuge tubes and mixed before adding Opti-MEM to a final volume of 500 µl. The DNA/Opti-MEM solutions were mixed and incubated at room temperature for five minutes. The volume of Lipofectamine 2000™ required for the transfection was added to the required volume of Opti-MEM and incubated at room temperature for five minutes. Five hundred and fifteen microlitres of the Lipofectamine 2000™/Opti-MEM mix was added to 500 µl of the

DNA/Opti-MEM mixes. The solutions were mixed by vortexing, incubated for 20 minutes at room temperature and 1000 µl added per plate. The media was removed the following day and replaced with 10 ml of fresh DMEM supplemented with 10% FCS, penicillin (1000 U/ml), streptomycin (100 µg/ml) and ciprobay (100 µg/ml). Forty-eight hours post transfection the cells were viewed at 456 nm (Zeiss Axiovision 100, Germany) and assessed for GFP expression.

2.10 Transfection of Huh7 cells using Calcium Chloride for total, nuclear and cytoplasmic RNA extraction

Prior to the day of transfection Huh7 cells were seeded at 40% confluency into 10 cm plates (TPP®, Switzerland) in DMEM supplemented with 10% FCS, which was replaced 4 hours prior to the transfection. Transfections were carried out on cells at a confluency of ~80%. Briefly, cells were transfected with 16µg of total DNA constituted by combining 15 µg of either a Mock (U6+1; H1 Mock; $tRNA^{Lys3}$ Mock or pCI-neo) or an effecter vector (U6 shRNA, H1 shRNA, $tRNA^{Lys3}$ shRNA or pri-miRNA-122 shuttle vectors) and 1 µg pCMV-GFP. The initial DNA concentrations (ng/µl) of the vectors were measured at 260 nm. Five hundred microlitres of nuclease free sterile water was aliquoted into a sterile 15 ml Falcon tube and the DNA was added. Five hundred microlitres of 2.5 M $CaCl_2$ (Appendix A.13) was added to the water/DNA mix and the sample vortexed for 5 seconds. In a separate sterile 15 ml Falcon tube, 1 ml of 2× HEPES buffer (Appendix A.14) was added and the tube vortexed whilst the DNA/$CaCl_2$ solution was added drop wise. The mixture was vortexed for 5 seconds to ensure thorough mixing before being incubated for 20 minutes at room temperature. One thousand microlitres was added drop wise to the cells whilst the plates were swirled continuously. The media was removed the following day and replaced with 10 ml of fresh DMEM supplemented with 10% FCS. Forty-eight hours post

transfection the cells were viewed at 456 nm (Zeiss Axiovision 100, Germany) and assessed for GFP expression.

2.11 Total RNA Extraction for Northern Blot Hybridisation

Forty-eight hours post transfection, the medium was removed and 1 ml of Tri® Reagent (Sigma, MO, USA) was added to the dish to lyse the cells. The lysate was pipetted several times and incubated at room temperature for five minutes before being transferred into a sterile 1.7 ml microcentrifuge tube. Two hundred microlitres of chloroform was added and the samples shaken vigorously for 15 seconds. The samples were incubated at room temperature for 2 minutes before being centrifuged at 12 000 × g for 15 minutes at 4°C. The aqueous phase containing the RNA (~500 µl) was removed and transferred to a sterile 1.7 ml microcentrifuge tube and mixed with 500 µl of isopropanol. The samples were stored overnight at -70°C. The following day, the samples were centrifuged at 12 000 × g for 30 minutes at 4°C to precipitate the RNA. The supernatant was removed and 500 µl of 70% ethanol (v/v) added to the RNA pellet. The samples were centrifuged at 8 000 × g for 5 minutes at 4°C. The supernatant was aspirated and the pellet was air-dried. The pellet was resuspended in 100 µl nuclease free water and the RNA stored at -70°C.

2.12 Nuclear and Cytoplasmic Fractionation

Three alternative methods (Appendix A.15; Appendix A.16 and Appendix A.17) were applied to fractionate transfected Huh7 cells before using the PARIS™ kit (Ambion, USA) according to the manufacturer's instructions. Briefly, Huh7 cells were cultured and co-transfected as described previously (Section 2.9 and Section 2.10). Forty-eight hours post transfection the medium was removed and the cells were washed three times with ice-cold saline-EDTA. The cells were trypsinised in 1 ml of 1× trypsin. Three milliliters of DMEM

was added to neutralise the trypsin. The cells were transferred to a sterile 15 ml Falcon tube and centrifuged at 120 × g for five minutes at 4°C. The supernatant was aspirated and the cells resuspended in one milliliter of ice cold saline and centrifuged at 120 × g for five minutes at 4°C. Cell pellets were gently resuspended in 300 µl ice-cold Cell Fractionation Buffer and incubated on ice for five minutes. The samples were centrifuged at 500 × g for 2 minutes at 4°C. The supernatant (cytoplasmic fraction) was aspirated and transferred into a sterile microcentrifuge tube and stored on ice. Three hundred microlitres ice cold Cell Fractionation Buffer was added to the pellet (nuclear fraction) before being centrifuged at 500 × g for one minute at 4°C. The supernatant was removed and 300 µl Cell Disruption Buffer was added to the pellet. The mixture was pipetted vigorously to lyse the nuclei. Initially, RNA was extracted from the lysates using the PARIS™ kit (Appendix A.18) however the yield was insufficient, thus the RNA was extracted from the nuclear and cytoplasmic fractions as described in Section 2.11.

2.13 DAPI Staining of Nucleic Acids

Ten microlitres of the nuclear and cytoplasmic lysates were pipetted onto the centre of clean microscopic slides. Five hundred microlitres of a gluteraldehyde (1% v/v) and formaldehyde (0.5% v/v) fixative was added to the nuclear fraction. A cover slip was placed over the mixture and the microscope slide incubated at room temperature for 20 minutes. The slide was rinsed in 1× phosphate buffered saline (PBS) and blotted gently on paper towel. Three hundred microlitres of the DAPI stain (300 nM) (Molecular Probes, CA, USA) was aliquoted onto the centre of the slide. The slide was incubated at room temperature for five minutes, before being rinsed in 1× PBS and gently blotted on paper towel. A drop of mounting fluid was placed on the centre of the slide and a clean cover slip gently lowered on top. The slide was incubated at room temperature for 24 hours to allow the mounting solution to solidify. The nuclear fractions were viewed using confocal

fluorescence microscopy at 365 nm (Zeiss Axiovision 100, Germany) and the stained nuclei were identified by their blue fluorescence.

2.14 Northern Blot Hybridisation

Thirty micrograms of RNA extracted from transfected cells was subjected to polyacrylamide gel electrophoresis (PAGE) on a 15% polyacrylamide gel (Appendix A.19). The RNA was transferred to a piece of positively charged nylon membrane (Hybond-N+, GE Healthcare, NJ, USA) that had been cut to the size of the gel. Thereafter the RNA on the membranes was cross-linked using ultraviolet (UV) radiation at 200 J/cm^2 followed by incubation at 80°C for one hour. The membrane was pre-hybridised in 10 ml of Rapid-hyb™ Buffer (GE Healthcare, NJ, USA) at 42°C for 20 minutes. An oligonucleotide probe against the guide strand of the processed shRNA 5 and pri-miRNA-122/5 (Table 2.4) was synthesised using standard phosphromadite chemistry (Inqaba, Pretoria, RSA). Lyophilised oligonucleotides were resuspended to 100 µM and working stocks of 10 µM prepared. The probe was radioactively labelled using ^{32}P (Appendix A.20), added to the membrane and incubated overnight in a rotating oven at 42°C. The membrane was subjected to an initial low stringency wash at 25°C for 20 minutes with 5× SSC (Appendix A.21) and 0.1% (w/v) sodium dodecyl sulphate (SDS). Thereafter, the membrane was washed twice at 42°C for 15 minutes (1× SSC; 0.1% SDS) and subjected to either autoradiography or phosphor imaging using the FLA-7000 (Fujifilm, Tokyo, Japan). The membrane was stripped (1% SDS) at 80°C for 30 minutes and probed for either U6 snRNA or tRNA (Table 2.4).

Table 2.4: Sequences of probes used in Northern Blot Hybridisation

Probe	Sequence
shRNA 5	5′CCGTGTGCACTTCGCTTC 3′
U6 snRNA	5′TAGTATATGTGCTGCCGAAGCGAGCA 3′
tRNA	5′GGACCCTCAGATTAAAAGTCTGATGCTC 3′

2.15 *In vivo* Analysis of Effecter Sequences Targeted to *HBx*

Eight groups of five mice each were hydrodynamically injected via the tail vein. Injection solutions were prepared containing 5 µg of the target vector pCH-9/3091, 5 µg of an effecter vector (U6 shRNA 5, H1 shRNA 5, $tRNA^{Lys3}$ shRNA 5 or pri-miRNA-122/5 shuttle) or Mock (U6 +1, H1 Mock, $tRNA^{Lys3}$ Mock or pCI-neo) and 5 µg of psiCHECK-2.2. A volume of saline (containing the DNA) equivalent to 10% of the mouse's body weight was injected into the tail vein over a short period of time (approximately 10 seconds). The mice were bled retro-orbitally on day three and day five post injection. The mice were sacrificed on day five and the livers harvested for further analysis. All experiments carried out on mice were in accordance with protocols approved by the University of the Witwatersrand Animal Ethics Screening Committee (Appendix B).

2.15.1 HBsAg Assay using ELISA

Twenty five microlitres of serum was diluted with seventy five microlitres of normal saline and subjected to HBsAg ELISA using the MONOLISA® Ag HBs PLUS Kit (Bio-Rad, CA, USA) according to the manufacturer's instructions (Appendix A.12).

2.15.2 Nucleic Acid Isolation of HBV DNA from Mouse Serum

Total nucleic acids were isolated from mouse serum using the MagNA Pure LC Total Nucleic Acid Isolation Kit (Roche, Germany) and the MagNA Pure Instrument (Roche, Germany) according to the manufacturer's instructions.

2.15.3 Extraction of Genomic DNA (gDNA) from Homogenised Liver

The harvested mouse livers were weighed and an equal volume of phosphate buffered saline (PBS) added. The livers were homogenised using a CAT X120 homogeniser at 30 000 rpm. Briefly, 100 mg of homogenised mouse liver was transferred into a sterile 15 ml Falcon tube and 1.2 ml digestion buffer (100 mM NaCl; 10 mM Tris-Cl pH 8.0; 25 mM EDTA pH 8.0; 0.5% SDS and 0,1 mg/ml Proteinase K) was added. The samples were incubated for 18 hours in a shaking water bath at 50°C. An equal volume of phenol:chloroform:isoamyl alcohol (25:24:1) was added to the digested liver solution. The tubes were gently agitated to ensure thorough mixing and centrifuged at 1700 × g for ten minutes at 4°C. One millilitre of the aqueous layer containing the genomic DNA (gDNA) was aspirated and transferred into a sterile 15 ml Falcon tube. Five hundred microlitres of ammonium acetate (7.5 M) was added and the tubes gently agitated. Two milliliters of absolute ethanol was added and the samples were stored overnight at -20°C. The following day the samples were centrifuged at 1700 × g for two minutes at 4°C to pellet the gDNA. The supernatant was aspirated and 1 ml of 70% ethanol (v/v) was added to the gDNA pellet. The samples were centrifuged at 1700 × g for two minutes at 4°C. The supernatant was aspirated and the pellet air-dried. The pellet was resuspended in 100 µl nuclease free water and stored at -20°C. The concentration of the gDNA was determined by measuring optical absorbance at 260 nm and working stocks of 100 ng/µl prepared.

2.15.4 Quantitative Real-time PCR (qRT-PCR) for the detection of rcDNA and cccDNA

The total amounts of circulating viral particles in the serum and liver were assessed by real-time quantitative PCR (qPCR) using the LightCycler® FastStart DNA Master^{PLUS} SYBR Green I kit (Roche, Germany) according to the manufacturer's instructions (Appendix A.22). Total amounts of HBV DNA, cccDNA and rcDNA within the harvested livers were measured using an in house assay (2). Total HBV was measured using the HBV rc/cccDNA primer sets which amplify the *pre*S1 region and cccDNA was detected using the cccDNA primer sets which were designed to flank the direct repeats (Table 2.5). Efficacy of DNA delivery to the liver was detected by the Rluc primer sets (Table 2.5), which amplify the Renilla *luciferase* sequence of psiCHECK 2.2.

Table 2.5: Primer sets used in real-time quantitative PCR

Quantification	Primer	Sequence
HBV rc-DNA	F	5′TTATTATCCAGAACATGTAGTTAATCATTACTTCC3′
	R	5′TTGATGGGATTGAAGTCCCAATCTGGATT 3′
HBV ccc-DNA	F	5′TTCTCATCTGCCGGTCCGTGT 3′
	R	5′TGGGACATGTACAAGAGATGATTAGGC 3′
Rluc	F	5′AAATCATCTTTGTGGGCCACGACTGG 3′
	R	5′GAACTCCTCAGGCTCCAGTTTCCGCAT3′

2.16 Statistical Analysis

All data was analysed using the software package GraphPad Prism® version 4.0 (GraphPad Software Inc.). All *in vitro* data were expressed as the mean ± the normalised standard deviation of the mean and the statistical differences of triplicate data determined using the two-tailed unpaired student t-test with a confidence interval (CI) of 95%.

In vivo HBsAg data were expressed as the mean ± the standard deviation of the mean and the statistical differences of data determined using the two-tailed unpaired student t-test with a confidence interval (CI) of 95%.

In vivo qPCR serum data were expressed as the mean ± the normalised standard deviation of the mean and the statistical differences of data determined using the two-tailed unpaired student t-test with a confidence interval (CI) of 95%.

In vivo qPCR liver data expressed as the mean ± the normalised standard deviation of the mean and the statistical differences of triplicate data determined using the two-tailed unpaired student t-test with a confidence interval (CI) of 95%.

3 RESULTS

3.1 Design and Generation of H1 shRNA expression cassettes

The H1 shRNA expression cassettes were designed to contain the anti-HBV effecter sequences as described by Carmona *et al* (5). The shRNAs comprised a 25 base pair (bp) anti-guide strand, a 10 bp loop, a 25 bp guide strand, which was homologous to the HBx target and a 6 bp termination site (Figure 3.1). The complete H1 shRNA expression cassettes were verified to be ~317 nucleotides (Appendix C.1). The sequences of the H1 shRNA expression cassettes were assessed and hairpin structures found to have a 100% homology to the predicted structures (Appendix C.2 to C5). A G→A base change was identified in the H1 promoter region at ~ 152 nt for all shRNA expression cassettes, however this had no influence on the transcriptional activity of the H1 promoter as demonstrated by the data observed in the investigation.

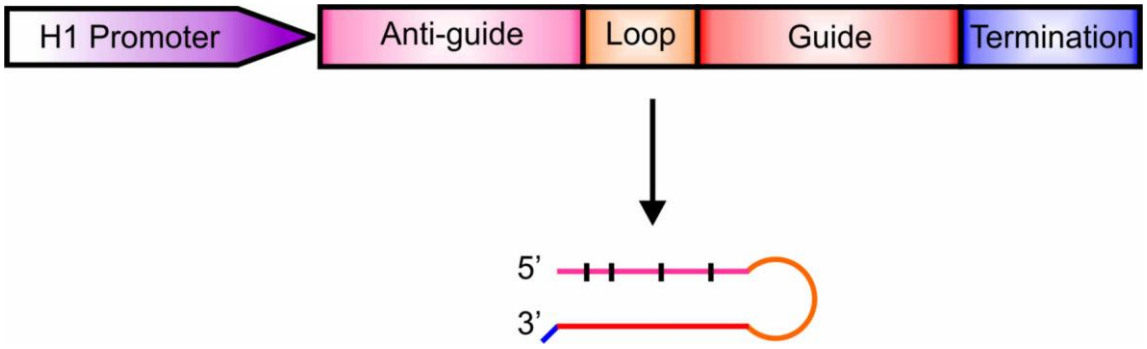


Figure 3.1: H1 shRNA expression cassette structure.
Driven by the RNA Pol III promoter H1, the shRNA expression cassettes were designed to be 66 nucleotides in length. The 25 bp anti-guide strand contained four G-U or C-A mismatches (black). The 10 bp loop was identical for all the shRNA expression cassettes. The 25 bp guide strand was complementary to the HBx target. (Diagram not to scale).

3.2 Design and Generation of the $tRNA^{Lys3}$ shRNA expression cassettes

The $tRNA^{Lys3}$ shRNA expression cassettes were comprised of a 21 bp anti-guide strand, a 9 bp loop, a 21 bp guide strand and a 6 bp termination site (Figure 3.2). The guide and anti-guide were designed to contain the anti-HBV sequences as described by Carmona *et al* (5).The shRNAs sequences were shortened by four nucleotides at the 3' and 5' end respectively. The 9 bp loop (5' TTT GTG TAG 3') was common to $tRNA^{Lys3}$ shRNA 5, shRNA 6 and shRNA 8. The five nucleotides preceding the loop structure of $tRNA^{Lys3}$ shRNA 9 and shRNA 10 (TTTTT) could cause early transcriptional termination (Appendix C.6). A single T→A nucleotide change in the first position of the loop (5' ATT GTG TAG 3') was incorporated as a preventative measure against early transcriptional termination. The sequences of the $tRNA^{Lys3}$ shRNA expression cassettes were assessed and the hairpin structures found to have 100% homology to the predicted structures (Appendix C.6 to C.11). A single base change (T136A) was observed within the $tRNA^{Lys3}$ promoter. The efficacy of the investigation demonstrated that this base change had no effect on the transcriptional capabilities of the promoter.

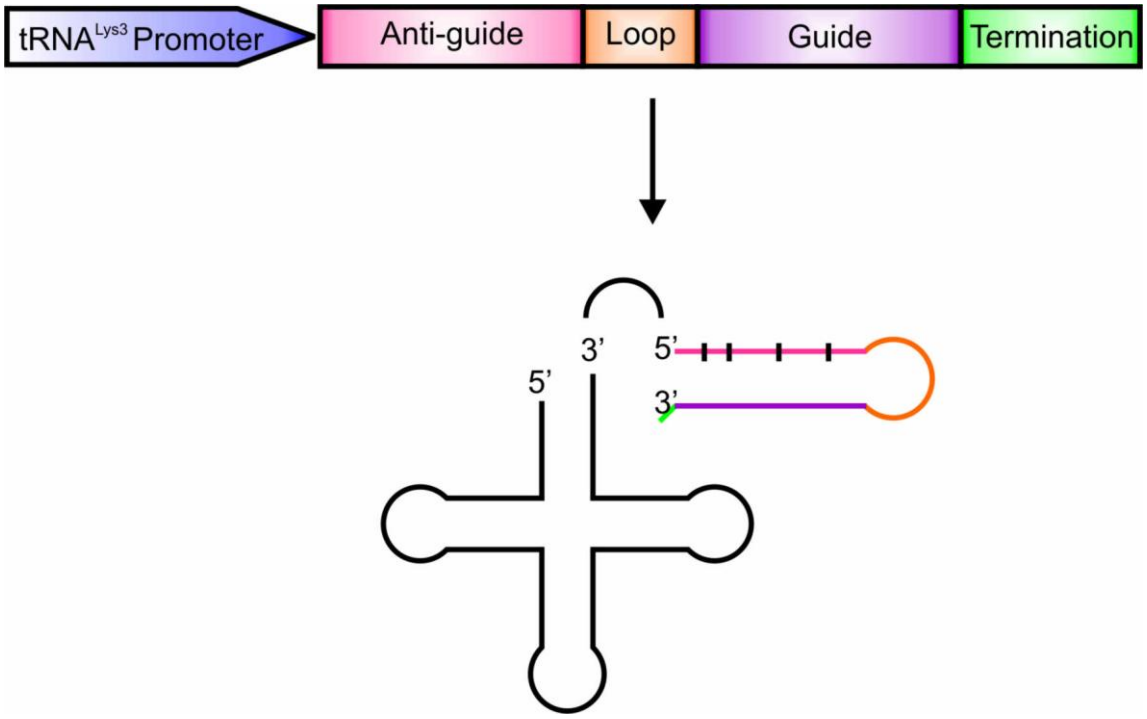


Figure 3.2: Schematic representation of the tRNA^{Lys3} shRNA expression cassettes.
The shRNA expression cassettes were designed with 21 bp anti-guide and guide strand. The anti-guide contained 4 G-U or C-A mismatches. The 9 bp loop was altered slightly for shRNA 9 and shRNA 10. The tRNA^{Lys3} promoter starts transcription within the promoter structure, thus the shRNA expression cassette will be transcribed onto the 3' GGCG acceptor arm. (Diagram not to scale).

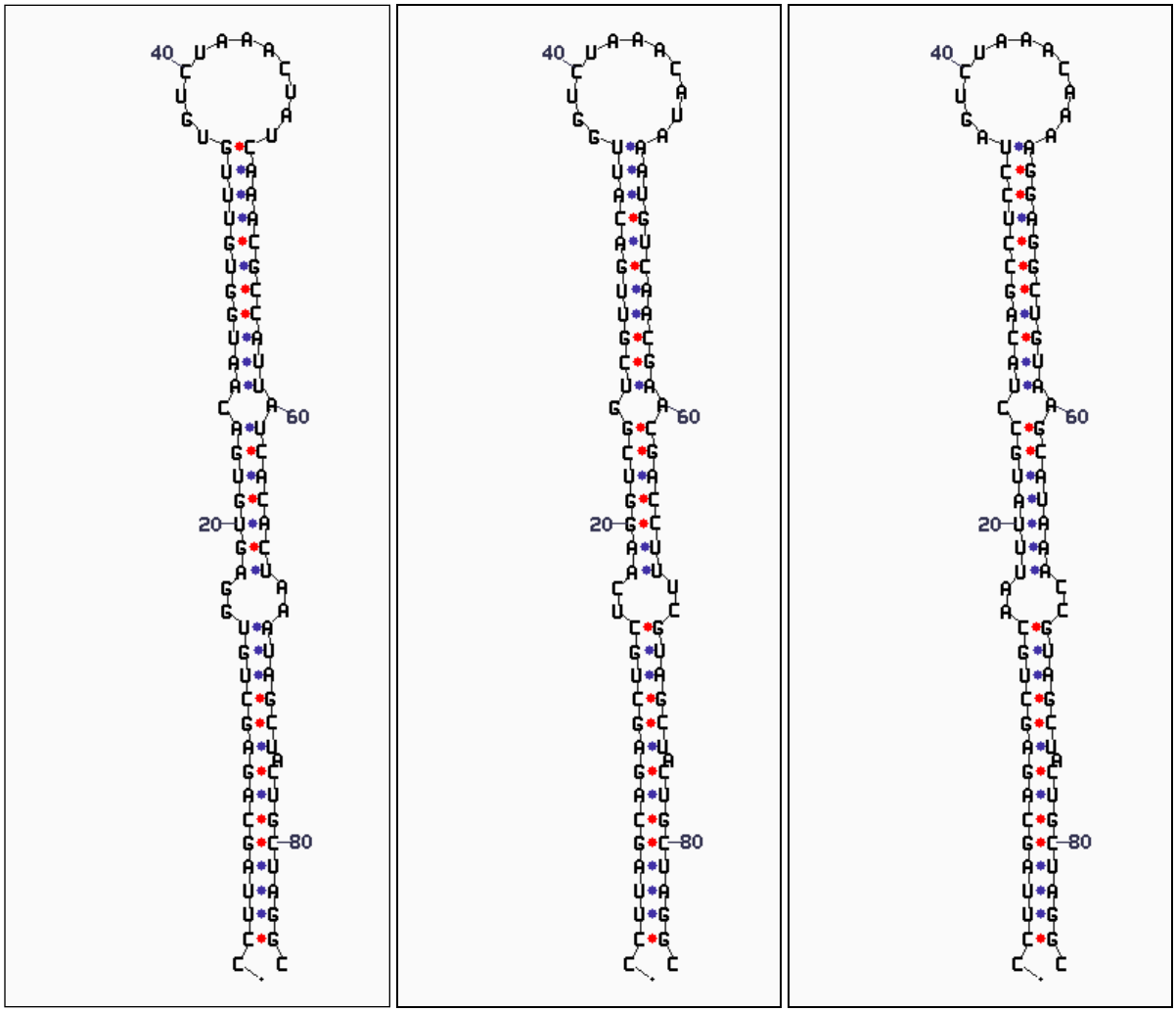
3.3 Design and Generation of pri-miRNA-122/8 and pri-miRNA-122/9 shuttles

The pri-miRNA-122/8 and pri-miRNA-122/9 shuttles were designed as described by Ely *et al* (15). The natural guide and complementary strand of pre-miRNA-122 wild type (wt) were replaced with the anti-HBV anti-guide and guide sequence of shRNA 8 and shRNA 9 as previously described designed (5) (Figure 3.3). The design of the pri-miRNA shuttles was assessed using the M-fold secondary folding structure programme. No significant difference was observed between the folding of the pri-miRNA-122/8 and pri-miRNA-122/9 shuttles when compared to the pri-miRNA-122/wt (Figure 3.4).



Figure 3.3: Design of pri-miRNA-122/8 and pri-miRNA-122/9 shuttles.

The pri-miRNA shuttles were designed to be structurally identical to the pri-miRNA-122/wt. The pre-miRNA-122/wt guide and anti-guide sequences were replaced with the guide sequence (purple) complementary to the *HBx* target. The anti-guide sequence (blue) and guide sequence indicate the processed pre-miRNA construct. Figure adapted from Ely *et al* (15).



Pri-miRNA-122/wt Pri-miRNA-122/8 Pri-miRNA-122/9

Figure 3.4: M-fold predictions of pri-miRNA-122/8 and pri-miRNA-122/9 shuttles.

There were no observed differences in the predicted secondary structure folding of the pri-miRNA-122/8 and pri-miRNA-122/9 effecter sequences when compared to pri-miRNA-122/wt. The ΔG values for pri-miRNA-122/8 and pri-miRNA-122/9 were ΔG=-47.6 and ΔG=-48.7 respectively. These values correspond to the pri-miRNA-122/wt (ΔG=-45.9) illustrating structural similarity of secondary folding.

3.4 GFP expression as a indicator of transfection efficacy

To assess the efficacy of DNA delivery, Huh7 cells were transfected with a eGFP-expressing plasmid and analysed for expression of the reporter gene. Figure 3.5 illustrates the consistency of expressed GFP confirming transfection efficacy and consistent delivery of DNA between Mock and U6 shRNA transfected cells. Consistent expression of GFP was observed over all *in vitro* transfections.

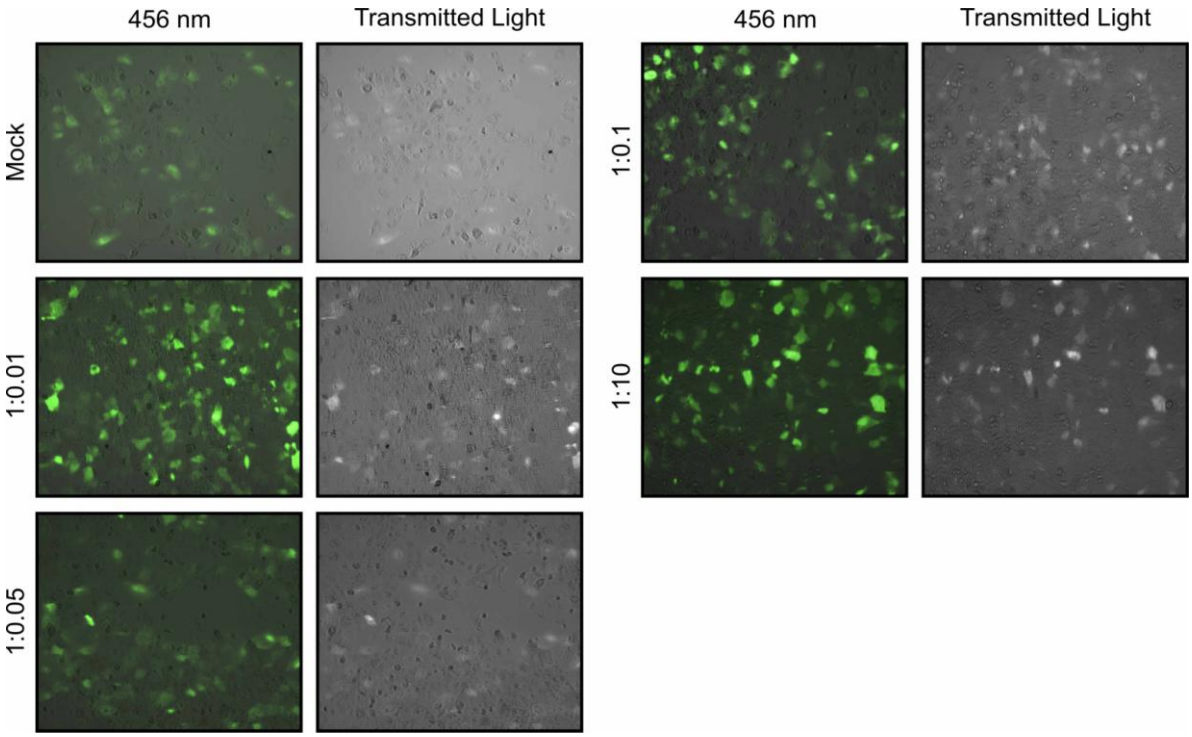


Figure 3.5: A representation of GFP expression in Huh7 cells as a measure of transfection efficacy.

Huh7 cells were co-transfected with RNA Pol III- or Pol-II expression cassettes at varying target to effecter ratios or a comparative Mock and the GFP expression vector pCMV-GFP. The morphology of the cells was assessed under transmitted light and the efficacy of GFP expression at 456 nm. The efficacy of transfection and delivery of DNA were consistent for these Huh7 cells transfected with U6 shRNA 9.

3.5. The efficacy of RNA Pol III and RNA Pol II transcribed effecter sequences to target *HB*x for knockdown

Previously, a panel of ten U6 shRNA expression cassettes was constructed to target highly conserved sites within the *HBx* sequence (5). Primary findings established four shRNA expression cassettes, which were particularly efficacious in targeting and inhibiting replicating HBV. U6 shRNA 5 and U6 shRNA 6 caused knockdown of between 80 and 95% in comparison to Mock treated cells, whilst U6 shRNA 8 and U6 shRNA 9 caused knockdown of between 80 – 85%. A fifth shRNA expression cassette, U6 shRNA 10, failed to knockdown the target. These five shRNAs were selected to investigate whether two different RNA Pol III promoters, H1 and $tRNA^{Lys3}$, could actively transcribe these shRNAs and target HBV as effectively as the U6 promoter-driven shRNAs.

To assess whether the H1 and $tRNA^{Lys3}$ shRNA expression cassettes were capable of *HBx* target knockdown, a co-transfection assay was performed. Huh7 cells were transfected with the shRNA expression cassettes and the target vector psiCHECK HBx at an effecter to target ratio of 10:1. The efficacy of the effecter sequences to knockdown the *HBx* target was measured by comparing the ratio of *Renilla* to Firefly luciferase activity. In comparison to Mock treated cells, H1 shRNA 5 caused knockdown of ~ 92% whilst $tRNA^{Lys3}$ shRNA 5 caused knockdown of ~ 90%. H1 shRNA 10 and $tRNA^{Lys3}$ shRNA 10 failed to knockdown the *HBx* target (data not shown). These data correlate with previous findings (5).

After establishing the RNA Pol III promoter-driven shRNA expression cassettes were capable of knocking down the *HBx* target*,* it was decided to compare the efficacies of these three different RNA Pol III promoter-driven shRNA expression cassettes to an RNA Pol II promoter-driven pri-miRNA shuttle. Five target to effecter ratios were chosen

(1:0.0025; 1:0.01; 1:0.05; 1:0.1 and 1:10) and the efficacy of *HBx* target knockdown assessed. All data were normalised to a comparative mock (n=3).

3.5.1 Effective *HBx* target knockdown by Pol II- and Pol III-driven effecter sequences 5 and 6

The shRNA 5 expression cassettes revealed a trend in knockdown with the most effective knockdown achieved at the highest RNAi effecter to target plasmid ratios (Figure 3.6). The U6, H1 and $tRNA^{Lys3}$ shRNA 5 expression cassettes caused knockdown of between 88% - 90% at a ratio of 1:10 and 80 - 88% at a ratio of 1:0.1, which was significantly different when compared to Mock transfected cells ($p<0.05$). Furthermore, significant target knockdown was observed at 1:0.05, 1:0.01 and 1:0.0025 (Appendix C.1). Taken together, these data indicate that even following a decrease of 100 fold in effecter ratio (1:10 to 1:0.1) the expressed effecter sequences are capable of substantial knockdown, and at a decrease of 200 fold (1:10 to 1:0.05), target knockdown is still greater than 60%.

At 1:10, pri-miRNA-122/5 caused significant target knockdown of ~88%, which decreased two-fold at 1:0.1 (Figure 3.6). Pri-miRNA-122/5 was incapable of significant knockdown at decreased effecter ratios (Appendix C.1). These data suggest the efficacy of the RNA Pol III shRNA 5 expression cassettes to target *HBx* is greater than the RNA Pol II pri-miRNA shuttle.

U6 shRNA 6 and H1 shRNA 6 showed a similar trend in knockdown to that observed for the RNA Pol III-promoter driven shRNA expression cassettes (Figure 3.6). U6 shRNA 6 and H1 shRNA 6 caused knockdown of ~90% at a ratio of 1:10 and between 85% - 90% at 1:0.1, which was significantly different when compared to Mock transfected cells ($p<0.05$). Furthermore, significant knockdown was observed for U6 shRNA 6 and H1 shRNA 6 at

1:0.05, 1:0.01 and at 1:0.0025 for U6 shRNA 6 (Figure 3.7). Taken together these data indicate a correlation in knockdown to U6 shRNA 5 and H1 shRNA 5.

The efficacy of target knockdown by $tRNA^{Lys3}$ shRNA 6 and pri-miRNA-122/6 was substantially reduced in comparison to U6 and H1 shRNA 6. In comparison to Mock transfected cells, $tRNA^{Lys3}$ shRNA 6 and pri-miRNA-122/6 were capable of significantly knocking down the *HBx* target by ~60% at 1:10 ($p>0.05$). At 1:0.01, target knockdown was no longer significant for $tRNA^{Lys3}$ shRNA 6 and pri-miRNA-122/6 (Figure 3.7) (Appendix C.2).

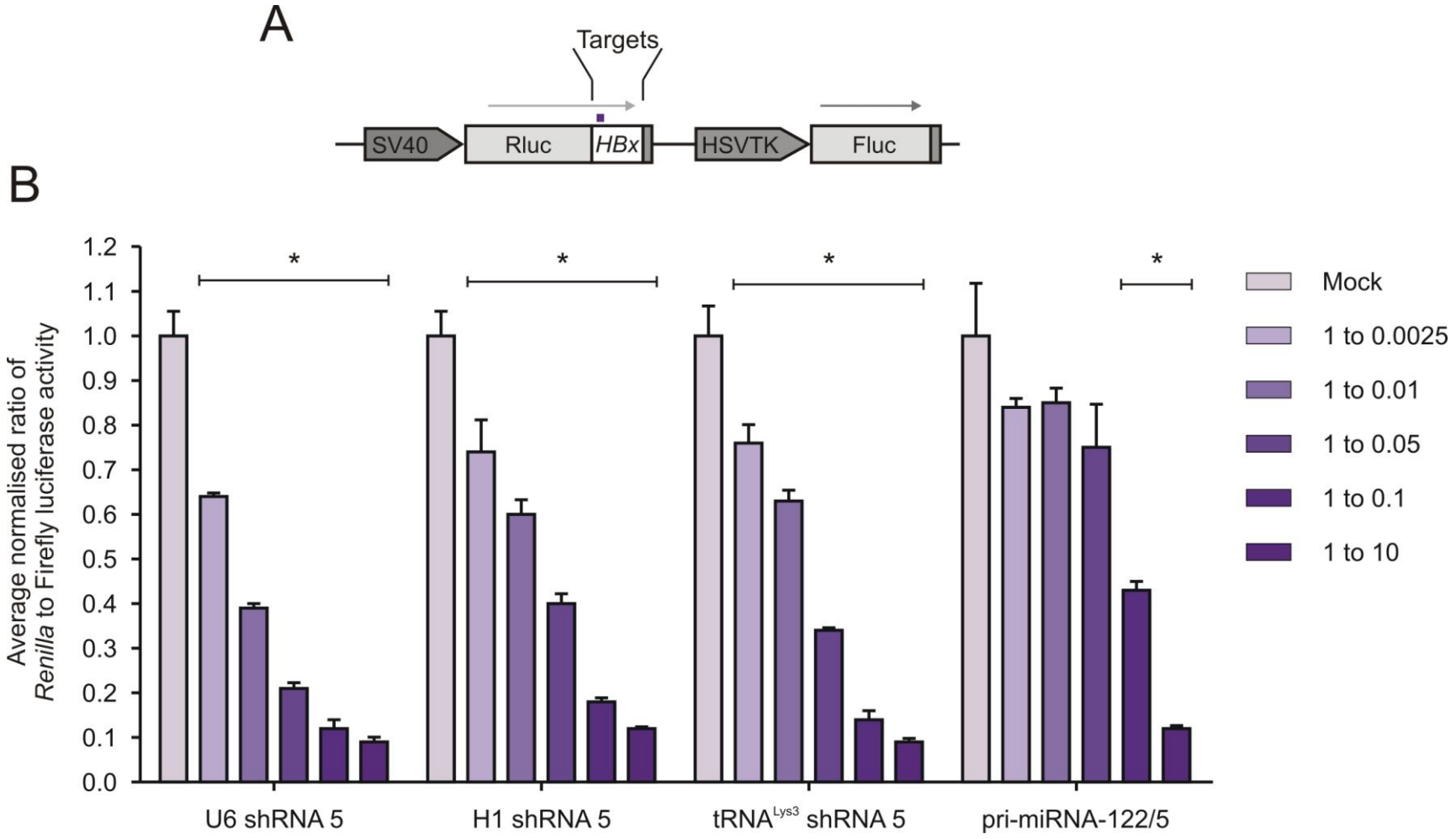


Figure 3. 6: *HBx* knockdown by Pol III-shRNA 5 and miRNA-122/5.

(A) Schematic representation of the psiCHECK HBx vector, indicating the target site of the effecter sequence (purple). **(B)** Knockdown of *HBx* was assessed using the dual luciferase assay. Cultured cells were co-transfected with a psiCHECK HBx target plasmid and either a RNA Pol II driven pri-miRNA-122/5 shuttle or Pol III-driven shRNA 5. Knockdown was normalised to the respective Mocks for comparison. Error bars indicate the normalised standard error of the mean (n=3). The p values are discussed within the text. *p<0.05.

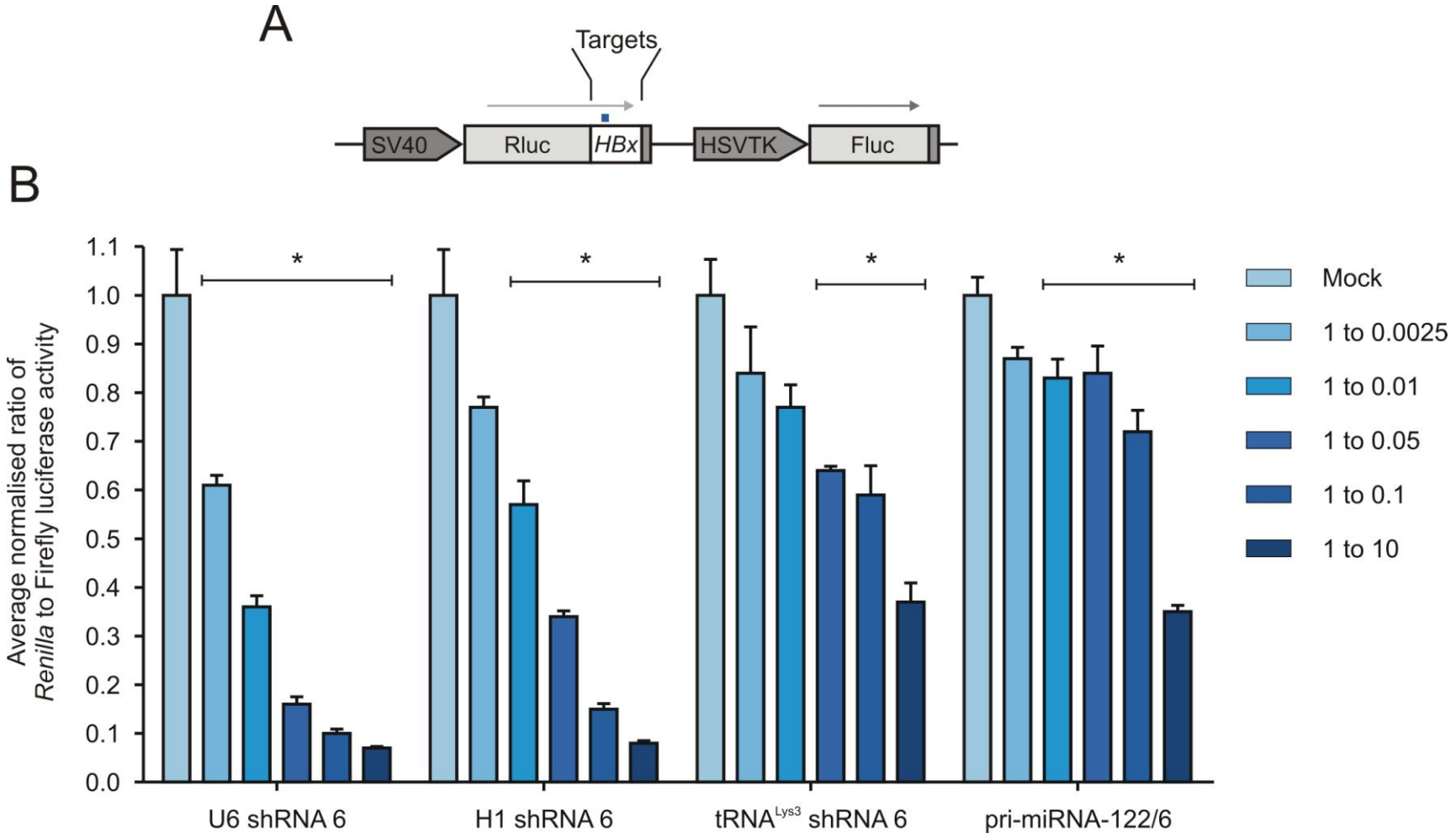


Figure 3.7: *HBx* knockdown by Pol III-shRNA 6 and miRNA-122/6.

(A) Schematic representation of the psiCHECK HBx vector, indicating the target site of the effecter sequence (blue). **(B)** Knockdown of *HBx* was assessed using the dual luciferase assay. Cultured cells were co-transfected with a psiCHECK HBx target plasmid and either a RNA Pol II driven pri-miRNA-122/6 shuttle or a Pol III-driven shRNA 6. Knockdown was normalised to the respective Mocks for comparison. Error bars indicate the normalised standard error of the mean (n=3). The p values are discussed within the text. *p<0.05.

3.5.2 Decreased *HBx* target knockdown by Pol II- and Pol III-driven effecter sequences 8, 9 and 10

The trend of knockdown previously observed for U6 was maintained by U6 shRNA 8. At an effecter to target ratio of 1:10, U6 shRNA 8 caused significant target knockdown of ~85% in comparison to Mock treated cells ($p<0.05$). At 1:0.1, target knockdown of ~65% was achieved, and the knockdown was no longer significant at 1:0.0025. H1 shRNA 8 followed a similar trend to U6 shRNA 8 (Appendix C.3). Although target knockdown of ~62% was significant at 1:10, and at 1:0.1 and 1:0.05 ($p<0.05$), the efficacy of knockdown at 1:0.1 and 1:0.05 was low at, ~20% and ~40% respectively (Figure 3.8). Although the knockdown efficacy of $tRNA^{Lys3}$ shRNA 8 and pri-miRNA-122/8 was considered significant at 1:10 and 1:0.1 ($p<0.05$), the percentage of knockdown failed to exceed 48%. Pri-miRNA-122/8 was slightly more efficacious with significant knockdown at 1:0.05, 1:0.01 and 1:0.0025. Taken together, these data indicate the effecter sequence is only capable of >80% knockdown when under the expression of the potent promoter, U6.

Figure 3.6 and Figure 3.7 indicate significant target knockdown primarily by the RNA Pol III promoters, U6 and H1. The trend of *HBx* target knockdown by U6 shRNA 9 and H1 shRNA 9 followed this established trend. At 1:10 target knockdown by U6 shRNA 9 and H1 shRNA 9 was significant, at ~ 80-85% in comparison to Mock treated cells ($p<0.05$). U6 and H1 shRNA 9 caused significant knockdown at 1:0.1, 1:0.05 and 1:0.01 (Figure 3.9). It was only at the lowest effecter 1:0.0025 at which knockdown was not significant (Appendix C.4). At an effecter ratio of 1:10, $tRNA^{Lys3}$ shRNA 9 and pri-miRNA-122/9 caused significant knockdown ($p<0.05$) of 77% and 68% respectively. As the effecter concentration decreased to 1:0.01, target knockdown was decreased to ~ 22% and 38%, which was analysed to be significantly different. Further decrease in effecter concentration

indicated limited knockdown by tRNA ^{Lys3} shRNA 9 and pri-miRNA-122/9 was not significant.

RNA Pol III-promoter driven shRNA 10 expression cassettes and RNA Pol II-promoter driven pri-miRNA-122/10 shuttle indicated no significant knockdown (Figure 3.10) (Appendix C.5). These data correlate with previous findings (5).[1]

[1] The complete statistical analyses can be found in Appendix Table C.1 to C.5

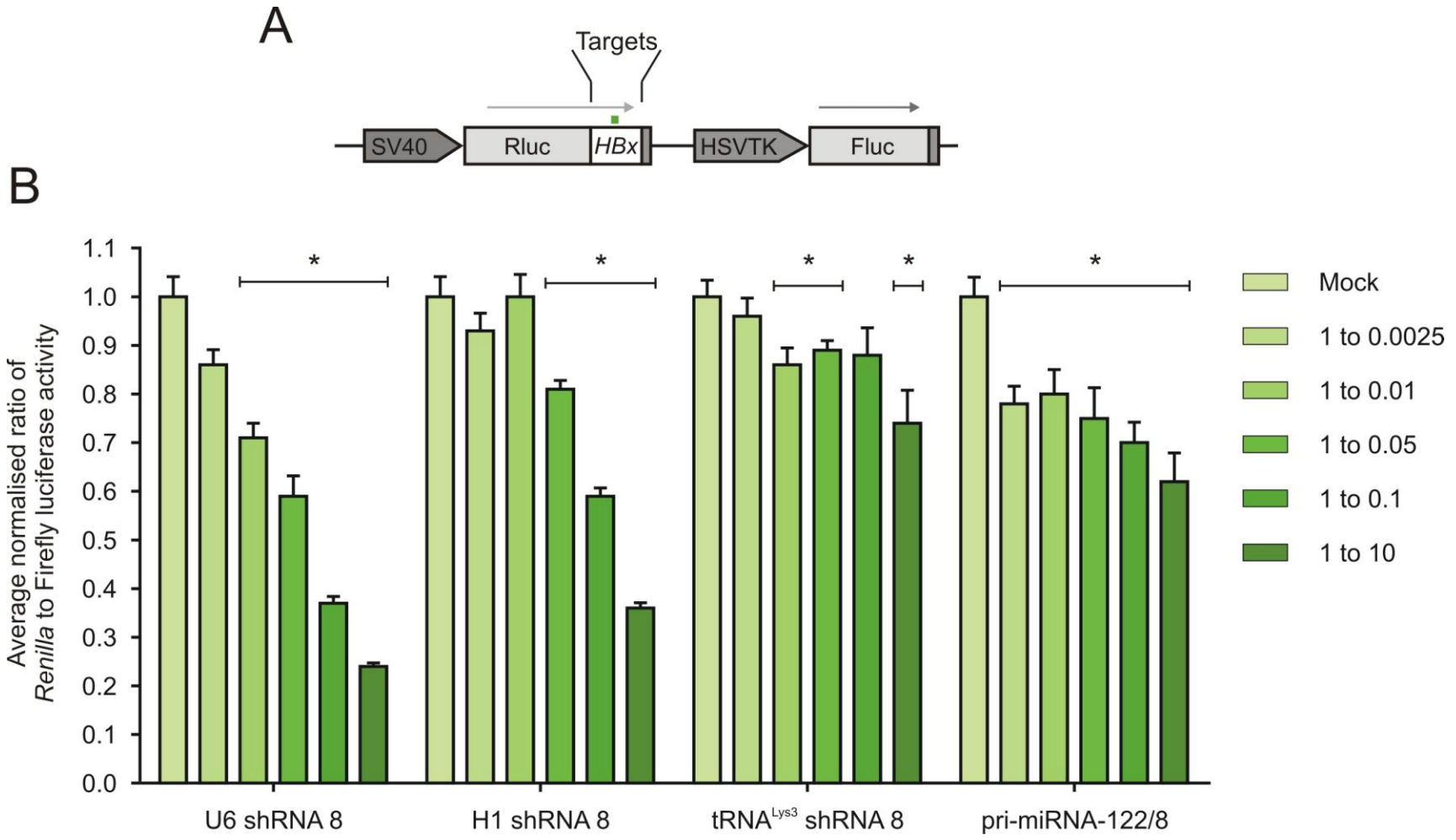


Figure 3.8: *HBx* knockdown by Pol III-shRNA 8 and miRNA-122/8.

(A) Schematic representation of the psiCHECK HBx vector, indicating the target site of the effecter sequence (green). **(B)** Knockdown of *HBx* was assessed using the dual luciferase assay. Cultured cells were co-transfected with a psiCHECK HBx target plasmid and either a RNA Pol II driven pri-miRNA-122/8 shuttle or a Pol III-driven shRNA 8. Knockdown was normalised to the individual Mocks for comparison. Error bars indicate the normalised standard error of the mean (n=3). The p-values are discussed within the text. *p<0.05.

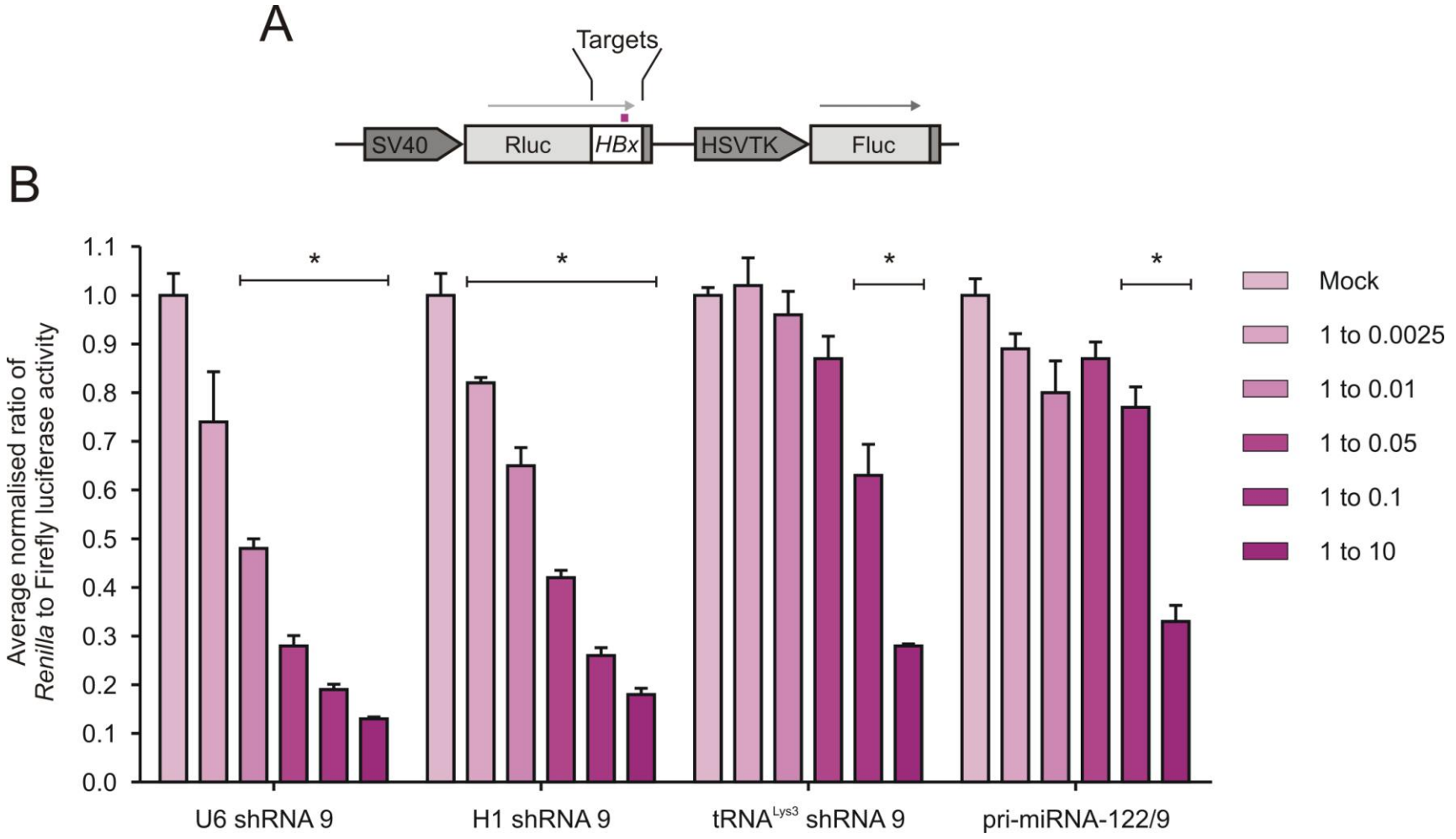


Figure 3.9: *HBx* knockdown by Pol III-shRNA 9 and miRNA-122/9.

(A) Schematic representation of the psiCHECK HBx vector, indicating the target site of the effecter sequence (pink). **(B)** Knockdown of *HBx* was assessed using the dual luciferase assay. Cultured cells were co-transfected with a psiCHECK HBx target plasmid and either a RNA Pol II driven pri-miRNA-122/9 shuttle or a Pol III-driven shRNA 9. Knockdown was normalised to the individual Mocks for comparison. Error bars indicate the normalised standard error of the mean (n=3). The p-values are discussed within the text. *p<0.05.

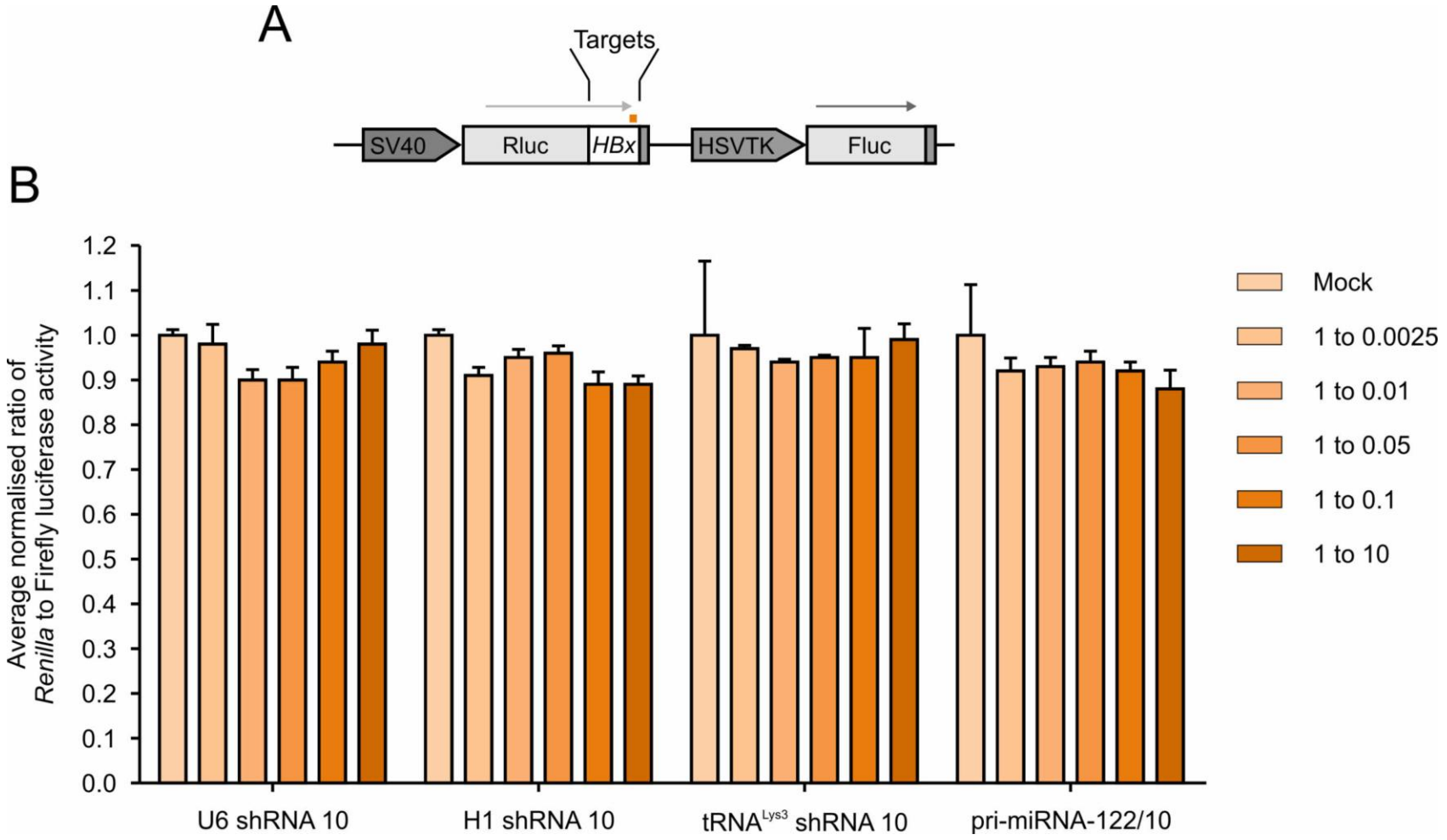


Figure 3.10: *HBx* knockdown by Pol III-shRNA10 and miRNA-122/10.

(A) Schematic representation of the psiCHECK HBx vector, indicating the target site of the effecter sequence (orange). **(B)** Knockdown of *HBx* was assessed using the dual luciferase assay. Cultured cells were co-transfected with a psiCHECK HBx target plasmid and either a RNA Pol II driven pri-miRNA-122/10 shuttle or a Pol III-driven shRNA 10. Knockdown was normalised to the individual Mocks for comparison. Error bars indicate the normalised standard error of the mean (n=3). The p-values are discussed within the text.

3.6. Effective inhibition of HBsAg secretion from cultured cells after transfection with by anti-HBV expression cassettes

After establishing that the shRNA expression cassettes and pri-miRNA shuttles effectively knocked down the expressed *HBx* target, the efficacy at which these effecter sequences could inhibit actively replicating virus was assessed. The target vector pCH-9/3091 was co-transfected with the shRNA expression cassettes, pri-miRNA shuttles and a comparative mock. The concentration of HBsAg secreted within the media of transfected cells was measured and the efficacy of inhibition determined. All data were normalised to a comparative mock (n=3).

The U6 promoter-driven shRNA 5, 6, 8 and 9 expression cassettes significantly inhibited HBsAg secretion by ~60% in comparison to the Mock treated cells ($p<0.05$) (Figure 3.11). Furthermore, a significant inhibition of HBsAg secretion was caused by H1 and $tRNA^{Lys3}$ shRNA 5, 6 and 9; and pri-miRNA-122/5 -/6 and -/9. (Figure 3.11 and Figure 3.12), however there was no significant inhibition ($p>0.05$) caused by H1 and $tRNA^{Lys3}$ shRNA 8 and pri-miRNA-122/8 (Appendix C.6). Taken together these data correlate with the findings in Section 3.5. A 2.5 fold increase in HBsAg was observed for U6 shRNA 10. In addition, H1 shRNA 10 and pri-miRNA-122/10 caused increases in HBsAg concentrations, which were significantly different to the Mock treated cells ($p<0.05$). This phenomenon has been observed in previous investigations, however a suitable explanation has not yet been established.

Taken together, the trend of HBsAg inhibition and targeted *HBx* knockdown identify the effecter sequences 5 and 6 as the most efficacious at targeting HBV, whilst U6 and $tRNA^{Lys3}$ were established to be the most effective promoters[2].

[2] The complete statistical analyses can be found in Appendix Table C.6

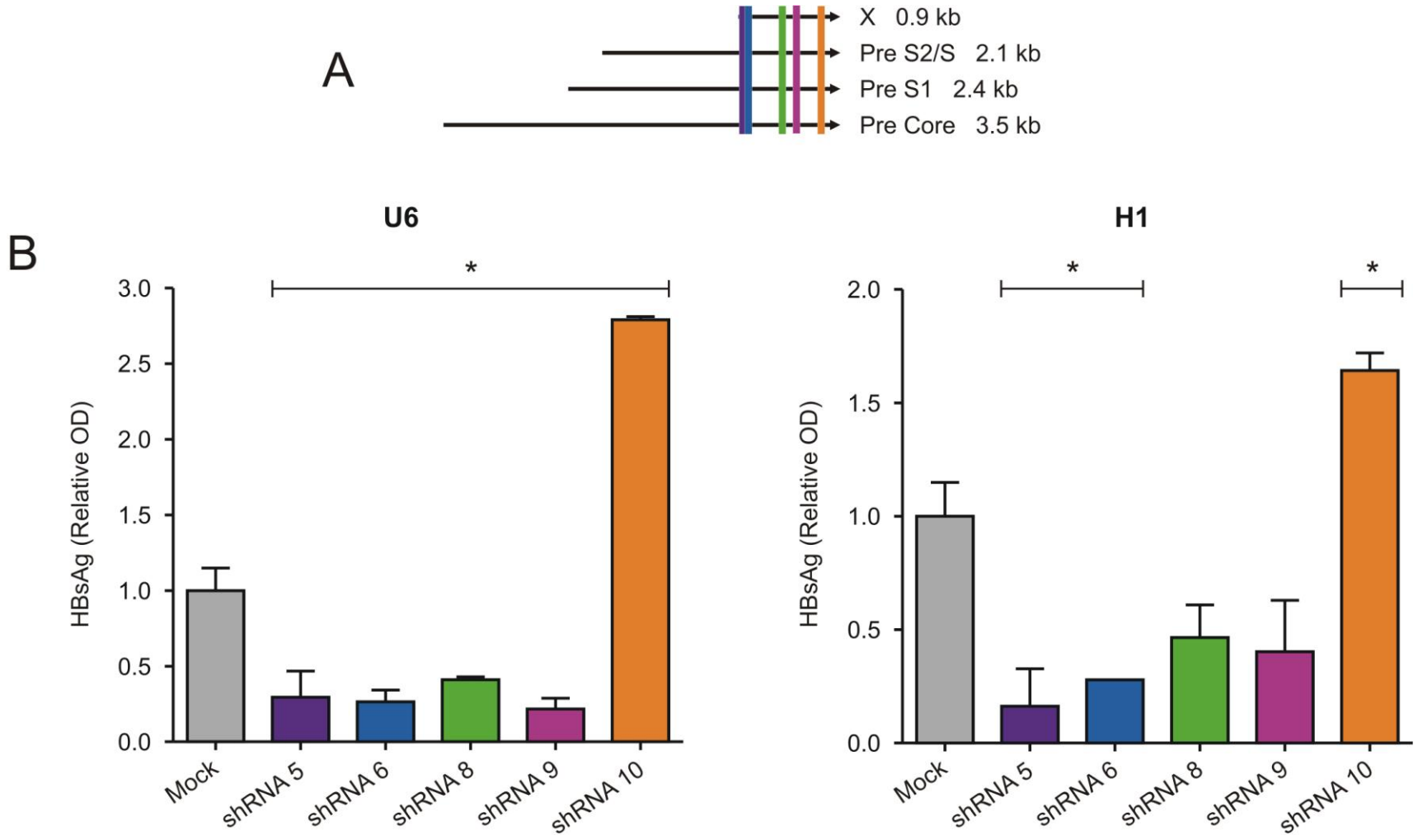


Figure 3.11: Inhibition of HBsAg by U6 and H1 promoter-driven shRNA expression cassettes.

(A) Schematic representation indicating the sites targeted by the different effecter sequences. **(B)** The target vector pCH-9/3091 was co-transfected with the shRNA expression cassettes and a mock for comparison. Error bars indicate the normalised standard error of the mean (n=3). *p<0.05.

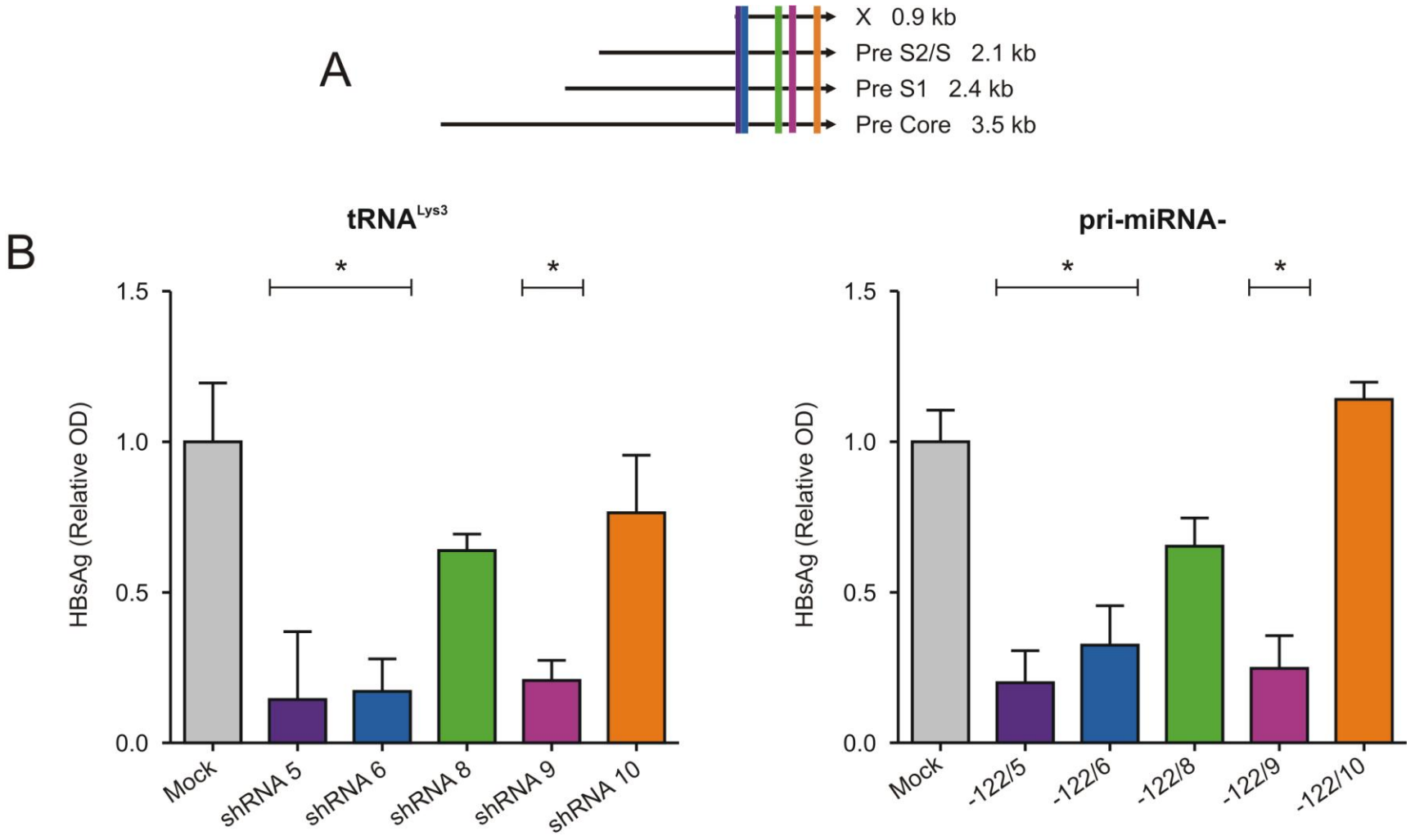


Figure 3.12: Inhibition of HBsAg by tRNA^{Lys3} and CMV promoter-driven shRNA expression cassettes.

(A) Schematic representation indicating the sites targeted by the different effecter sequences. **(B)** The target vector pCH-9/3091 was co-transfected with the shRNA expression cassettes and a mock for comparison. Error bars indicate the normalised standard error of the mean (n=3). *p<0.05.

3.7 Pol III- and Pol II- expression cassettes do not saturate the RNAi pathway.

The introduction of exogenous RNAi effecter sequences have been known to cause toxic effects including off-target silencing and saturation of the endogenous RNAi pathway. To assess potential saturation of the endogenous miRNA pathway by exogenous RNAi effecter sequences disruption of miR-16 silencing of a luciferase target was assessed. The shRNA 5 and shRNA 6 expression sequences and the pri-miRNA-122/5 and -122/6 shuttles were selected to challenge miR-16 functionality, as these effecter sequences caused the greatest knockdown of the *HBx* target. As a positive control for disruption of miR-16 functionality a miR-16 sponge expression cassette (pTZ-U6-miR-16S×7) (14) was included. Neither of the effecter sequences was found to disrupt miR-16 target silencing ($p<0.05$), whereas the sponge sequence significantly derepressed target expression (Figure 3.13). This is a clear indication that the effecter sequences do not saturate the endogenous RNAi pathway[3].

[3] The complete statistical analyses can be found in Appendix Table C.7

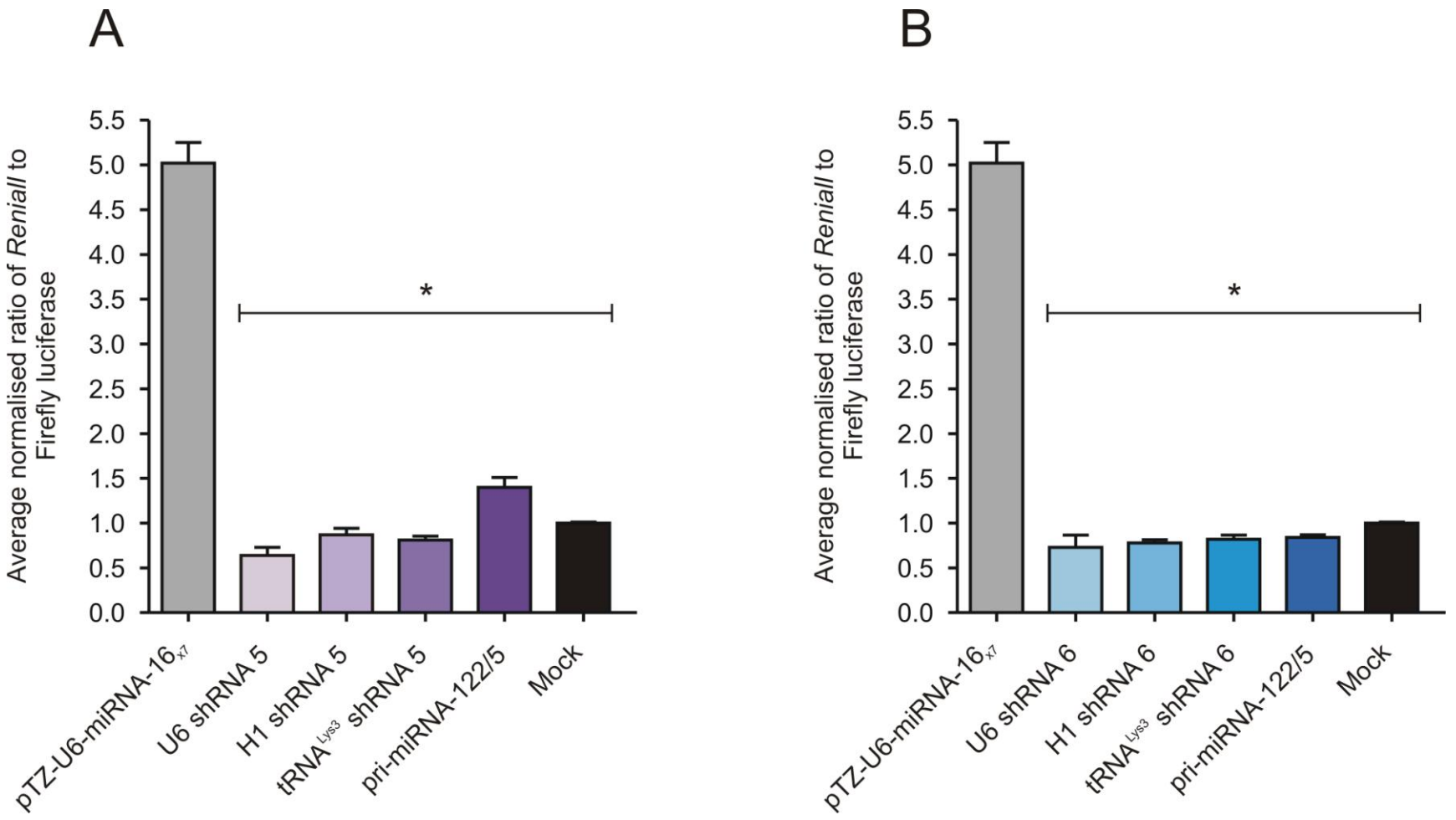


Figure 3.13: Saturation assay of miR-16.

To assess disruption of the endogenous miRNA pathway, cultured cells were co-transfected with a miR-16 luciferase target plasmid and various RNA Pol II- and Pol III-driven expression cassettes. pTZ-U6-miR-16S×7 sponge is a positive control for disruption of miR-16 silencing activity. All data were carried out in triplicate and normalised to the Mock. Bars indicate normalised standard error of the mean (n=3). The p values discussed within the text. *$p<0.05$

3.8 DAPI Stain

To assess whether the fractionation of the nuclear and cytoplasmic components were effective and if contamination had occurred between the fractions, the lysates were stained with DAPI and assessed for the presence of nucleic acids within the nuclei. The nuclear lysates obtained from Method 1 (19), Method 3 (4) and the PARIS™ kit was compared. The fractionated lysates from the PARIS™ kit indicate minimal amounts of nucleic acids within the cytoplasmic fraction, when compared to the nuclear fraction (Figure 3.14). Taken together this data indicates a slight contamination of the nuclear fraction within the cytoplasmic fraction.

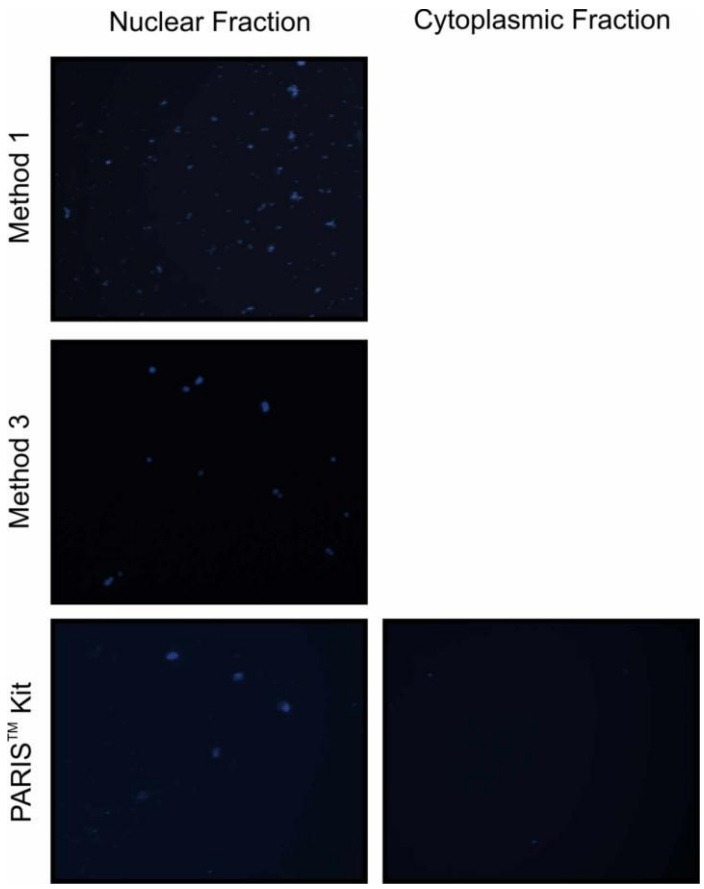


Figure 3.14: Presence of nucleic acids within fractionated lysates at 10 x Magnification.
Nulceic acids were depicted within the nuclear lysates, with minimal amounts in the cytoplasmic fraction for the PARIS™ kit

3.9 Expression and processing of anti-HBV effecter sequences in total, nuclear and cytoplasmic fractions

Northern blot hybridisation was used to detect the Dicer processed anti-HBV effecter sequence from the different shRNA 5 expression cassettes and pri-miRNA-122/5 shuttle in total, nuclear and cytoplasmic RNA extracts.

3.9.1 Processed anti-HBV guide strands detected in Total RNA

Hybridisation to a radiolabelled probe complementary to the processed guide sequence 5 detected a band at ~21 nucleotides for U6, H1 and $tRNA^{Lys3}$ shRNA 5 (Figure 3.15) indicating processed mature guide strand. The processed guide strands for U6, H1 and $tRNA^{Lys3}$ were detected after 24 hours exposure, however the miRNA-122/5 remained undetected, even when exposed for 5 days. Large amounts of U6 and H1 precursors were detected at ~ 65 nt. $tRNA^{Lys3}$ precursors were detected at > 100 nt and at ~55 nt which conform to the expected sizes of unprocessed pre-$tRNA^{Lys3}$ shRNA 5 and unprocessed $tRNA^{Lys3}$ shRNA 5. The amount of U6 and H1 precursors in comparison to H1 and $tRNA^{Lys3}$ indicates a high level of expression for U6 and decreased expression, which is in accordance with published literature. Hybridisation of a radiolabelled probe complementary to U6 snRNA confirmed equal loading of the RNA samples.

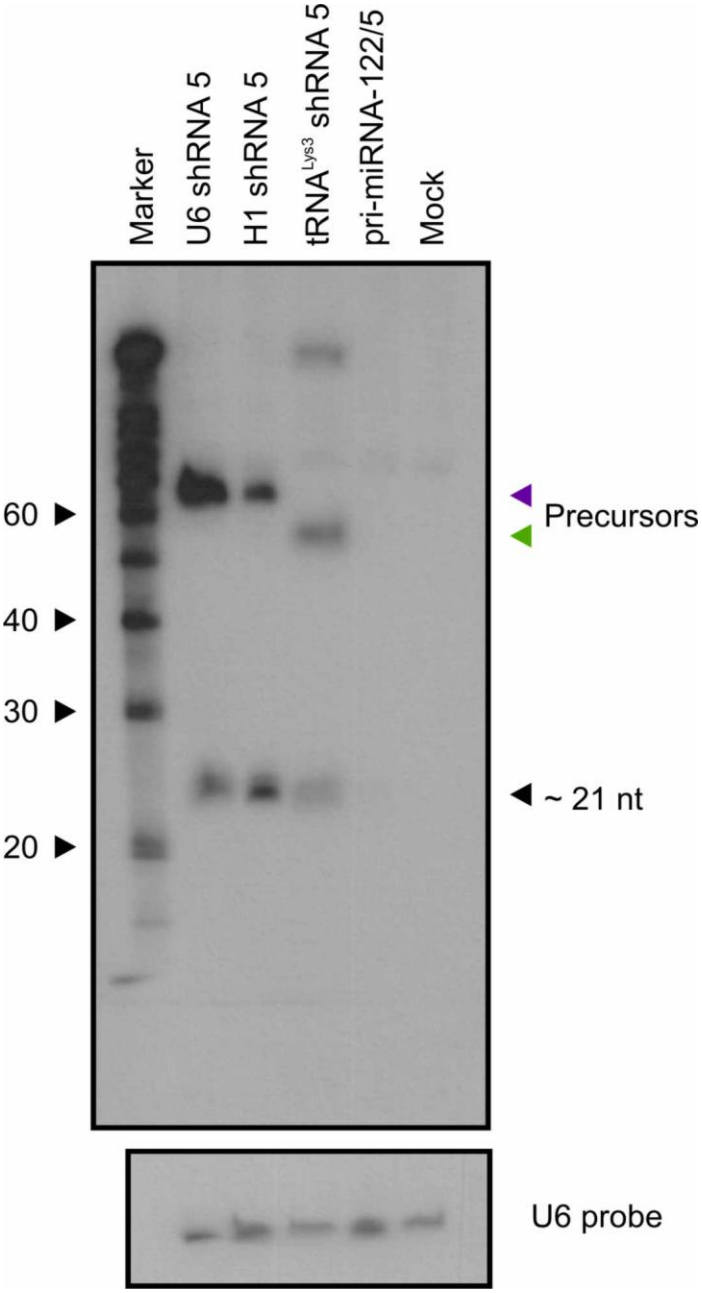


Figure 3.15: Northern blot hybridisation of processed anti-HBV effecter sequences of a total RNA lysate.

Total RNA was extracted from Huh7 cells that ad been transfected with the U6, H1 or tRNA^{Lys3} shRNA 5, pri-miRNA-122/5 or Mock (pCI-neo) plasmids. Signals were detected following the hybridisation of a radioalabelled probe to the processed anti-HBV guide 5. The processed guide strand was detected at 21 nucleotides. Precursors of the processed product were detected for U6 and H1 (purple arrow) and tRNA^{Lys3} (green arrow). Processed miRNA-122/5 was not detected. The blot was stripped and reprobed with U6 snRNA to confirm equal loading of RNA.

3.9.2 Processed anti-HBV guide strands detected in Total and Cytoplasmic RNA

To assess in which compartment of the cell the majority of the mature guide strand occurred, Lipofectamine2000™ transfected Huh7 cells were fractionated into nuclear and cytoplasmic lysates (Method 1) and the RNA extracted. The overall yield of nuclear RNA was ~ 20 ng, thus the fraction was excluded. Twenty-four hours post exposure the processed guide strand was detected as a band at ~21 nucleotides for U6, H1 and $tRNA^{Lys3}$ shRNA 5, in the total and cytoplasmic fractions. The guide strand processed from miRNA-122/5 remained undetected, even at 5 days exposure (Figure 3.16). Precursors were detected for U6, H1 and $tRNA^{Lys3}$. Hybridisation of a radiolabelled probe complementary to U6 snRNA was used to confirm equal loading of the RNA samples and to detect nuclear RNA. High levels of nuclear RNA were detected in the cytoplasmic fraction, suggesting lysis of the nuclei prior to the separation of the fractions. Hybridisation of a radiolabelled probe complementary to tRNA detected high levels within the cytoplasmic fraction. The tRNA occurring in the cytoplasmic fraction was detected at higher levels than the previously detected nuclear RNA and the levels of tRNA within the cytoplasmic fraction are comparable and almost identical to the levels detected in the total lysate. Taken together, these data suggest the majority of the RNA is concentrated in the cytoplasmic fraction however the nuclear fraction is required to corroborate this finding.

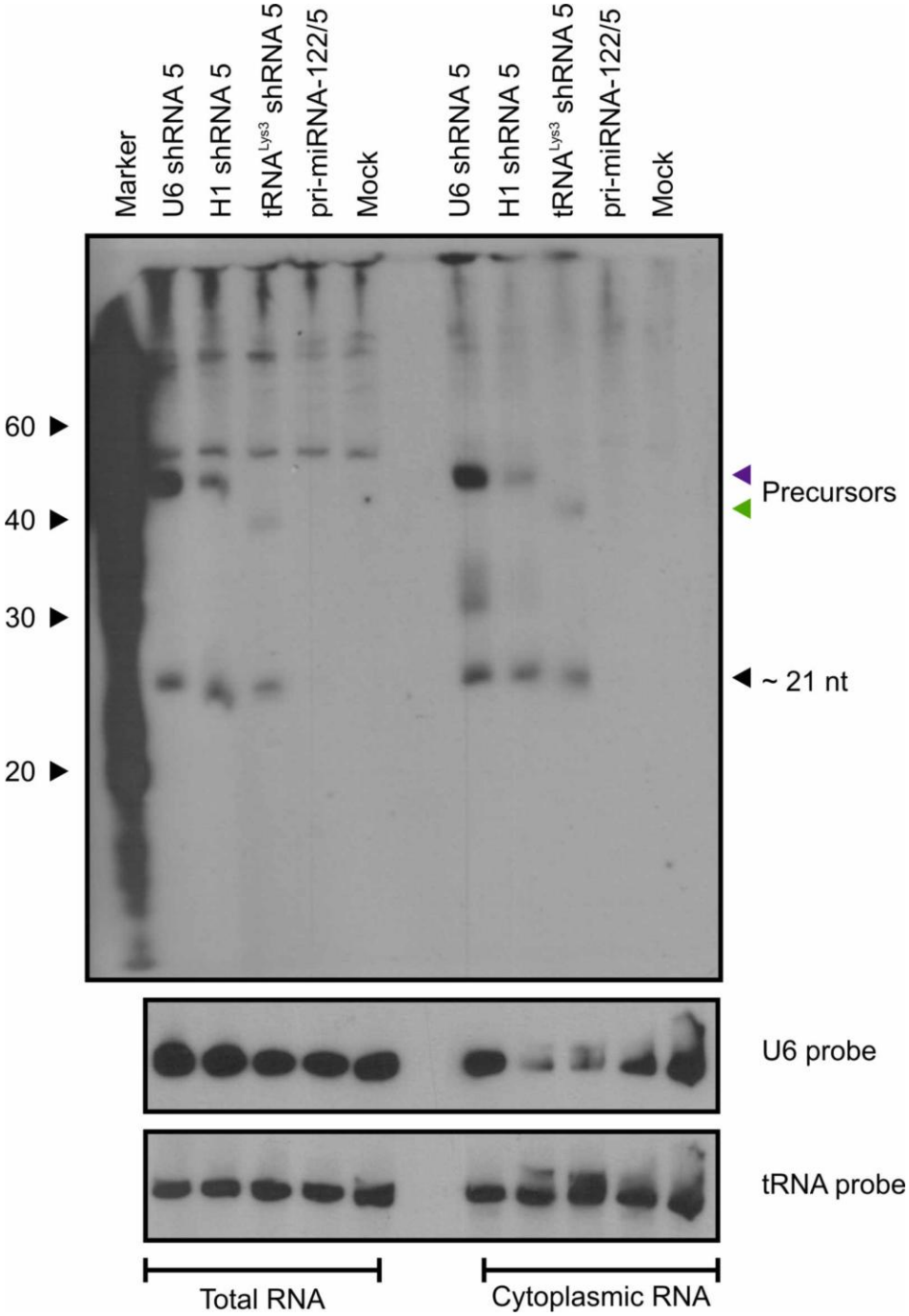


Figure 3.16: Northern blot hybridisation of the processed anti-HBV effecter sequence (guide 5) within total lysate and cytoplasmic RNA fraction.

Hybridisation of a radiolabelled probe detected the processed anti-HBV guide 5 at ~21 nt for U6, H1 and tRNA^{Lys3} shRNA 5. Precursors of U6 and H1 (purple arrow) and tRNA^{Lys3} (green arrow) were detected. Processed miRNA-122/5 was not detected. The blot was stripped and reprobed for U6 snRNA, to confirm equal loading of the RNA samples and to detect nuclear RNA in the cytoplasmic fraction. The blot was stripped again and reprobed for tRNA.

3.9.3 Detection of processed anti-HBV guide strands in total, nuclear and cytoplasmic RNA

Three different methods for fractionating the nucleus and cytoplasm were attempted to obtain suitable RNA concentrations from the respective fractions. The overall yields of extracted nuclear RNA seldom exceeded 200 ng in 10^6 cells and in the cases where a suitable concentration was obtained, the RNA was severely degraded (Appendix C.12 and C.13). Combining the most efficient method of fractionation and RNA extraction, the nuclear and cytoplasmic fractions yielded ~ 20 μg of RNA for the majority of each fraction. Nuclear RNA obtained from the U6 shRNA 5, $tRNA^{Lys3}$ and $tRNA^{Lys3}$ shRNA 5 fractions yielded <1 μg and there was no detectable RNA when the samples were subjected polyacrylamide gel electrophoresis (Appendix C.14).

Figure 3.17 indicates the processed guide strand detected as a band of ~ 21 nt. The guide strand was detected in the total and cytoplasmic RNA of U6 shRNA 5 and in the total, nuclear and cytoplasmic RNA for H1 shRNA 5. As indicated in the polyacrylamide gel, there was no detectable RNA for U6 shRNA 5 nuclear fraction hence no detectable processed guide within the nuclear lane. U6 and H1 precursors were detected. Hybridisation of a radiolabelled probe complementary to U6 snRNA detected contamination of nuclear RNA within the cytoplasmic fractions of U6 shRNA 5, U6+1, H1 shRNA 5 and H1 Mock, indicating lysis of the nuclei during the fractionation. The U6 probe confirmed equal loading of the total RNA between the samples, and equivalent loading of the nuclear and cytoplasmic fractions. Hybridisation of a radiolabelled probe complementary to tRNA detected RNA within the cytoplasmic fraction but no cytoplasmic RNA was detected in the nuclear fractions. There were two bands observed in the cytoplasmic fraction, which is likely due to different RNA species or non-specific binding.

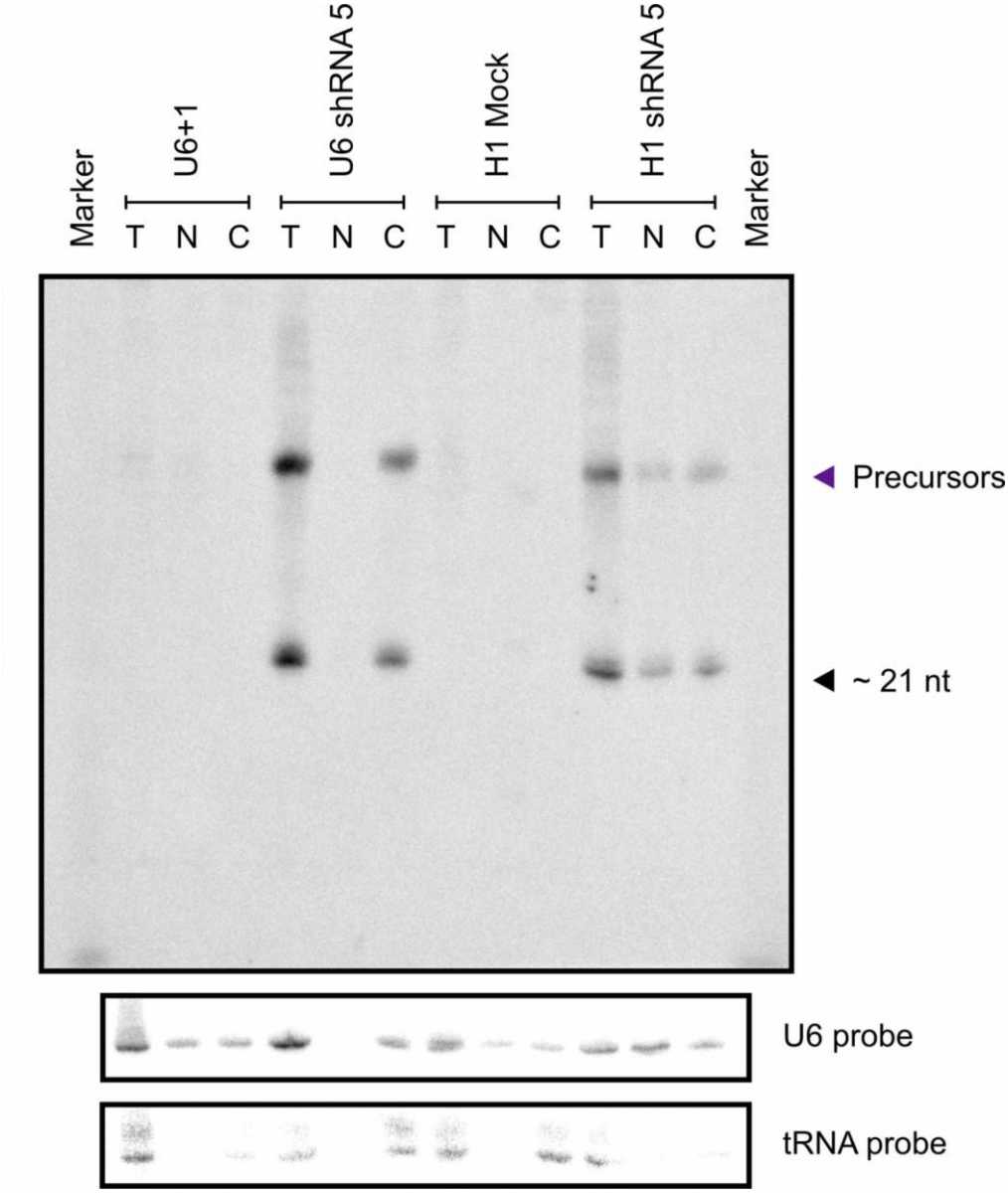


Figure 3.17: Northern blot hybridisation of U6 and H1 processed anti-HBV effecter sequences of total, cytoplasmic and nuclear RNA.

Total, nuclear and cytoplasmic RNA were extracted from Huh7 cells transfected with U6 and H1 shRNA 5 and complementary U6+1 and H1 Mock plasmids. Hybridisation of a radioactively labeled probe detected processed anti-HBV guide 5 at 21 nucleotides. Precursors of the processed products were detected (purple arrow). The blot was stripped and probed for U6 snRNA, confirming RNA loading control. The blot was stripped and reprobed for tRNA. (T) - Total; (N) - Nuclear; (C) - Cytoplasmic. Huh7 cells were transfected using calcium chloride and fractionated using the PARIS™ kit.

Figure 3.18 indicates the processed guide strand detected as a band at ~21 nucleotides for $tRNA^{Lys3}$ shRNA 5 in the total and cytoplasmic fraction and for pri-miRNA-122/5 in the total RNA. There were no detectable bands for the pri-miRNA-122/5 nuclear or cytoplasmic fractions, even after 12 days exposure. The lack of processed guide within the $tRNA^{Lys3}$ shRNA 5 nuclear fraction correlates with the lack of detectable RNA as identified in the polyacrylamide gel. Precursors were detected in the total and cytoplasmic fractions of $tRNA^{Lys3}$ shRNA 5. Hybridisation of a radiolabelled probe complementary to U6 snRNA detected contamination of nuclear RNA within the cytoplasmic fractions of $tRNA^{Lys3}$ shRNA 5, $tRNA^{Lys3}$ Mock, pri-miRNA-122/5 and pCI-neo. There was no nuclear RNA detected in the nuclear fractions of $tRNA^{Lys3}$ Mock and $tRNA^{Lys3}$ shRNA 5, which corroborates the lack of RNA isolated from the fraction. The U6 probe confirmed equal loading of the total RNA between the samples. Hybridisation of a radiolabelled probe complementary to tRNA detected RNA within the cytoplasmic fraction but no cytoplasmic RNA was detected in the nuclear fractions.

Taken together these findings indicate that the nuclei are being lysed during the fractionation step, causing contamination within the cytoplasmic fractions. The cytoplasmic fraction, however, is removed in its entirety without contaminating the nuclear fraction.

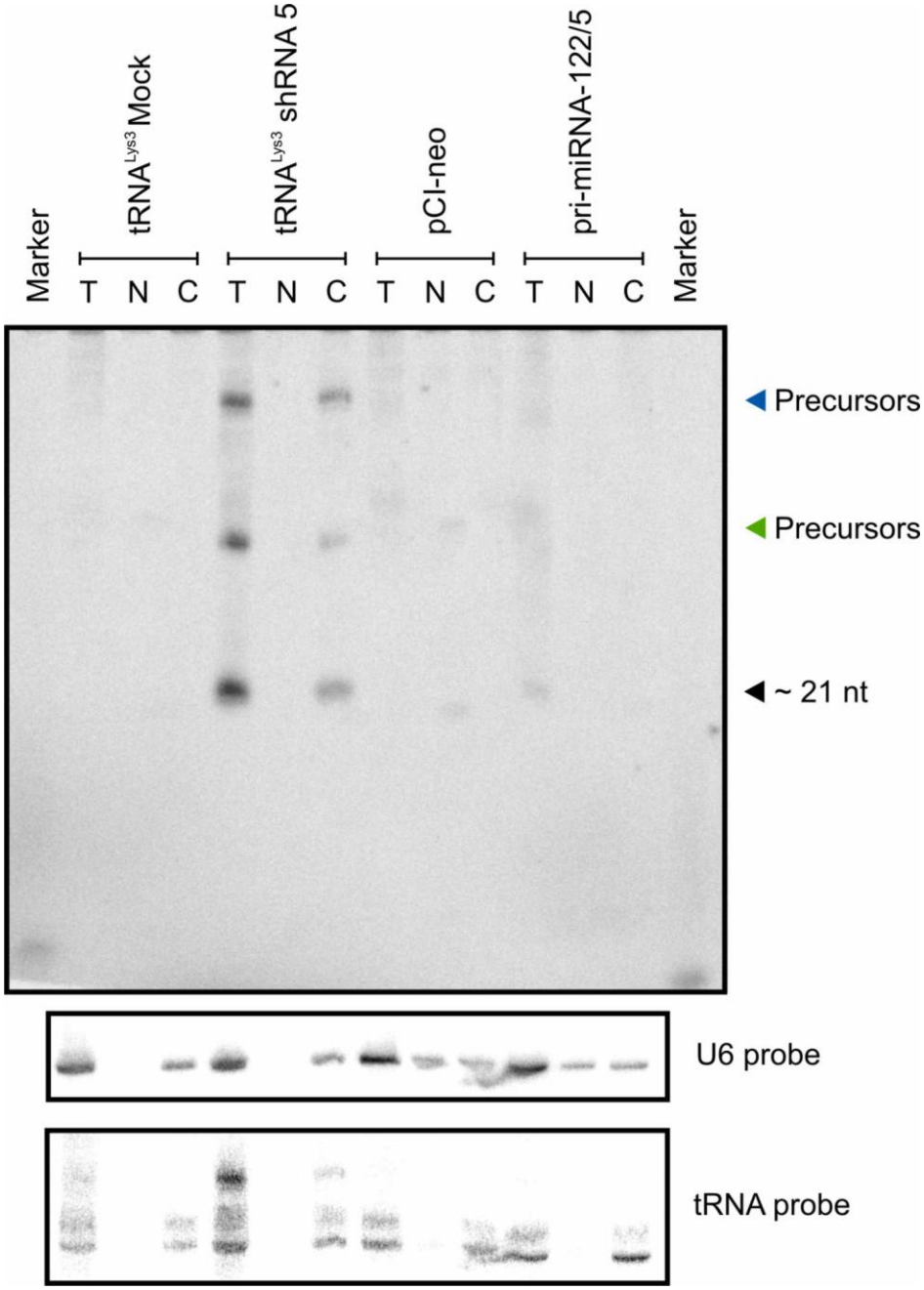


Figure 3.18: Northern blot hybridisation of processed tRNA^{Lys3} and pri-miRNA-122/5 anti-HBV effecter sequences of total, nuclear and cytoplasmic RNA.

Hybridisation of a radioactively labeled probe detected processed anti-HBV guide 5 at 21 nucleotides. Precursors of tRNA^{Lys3} were identified (blue and green arrow). The blot was stripped and probed for U6 snRNA, confirming RNA loading control and the contamination of nuclear RNA in the cytoplasmic fractions. The blot was stripped and reprobed for tRNA. (T) - Total; (N) - Nuclear; (C) - Cytoplasmic. Huh7 cells were transfected using calcium chloride and fractionated using the PARIS™ kit.

3.10 Inhibition of HBV within an *In vivo* Mouse model

3.10.1 Kaplan-Meier survival curve of mice post hydrodynamic tail vein injection

It has been established that the RNA Pol III promoter-driven shRNA 5 effecter sequences and the pri-miRNA-122/5 shuttle are highly efficacious at knocking down the expressed target *HBx*, and at inhibiting production of viral antigens *in vitro*. To assess whether the effect would be as efficient in an *in vivo* model, eight groups of five mice each (n=40) were hydrodynamically injected (HDI) via the tail vein with, either the U6, H1 or $tRNA^{Lys3}$ shRNA 5 expression cassettes, pri-miRNA122/5 shuttle sequence or comparable mock plasmids (U6+1; H1 Mock, $tRNA^{Lys3}$ Mock and pCI-neo) and pCH-9/3091. The administrations of the HDIs were scored out of 5, which provided an indication for delivery efficacy (data not shown). Twenty-four hours post HDI, four mice had died (Figure 3.19). The Kaplan-Meier survival curve indicates a 20% survival decrease in the experimental group U6 shRNA 5 and control group U6+1. A 40% survival decrease was observed in the control group $tRNA^{Lys3}$ Mock. All mice were sacrificed on day 5.

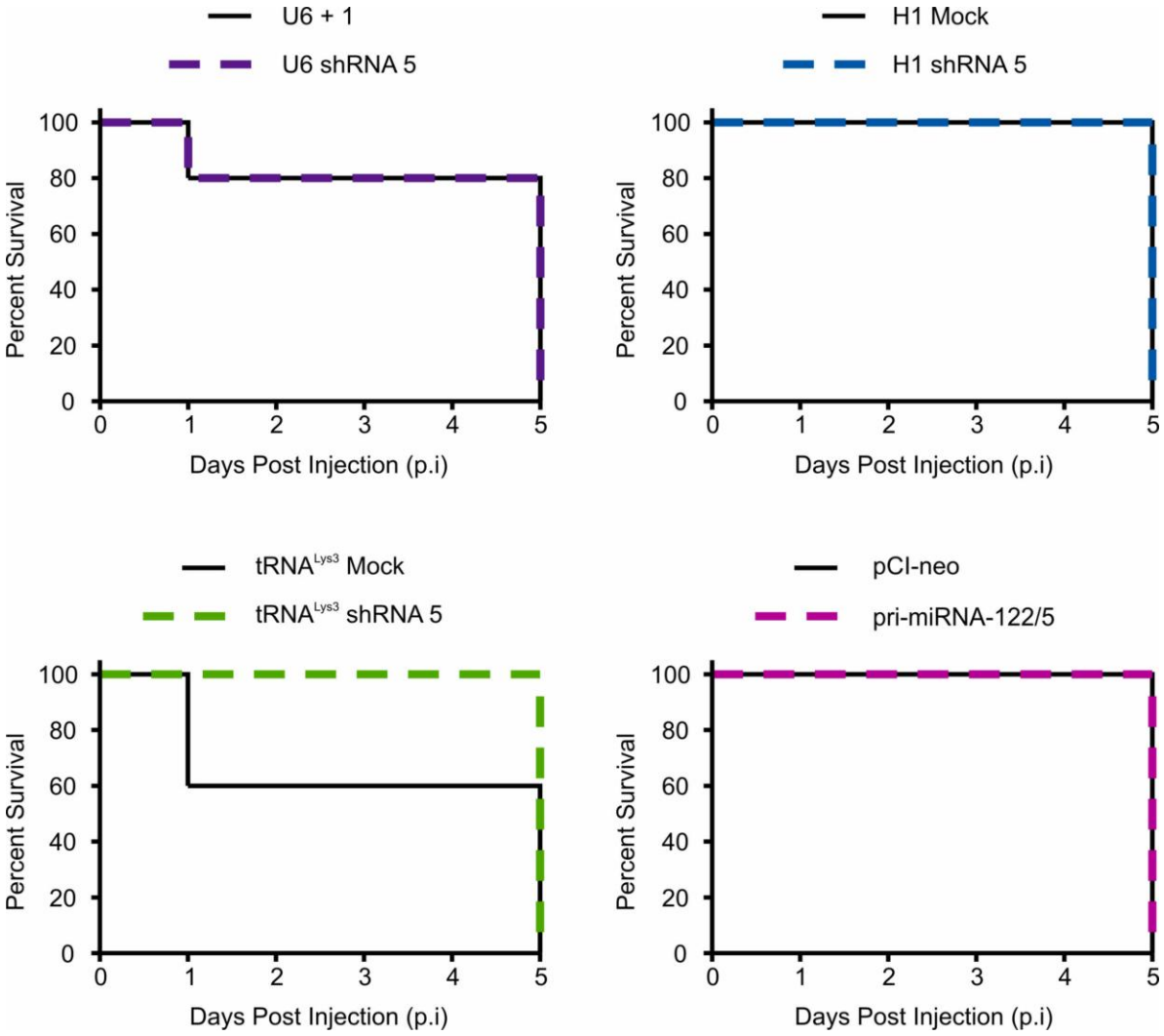


Figure 3.19: Kaplan-Meier survival curves of the hydrodynamically injected mice.

Eight groups of five mice each were hydrodynamically injected via the tail vein. Four groups received either U6 shRNA 5 (purple); H1 shRNA 5 (blue); tRNA^{Lys3} shRNA 5 (green) expression cassettes or pri-miRNA-122/5 shuttle (pink), whilst the remaining four groups served as controls and received the corresponding mocks (black). Twenty-four hours post injection four mice had died. Two mice were from the tRNA^{Lys3} Mock group and one mouse each from the U6 shRNA 5 and U6+1 groups. The surviving mice were sacrificed on day 5 p.i.

3.10.2 Inhibition of HBsAg secretion

Inhibition of HBsAg by the anti-HBV effecter sequences was measured in sera of HDI mice on 3 and 5 days post injection. The differences in the concentrations of HBsAg were measured between the anti-HBV effecter sequence and the mock for comparison. On day 3, U6 shRNA 5 ($p<0.005$) and $tRNA^{Lys3}$ shRNA5 ($p<0.005$) indicated a >95% decrease of serum HBsAg concentration whilst H1 shRNA 5 ($p<0.005$) and miRNA-122/5 ($p<0.005$) resulted in inhibition >80% (Figure 3.20). On day 5, U6 shRNA 5 ($p<0.005$) and pri-miRNA-122/5 ($p<0.005$) inhibited HBsAg secretion to approximately 80%, which is decreased in comparison to day 3. H1 shRNA 5 ($p<0.005$) and $tRNA^{Lys3}$ shRNA 5 ($p<0.005$), continued to inhibit HBsAg secretion, by 85% and 98% respectively. The ability of the RNA Pol III promoters, H1 and $tRNA^{Lys3}$ to increase the inhibition of HBsAg over five days suggests the effecter sequences are being transcribed at a rate comparable to the transcription of the virus.

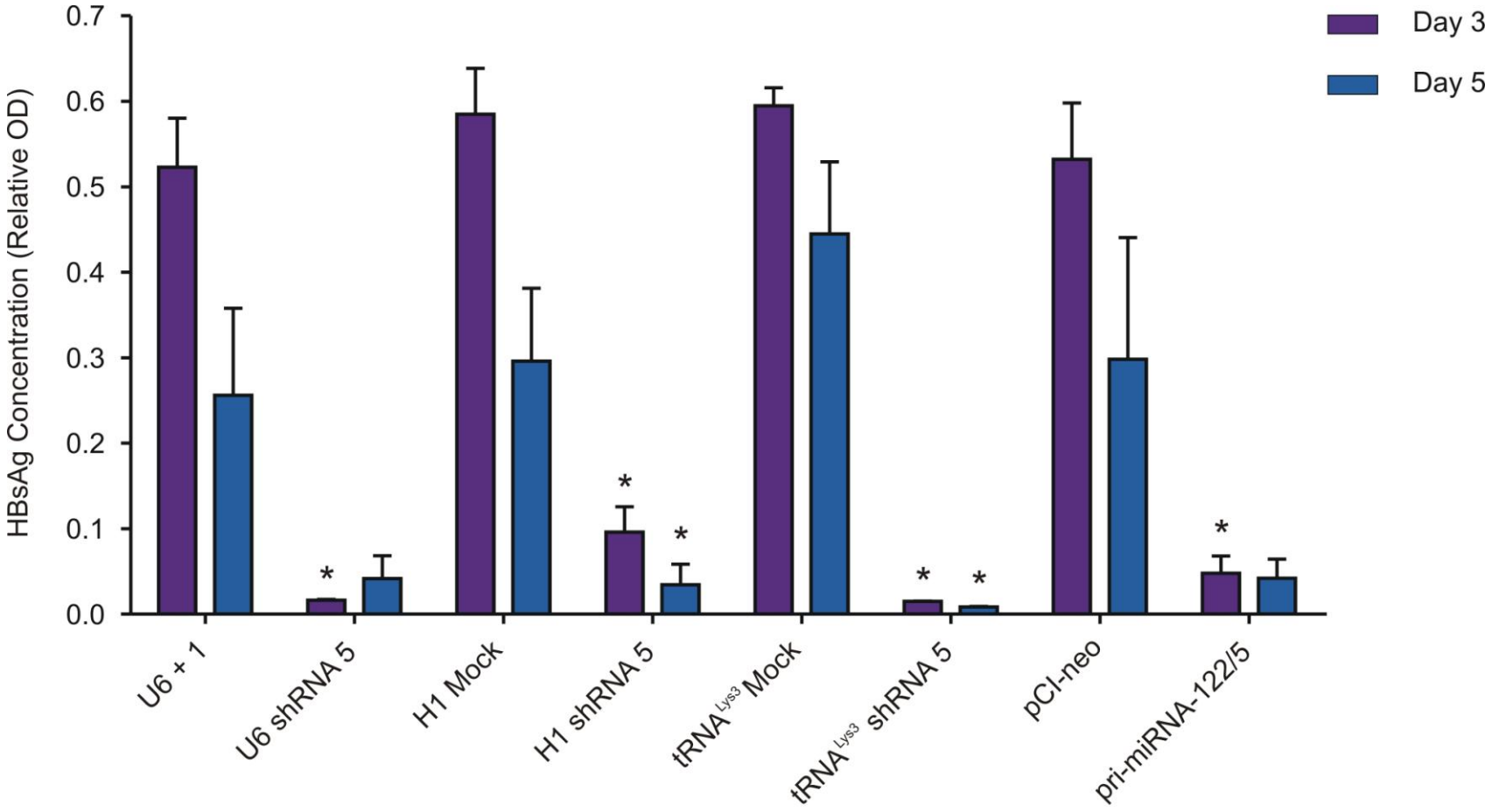


Figure 3.20: Decrease of serum HBsAg in mice following HDI treatment.

Plasmid DNAs containing the anti-HBV effecter sequences or complementary mocks were co-administered with the target vector pCH9/3091 to mice by hydrodynamic tail vein injection. Inhibition of HBsAg secretion in mouse sera was measured 3 and 5 days post injection. Error bars indicate the standard error of the mean (n=36). *p<0.05. The p-values are discussed within the text.

3.10.3 Detection of total HBV, cccDNA and rcDNA

To assess the amount of circulating viral particles within the sera of the HDI treated mice, primer sets were used to amplify the preS1 region and the concentration determined using a pre-designed standard curve. The minimum detection limit for total HBV was determined at 84 copies (9). The only significant difference was observed on day 3 between $tRNA^{Lys3}$ shRNA 5 and the $tRNA^{Lys3}$ Mock ($p<0.05$) (Figure 3.21) which correlates with the increased inhibition of HBsAg by $tRNA^{Lys3}$ shRNA 5. There was no statistical significance observed day 5 for any of the anti-HBV effecter sequences.

The data shows a clear trend in the amount of detectable HBV DNA, which is comparable to the trend observed in HBsAg inhibition. Decreases in the amount of HBV DNA were observed in all the Mock treated animals on day 5 indicating the probable clearing of the virus by the mice's natural immune system. In addition there is an increase in HBV DNA observed on day 5 for U6 shRNA 5 and pri-miRNA-122/5, and a decrease observed for H1 and $tRNA^{Lys3}$.

To assess the amount of total HBV, cccDNA and rcDNA in the liver, extracted DNA was analysed using an in house assay (2). Initially, the efficacies at which the target vector and DNA expressing plasmids were delivered to the liver following HDI were determined by amplification the Renilla *luciferase.* The delivery was variable between the eight groups, up to 1.5 fold difference (Appendix C.15). However, for the mock and experimental groups of the H1, $tRNA^{Lys3}$ and CMV promoters, the delivery is relatively consistent within each group itself and then between the two groups. Delivery of the U6 shRNA 5 group was almost 1 fold lower when compared to the U6+1 group.

Total HBV DNA and cccDNA was quantified, and the amount of rcDNA obtained by subtracting cccDNA from total HBV. There was no visual difference in the amount of total HBV and rcDNA observed between the U6 +1 and U6 shRNA 5 groups (Figure 3.22), however a decrease was observed in the experimental groups for H1(Figure 3.22), $tRNA^{Lys3}$ and pri-miRNA-122/5 (Figure 3.23). Although a decrease is evident, there was no significant difference observed between each of the control and the relative experimental groups, for either the total, cccDNA or rcDNA.

The data indicates the same trend, which has been observed throughout the *in vivo* experiments, essentially indicating a decrease in HBV DNA due to the inhibition of replication by the effecter sequences.

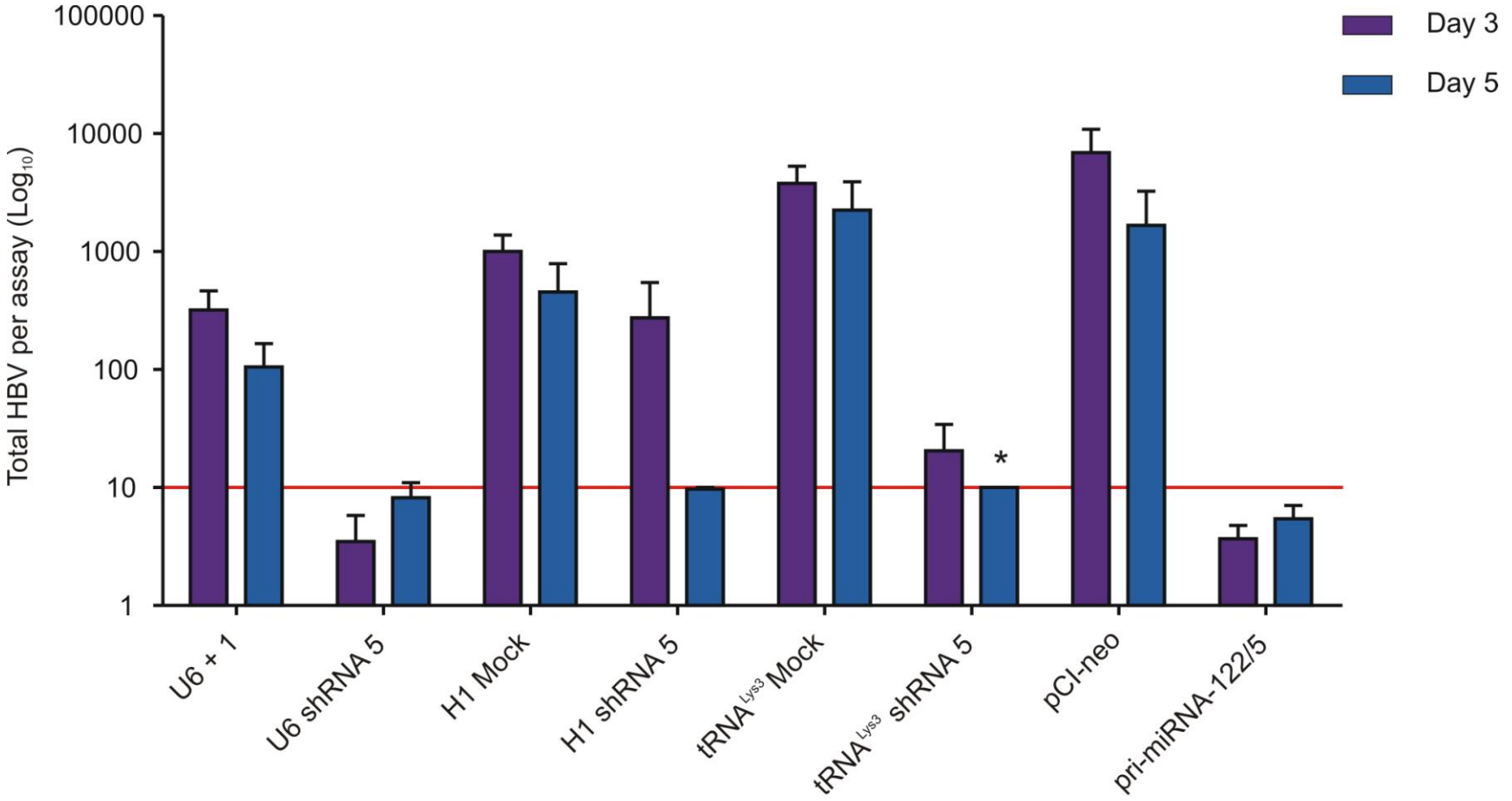


Figure 3.21: Quantification of total HBV DNA isolated from livers of mice subjected to HDI.

Hydrodynamic tail injections were used to co-administer pCH9/3091 and the shRNA expression cassette, pri-miRNA shuttle or complementary mocks. Total HBV was detected in the sera collected from mice on day 3 and day 5. The minimum detection limit (red line) of viral particles was 84 copies per microlitre. Error bars indicate the normalised standard error of the mean (n=36). *p<0.05.

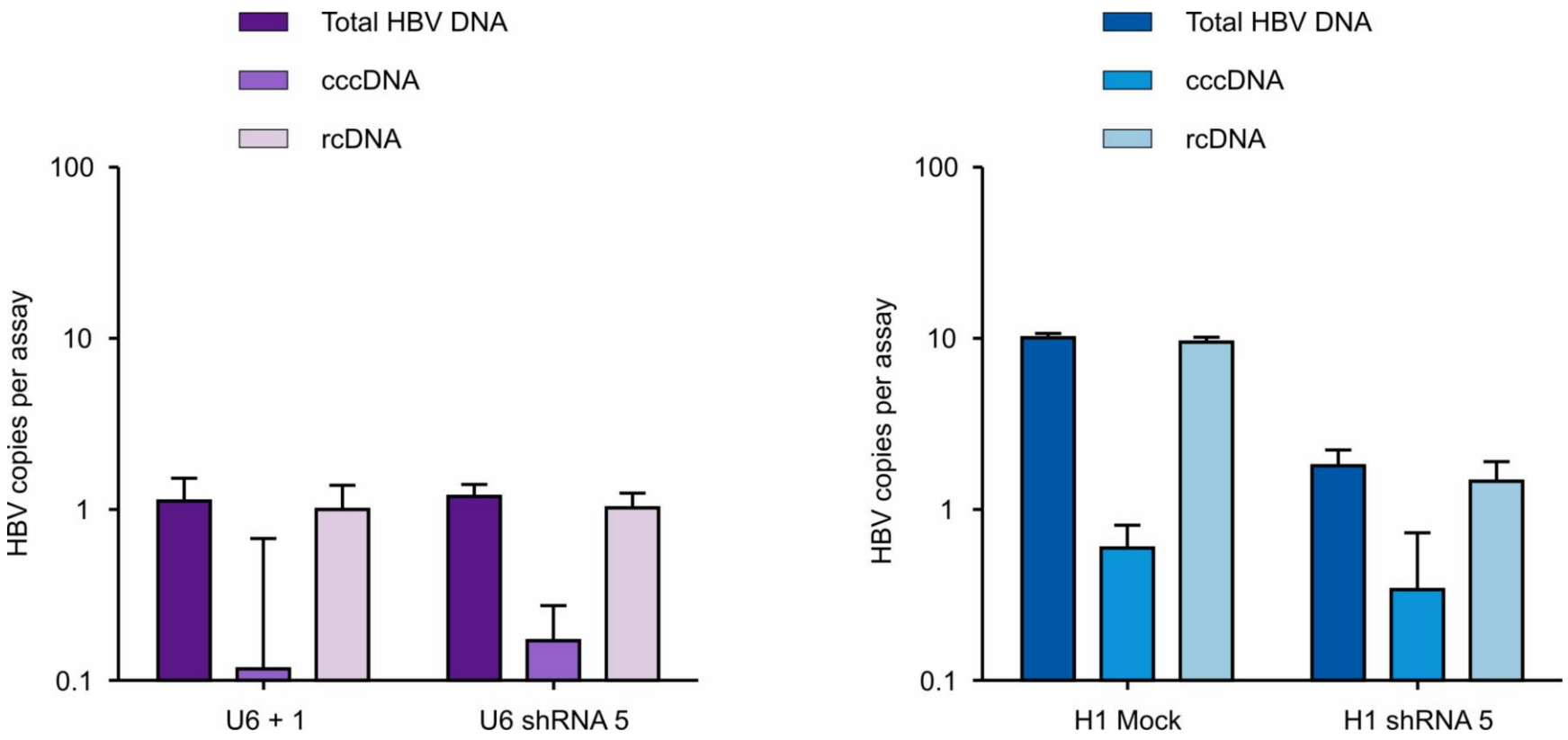


Figure 3.22: Quantification of U6 and H1 total HBV, cccDNA and rcDNA isolated from livers of mice subjected to HDI.

The amount of rcDNA was quantified in the liver of HDI mice treated using the HDI procedure. There was no significant difference between the control and experimental groups, however a trend of decrease is observed between H1 Mock and H1 shRNA 5 injected mice. The amount of rcDNA within the liver constitutes the majority of the total HBV DNA. Error bars indicate the standard normalized error of the mean (n=3).

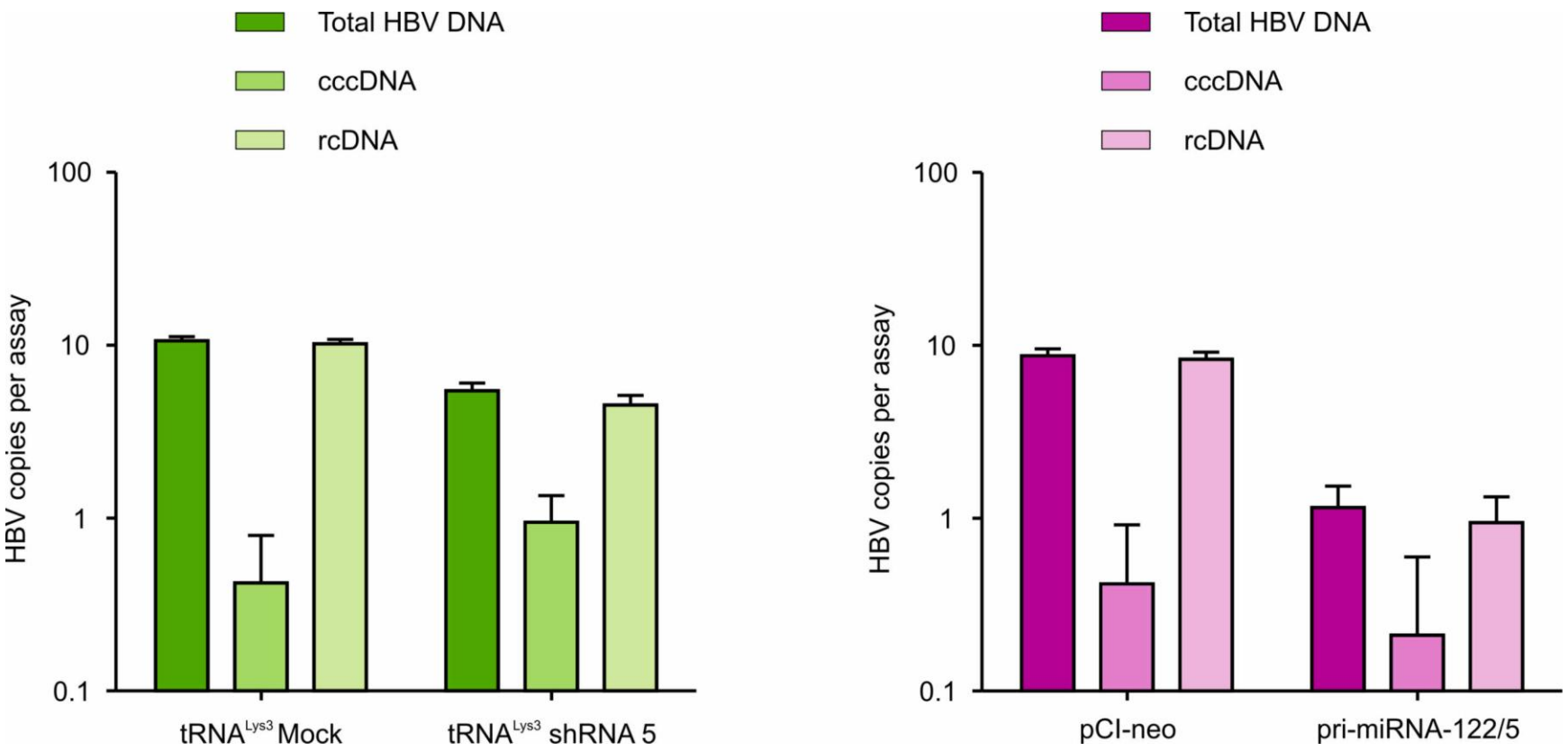


Figure 3.23: Quantification of $tRNA^{Lys3}$ and CMV total HBV, cccDNA and rcDNA isolated from livers of mice subjected to HDI.

There was no significant difference between the control and experimental groups, however the amount of rcDNA within the liver constitutes the majority of the total HBV DNA. Error bars indicate the standard normalized error of the mean (n=3).

4 DISCUSSION

Harnessing of the endogenous RNAi pathway through the introduction of exogenous effecter cassettes to target conserved regions within the HBV genome is proving to be a substantially effective approach to antiviral gene therapy.

McCaffrey *et al* (37) pioneered the initial use of RNAi *in vivo* to effectively target HBV. shRNAs with a guide sequence 25 bp in length and driven by the human U6 promoter were designed to target the four genes (core antigen, surface antigen, polymerase and X protein). The investigation showed a decrease of between 75-99% in HBV DNA, RNA, HBsAg and HBcAg. Numerous investigations into identifying a potent RNAi target, utilising different promoters (human U6 and H1 and mouse U6) to drive variable length shRNA constructs (reviewed in (21)) followed these initial findings. In 2006, Carmona *et al* (5) demonstrated effective inhibition of a particular HBV genotype in cultured cells and subsequently in an *in vivo* model. A potent RNAi sequence, which can rapidly silence target genes is essential in mediating effective knockdown of the virus.

In 2006, the effects of long-term shRNA expression in mice were assessed by (22). Following the administration of an AAV vector capable of continuously expressing shRNAs (200 copies per cell) targeted to HBV, dose-dependent liver injury and subsequent death were observed. It was determined that the exogenous shRNAs were competing with the endogenous miRNAs causing saturation of the RNAi pathway.

The current investigation aimed to assess the efficacy of three different Pol III promoters and a Pol II promoter to drive the expression of five different effecter cassettes targeted to

the conserved regions of *HBx,* without causing saturation of the endogenous RNAi pathway.

4.1 Efficacy of RNA Pol II and RNA Pol III promoter-driven effecter cassettes

In this study, the ability of five expression cassettes, each driven by one of four different promoters, to knockdown the *HBx* target was assessed. A definitive trend in target knockdown was established between the Pol III promoters U6, H1 and $tRNA^{Lys3}$ driving the effecter sequences targeting nucleotides 1575-1599 (shRNA 5). The effecter sequence targeting nucleotides 1580-1604 (shRNA 6) which has a 19 nucleotide overlap with shRNA 5 were effective in targeting *HBx* when driven by the U6 and H1 promoters. Similarly, the *in vitro* assay assessing the inhibition of HBsAg revealed that shRNA 5; pri-miRNA-122/5; shRNA 6 and pri-miRNA-122/6 caused significant inhibition, which was consistent with each of the four Pol II and Pol III promoters. Taken together it is clear that the effecter sequence cleaved from the shRNA 5 expression cassettes and pri-miRNA-122/5 shuttle were the greatest inhibitors of HBV, which correlates with previous findings (5, 15).

Published findings have generally compared U6 promoter-driven effecter cassettes with H1, $tRNA^{Lys3}$ or CMV promoter-driven effecter cassettes. There have been no investigations comparing efficacy of four different promoters expressing anti-HBV effecter sequences. Establishing the efficacy of these promoters to drive expression cassettes is important in that the lowest concentration of effecter required to cause optimal knockdown can be established. Furthermore, it is important to determine whether the expressed cassettes result in off-target or saturation effects due to the level of expression within a cell. The knockdown assays established that the effecter cassettes driven by the Pol III promoters U6 and H1 were the most efficacious in targeting HBV, however knockdown by

$tRNA^{Lys3}$ proved to be as effective as U6 and H1 when expressing shRNA 5. These data demonstrated that even when expressed at a lower level, the ability of the effecter sequence to target HBV was maintained, which is significant when considering a construct for utilisation in antiviral gene therapy.

4.2 Saturation and off-targeting

The endogenous RNAi pathway was assessed for potential saturation by the most effective exogenous effecter cassettes generated in this investigation. No derepression of the miR-16 target expression by the exogenous cassettes was observed, confirming there was no interference with the endogenous RNAi pathway. Notably, U6 shRNA 5 and $tRNA^{Lys3}$ shRNA 5 caused the least amount of interference. This was an important observation in that it demonstrated that at a high (U6 shRNA 5) and low level of expression ($tRNA^{Lys3}$ shRNA 5) there was no endogenous saturation. Taken together, this corroborates the previous findings in demonstrating the importance and usefulness of $tRNA^{Lys3}$ shRNA 5 as a suitable construct for antiviral gene therapy.

4.3 Processing of shRNA and pri-miRNA expression cassettes

Hybridisation of a radiolabelled probe complementary to the anti-HBV guide sequence detected processed products at 21 nt, demonstrating the processing of the guide strand from each of the promoter-driven expression cassettes occurred according to the intended design. Furthermore, the detection of these processed products showed that the guide strand was being selected for the incorporation into RISC. The expression level and processing of the guide strands from the U6 shRNA 5 and pri-miRNA-122/5 cassettes, assessed by northern blot hybridisation supported previous findings (15). The expression levels of the H1 and $tRNA^{Lys3}$ shRNA 5 precursors were considerably lower when compared to U6 shRNA 5 precursor. These findings support the notion that H1 and

tRNA^{Lys3} express at a lower level. Notably, the precursor denoting the pre-tRNA^{Lys3}-shRNA 5 demonstrated no effect on the processing of the shRNA, or the guide sequence from the tRNA. Notably, the majority of the expressed U6 shRNA 5 was not processed, indicating the inability of Dicer to process the shRNAs as quickly as they were transcribed. Although there was no detectable saturation of the endogenous RNAi pathway at 48 hours, the accumulation of these shRNAs could cause potential interference in the export pathway following long-term expression. H1 and tRNA^{Lys3} shRNA 5 were processed at lower level, which allowed for the majority of the effecter cassettes to be processed. Pri-miRNA-122/5 was processed at a rate equivalent to that of effecter cassette expression, which supported previous findings (15).

Comparative analysis of the nuclear and cytoplasmic compartments for the presence of processed effecter cassettes proved challenging. Contamination of the cytoplasmic fraction with nuclear RNA occurred within every fractionation, suggesting lysis of the nuclei prior to separation of the fractions. The initial lysing of the plasma membrane may cause indirect lysis of the nuclei through the shearing forces associated with the resuspension of the cell pellet with the lysis buffer. Alternatively, centrifugation of the mixture may cause released intact nuclei to lyse. The findings established that the majority of the expressed cassettes were localised within the cytoplasm and not the nucleus, which was expected as the shRNAs are transported out of the nucleus by exportin-5 and processed by Dicer in the cytoplasm of cells.

4.4 *In vivo* Efficacy

Previous comparisons between U6 and tRNA^{Lys3} expressed effecter cassettes by Scherer *et al* (45) demonstrated a comparable efficacy of Dicer processing and incorporation of the guide strand into the RISC complex between the expressed constructs. Furthermore, the

comparison of U6 and $tRNA^{Val}$ expressed effecter cassettes by Kawasaki in 2003 (27) established the processing of the tRNA-dsDNA to be significantly efficacious. Taken together these findings are supported by the data obtained after transfection of cells in culture, which identified U6 shRNA 5 and $tRNA^{Lys3}$ shRNA 5 as the most efficacious anti-HBV effecter cassettes.

The possibility exists that the established efficacy of an anti-HBV effecter cassette found to function optimally *in vitro* could function with less efficacy when introduced to an *in vivo* environment*. In vivo* analysis of the shRNA 5 expression cassettes and pri-miRNA-122/5 shuttle substantiated this hypothesis. The knockdown efficacy by U6 shRNA 5 and pri-miRNA-122/5 proved effective for an initial 72 hours, however the inability of the effecter cassette to maintain consistent knockdown was evident 120 hours post injection. As previously found, U6 is a highly potent promoter and the effecter sequences are incapable of being processed at a rate equivalent to that at which they are expressed. Based on this, it can be deduced that the increased amount of exogenous shRNAs within the cytoplasm of cells resulted in the activation of the innate immune response. Alternatively, it could be associated with the variable delivery of DNA to the liver. H1 and $tRNA^{Lys3}$ shRNA 5 which are expressed at a consistently low level, caused significant inhibition of HBV in sera 72 hours post injection, which continued to increase 120 hours post injection. The increase in inhibition indicates the shRNAs are being expressed at a rate, which is optimal for the processing machinery of the endogenous RNAi pathway. These findings were supported by the observations in the liver of the mice. Overall, the *in vivo* findings found RNA^{Lys3} to be the most effective in targeting HBV, which supported the findings observed in cultured cells.

5 CONCLUSIONS

The preliminary investigation has found $tRNA^{Lys3}$ shRNA 5 to be the most effective expression cassette to target and silence HBV *in vitro* and *in vivo* when compared the remaining RNAi effecter sequences. The ability of $tRNA^{Lys3}$ to express the effecter cassettes at a lower level whilst maintaining knockdown which was comparable to stronger promoters (U6 and CMV) and at times more efficient than these promoters, has defined the importance of this construct as a novel approach towards antiviral gene therapy. The primary *in vivo* investigations provided an insight into how exogenous expression cassettes function within a living organism expressing HBV over a short period of time. A plethora of investigations have assessed short-term expression of effecter cassettes, however the efficacy and duration of expression should be assessed over extended time periods.

The investigation identified the RNAi effecter sequences (5 and 6) to be highly effective in targeting and inhibiting HBV when assessed in cell culture. The ability of these effecter sequences to silence HBV even when expressed at lower levels by H1 and $tRNA^{Lys3}$ demonstrated the potency of these expression cassettes. This is of importance, as it supports the requirement of optimal silencing at lower expression levels.

It would be advisable to assess the effects of $tRNA^{Lys3}$ shRNA 5 in a transgenic mouse model, which actively expresses HBV. Alternatively, a natural host of HBV such as the woodchuck would prove even more efficacious as an *in vivo* model. This would allow a baseline of initial infection (circulating viral particles) to be established before administering the therapeutic construct. Furthermore, as this investigation has shown, a lower target to effecter ratio (1:0.1) was as effective as a higher target to effecter ration (1:10) at knocking down HBV, thus administration of a lower effecter dose warrants investigation.

Antiviral gene therapy is redirecting the way research therapeutics is approached. There are particular aspects associated with the treatment by antiviral gene therapy, which require further research. A combinatorial approach investigating the effects of combining H1 and $tRNA^{Lys3}$ promoter-driven effecter cassettes could be assessed. Combinatorial therapy of multi expressing cassettes would allow two different effecter sequences to be individually expressed by a low transcriptional promoter and may prove more effective in long-term therapy. Furthermore, combinatorial therapy has the important advantage of limiting the emergence of escape mutants because multiple gene sites are targeted, which renders it unlikey that the virus could mutate at all of the target sites. The delivery of therapeutic constructs to liver is of particular importance. The introduction of exogenous effecter cassettes via viral vectors, (adenoviruses, AAVs and lentiviruses), is being pursued as a possible vehicle for site-specific delivery. Adenoviruses and AAVs are particularly efficient in transducing hepatocytes, which would allow stable expression of the effecter sequences at a localised area, thereby prohibiting toxicity effects (20, 22). Exploitation of the RNAi pathway is paving the way in therapeutic approaches (42), and an advance in targeting HBV is progressing.

6 REFERENCES

1. **Baer, M., T. W. Nilsen, C. Costigan, and S. Altman.** 1990. Structure and transcription of a human gene for H1 RNA, the RNA component of human RNase P. Nucleic Acids Res **18:**97-103.

2. **Bloom, K.** 2010. The design and application of a Real Time PCR Assay to assess rcDNA abd cccDNA produced by HBV during infection. . Thesis Dissertation**:**1-106.

3. **Bogenhagen, D. F., and D. D. Brown.** 1981. Nucleotide sequences in Xenopus 5S DNA required for transcription termination. Cell **24:**261-70.

4. **Busch, H., M. Muramatsu, H. Adams, W. J. Steele, M. C. Liau, and K. Smetana.** 1963. Isolation of Nucleoli. Exp Cell Res **24:**SUPPL9:150-63.

5. **Carmona, S., A. Ely, C. Crowther, N. Moolla, F. H. Salazar, P. L. Marion, N. Ferry, M. S. Weinberg, and P. Arbuthnot.** 2006. Effective inhibition of HBV replication in vivo by anti-HBx short hairpin RNAs. Mol Ther **13:**411-21.

6. **Castanotto, D., H. Li, and J. J. Rossi.** 2002. Functional siRNA expression from transfected PCR products. Rna **8:**1454-60.

7. **Chambon, P.** 1975. Eukaryotic nuclear RNA polymerases. Annu Rev Biochem **44:**613-38.

8. **Chang, Z., S. Westaway, S. Li, J. A. Zaia, J. J. Rossi, and L. J. Scherer.** 2002. Enhanced expression and HIV-1 inhibition of chimeric tRNA(Lys3)-ribozymes under dual U6 snRNA and tRNA promoters. Mol Ther **6:**481-9.

9. **Chattopadhyay, S., A. Ely, K. Bloom, M. S. Weinberg, and P. Arbuthnot.** 2009. Inhibition of hepatitis B virus replication with linear DNA sequences expressing antiviral micro-RNA shuttles. Biochem Biophys Res Commun **389:**484-9.

10. **Chen, J. F., E. M. Mandel, J. M. Thomson, Q. Wu, T. E. Callis, S. M. Hammond, F. L. Conlon, and D. Z. Wang.** 2005. The role of microRNA-1 and microRNA-133 in skeletal muscle proliferation and differentiation. Nature genetics **38:**228-233.

11. **Chen, M., L. Zhang, H. Y. Zhang, X. Xiong, B. Wang, Q. Du, B. Lu, C. Wahlestedt, and Z. Liang.** 2005. A universal plasmid library encoding all permutations of small interfering RNA. Proc Natl Acad Sci U S A **102:**2356-61.

12. **Chisari, F. V., C. Ferrari, and M. U. Mondelli.** 1989. Hepatitis B virus structure and biology. Microb Pathog **6:**311-25.

13. **Elbashir, S. M., J. Harborth, W. Lendeckel, A. Yalcin, K. Weber, and T. Tuschl.** 2001. Duplexes of 21-nucleotide RNAs mediate RNA interference in cultured mammalian cells. Nature **411:**494-8.

14. **Ely, A., T. Naidoo, and P. Arbuthnot.** 2009. Efficient silencing of gene expression with modular trimeric Pol II expression cassettes comprising microRNA shuttles. Nucleic Acids Res **37:**e91.

15. **Ely, A., T. Naidoo, S. Mufamadi, C. Crowther, and P. Arbuthnot.** 2008. Expressed anti-HBV primary microRNA shuttles inhibit viral replication efficiently in vitro and in vivo. Mol Ther **16:**1105-12.

16. **Fire, A., S. Xu, M. K. Montgomery, S. A. Kostas, S. E. Driver, and C. C. Mello.** 1998. Potent and specific genetic interference by double-stranded RNA in Caenorhabditis elegans. Nature **391:**806-11.

17. **Gearhart, T. L., and M. J. Bouchard.** 2010. The Hepatitis B Virus X Protein Modulates Hepatocyte Proliferation Pathways to Stimulate Viral Replication. J Virol **84:**2675-86.

18. **Giering, J. C., D. Grimm, T. A. Storm, and M. A. Kay.** 2008. Expression of shRNA from a tissue-specific pol II promoter is an effective and safe RNAi therapeutic. Mol Ther **16:**1630-6.

19. **Gillman, M.** 2000. Preparation of RNA from Eukaryotic and Prokaryotic cells. F. M. Ausubel, R. Brent, R. E. Kingston *et al*. John Wiley & Sons, Inc. . Current Protocols in Molecular Biology. **1:**4.1.2-4.1.5.

20. **Grimm, D., and M. A. Kay.** 2007. Combinatorial RNAi: a winning strategy for the race against evolving targets? Mol Ther **15:**878-88.

21. **Grimm, D., and M. A. Kay.** 2006. Therapeutic short hairpin RNA expression in the liver: viral targets and vectors. Gene Ther **13:**563-75.

22. **Grimm, D., K. L. Streetz, C. L. Jopling, T. A. Storm, K. Pandey, C. R. Davis, P. Marion, F. Salazar, and M. A. Kay.** 2006. Fatality in mice due to oversaturation of cellular microRNA/short hairpin RNA pathways. Nature **441:**537-41.

23. **Han, J., J. S. Pedersen, S. C. Kwon, C. D. Belair, Y. K. Kim, K. H. Yeom, W. Y. Yang, D. Haussler, R. Blelloch, and V. N. Kim.** 2009. Posttranscriptional crossregulation between Drosha and DGCR8. Cell **136:**75-84.

24. **He, L., and G. J. Hannon.** 2004. MicroRNAs: small RNAs with a big role in gene regulation. Nature Reviews Genetics **5:**522-531.

25. **Helm, M., and G. Attardi.** 2004. Nuclear control of cloverleaf structure of human mitochondrial tRNA(Lys). J Mol Biol **337:**545-60.

26. **Karayiannis, P.** 2003. Hepatitis B virus: old, new and future approaches to antiviral treatment. J Antimicrob Chemother **51:**761-85.

27. **Kawasaki, H., and K. Taira.** 2003. Short hairpin type of dsRNAs that are controlled by tRNA(Val) promoter significantly induce RNAi-mediated gene silencing in the cytoplasm of human cells. Nucleic Acids Res **31:**700-7.

28. **Kim, D. H., and J. J. Rossi.** 2007. Strategies for silencing human disease using RNA interference. Nat Rev Genet **8:**173-84.

29. **Kunkel, G. R., R. L. Maser, J. P. Calvet, and T. Pederson.** 1986. U6 small nuclear RNA is transcribed by RNA polymerase III. Proc Natl Acad Sci U S A **83:**8575-9.

30. **Kutay, U., G. Lipowsky, E. Izaurralde, F. R. Bischoff, P. Schwarzmaier, E. Hartmann, and D. Gorlich.** 1998. Identification of a tRNA-specific nuclear export receptor. Mol Cell **1:**359-69.

31. **Lee, Y., C. Ahn, J. Han, H. Choi, J. Kim, J. Yim, J. Lee, P. Provost, O. Radmark, S. Kim, and V. N. Kim.** 2003. The nuclear RNase III Drosha initiates microRNA processing. Nature **425:**415-9.

32. **Lee, Y., K. Jeon, J. T. Lee, S. Kim, and V. N. Kim.** 2002. MicroRNA maturation: stepwise processing and subcellular localization. Embo J **21:**4663-70.

33. **Lee, Y., M. Kim, J. Han, K. H. Yeom, S. Lee, S. H. Baek, and V. N. Kim.** 2004. MicroRNA genes are transcribed by RNA polymerase II. Embo J **23:**4051-60.

34. **Lipowsky, G., F. R. Bischoff, E. Izaurralde, U. Kutay, S. Schafer, H. J. Gross, H. Beier, and D. Gorlich.** 1999. Coordination of tRNA nuclear export with processing of tRNA. Rna **5:**539-49.

35. **Makinen, P. I., J. K. Koponen, A. M. Karkkainen, T. M. Malm, K. H. Pulkkinen, J. Koistinaho, M. P. Turunen, and S. Yla-Herttuala.** 2006. Stable RNA interference: comparison of U6 and H1 promoters in endothelial cells and in mouse brain. J Gene Med **8:**433-41.

36. **Martinez, J., A. Patkaniowska, H. Urlaub, R. Luhrmann, and T. Tuschl.** 2002. Single-stranded antisense siRNAs guide target RNA cleavage in RNAi. Cell **110:**563-74.

37. **McCaffrey, A. P., H. Nakai, K. Pandey, Z. Huang, F. H. Salazar, H. Xu, S. F. Wieland, P. L. Marion, and M. A. Kay.** 2003. Inhibition of hepatitis B virus in mice by RNA interference. Nat Biotechnol **21:**639-44.

38. **Napoli, C., C. Lemieux, and R. Jorgensen.** 1990. Introduction of a Chimeric Chalcone Synthase Gene into Petunia Results in Reversible Co-Suppression of Homologous Genes in trans. Plant Cell **2:**279-289.

39. **Nassal, M., M. Junker-Niepmann, and H. Schaller.** 1990. Translational inactivation of RNA function: discrimination against a subset of genomic transcripts during HBV nucleocapsid assembly. Cell **63:**1357-63.

40. **Neurath, A. R., S. B. Kent, N. Strick, and K. Parker.** 1986. Identification and chemical synthesis of a host cell receptor binding site on hepatitis B virus. Cell **46:**429-36.

41. **Neurath, A. R., B. Seto, and N. Strick.** 1989. Antibodies to synthetic peptides from the preS1 region of the hepatitis B virus (HBV) envelope (env) protein are virus-neutralizing and protective. Vaccine **7:**234-6.

42. **Oshima, K., H. Kawasaki, Y. Soda, K. Tani, S. Asano, and K. Taira.** 2003. Maxizymes and small hairpin-type RNAs that are driven by a tRNA promoter

specifically cleave a chimeric gene associated with leukemia in vitro and in vivo. Cancer Res **63:**6809-14.

43. **Paran, N., B. Geiger, and Y. Shaul.** 2001. HBV infection of cell culture: evidence for multivalent and cooperative attachment. Embo J **20:**4443-53.

44. **Passman, M., M. Weinberg, M. Kew, and P. Arbuthnot.** 2000. In situ demonstration of inhibitory effects of hammerhead ribozymes that are targeted to the hepatitis Bx sequence in cultured cells. Biochem Biophys Res Commun **268:**728-33.

45. **Scherer, L. J., R. Frank, and J. J. Rossi.** 2007. Optimization and characterization of tRNA-shRNA expression constructs. Nucleic Acids Res **35:**2620-8.

46. **Scherer, L. J., Y. Yildiz, J. Kim, L. Cagnon, B. Heale, and J. J. Rossi.** 2004. Rapid assessment of anti-HIV siRNA efficacy using PCR-derived Pol III shRNA cassettes. Mol Ther **10:**597-603.

47. **Seeger, C., and W. S. Mason.** 2000. Hepatitis B virus biology. Microbiol Mol Biol Rev **64:**51-68.

48. **Shibata, S., M. Sasaki, T. Miki, A. Shimamoto, Y. Furuichi, J. Katahira, and Y. Yoneda.** 2006. Exportin-5 orthologues are functionally divergent among species. Nucleic Acids Res **34:**4711-21.

49. **Starkey, J. L., E. F. Chiari, and H. C. Isom.** 2009. Hepatitis B virus (HBV)-specific short hairpin RNA is capable of reducing the formation of HBV covalently closed circular (CCC) DNA but has no effect on established CCC DNA in vitro. J Gen Virol **90:**115-26.

50. **van der Krol, A. R., L. A. Mur, M. Beld, J. N. Mol, and A. R. Stuitje.** 1990. Flavonoid genes in petunia: addition of a limited number of gene copies may lead to a suppression of gene expression. Plant Cell **2:**291-9.

51. **Weinberg, M. S., A. Ely, S. Barichievy, C. Crowther, S. Mufamadi, S. Carmona, and P. Arbuthnot.** 2007. Specific inhibition of HBV replication in vitro and in vivo with expressed long hairpin RNA. Mol Ther **15:**534-41.

52. **Weinberg, M. S., A. Ely, M. Passman, S. M. Mufamadi, and P. Arbuthnot.** 2007. Effective anti-hepatitis B virus hammerhead ribozymes derived from multimeric precursors. Oligonucleotides **17:**104-12.

53. **Weinberg, M. S., and J. J. Rossi.** 2005. Comparative single-turnover kinetic analyses of trans-cleaving hammerhead ribozymes with naturally derived non-conserved sequence motifs. FEBS Lett **579:**1619-24.

54. **Wienholds, E., W. P. Kloosterman, E. Miska, E. Alvarez-Saavedra, E. Berezikov, E. de Bruijn, H. R. Horvitz, S. Kauppinen, and R. H. A. Plasterk.** 2005. MicroRNA expression in zebrafish embryonic development. Science **309:**310.

55. **Yeom, K. H., Y. Lee, J. Han, M. R. Suh, and V. N. Kim.** 2006. Characterization of DGCR8/Pasha, the essential cofactor for Drosha in primary miRNA processing. Nucleic Acids Res **34:**4622-9.

56. **Ying, R. S., C. Zhu, X. G. Fan, N. Li, X. F. Tian, H. B. Liu, and B. X. Zhang.** 2007. Hepatitis B virus is inhibited by RNA interference in cell culture and in mice. Antiviral Res **73:**24-30.

57. **Zeng, Y., R. Yi, and B. R. Cullen.** 2003. MicroRNAs and small interfering RNAs can inhibit mRNA expression by similar mechanisms. Proc Natl Acad Sci U S A **100:**9779-84.

58. **Zhou, H., C. Huang, and X. G. Xia.** 2008. A tightly regulated Pol III promoter for synthesis of miRNA genes in tandem. Biochim Biophys Acta **1779:**773-9.

59. **Zoulim, F., J. Saputelli, and C. Seeger.** 1994. Woodchuck hepatitis virus X protein is required for viral infection in vivo. J Virol **68:**2026-30.

APPENDIX A

A.1 Preparation of Agarose Gels

Agarose (WhiteSci, Cape Town, RSA) was weighed into a clean 500 ml Erlenmeyer flask and reconstituted with 1× Tris-acetate-EDTA (TAE) buffer (Appendix A.1.1). The mixture was boiled to ensure complete dissolution of the agarose before being poured into a prepared casting tray and allowed to set. The samples, which were to be subjected to electrophoresis, were mixed with 6× Orange Loading Dye (Fermentas, MD, USA) at a ratio of 1:5 and loaded into the wells of the gel. Ten microliters of O'Gene Rule 100 bp DNA ladder (Fermentas, MD, USA) was always loaded into lane 1 of the gels. The DNA fragments were viewed under UV light and the resultant images captured (Gel Logic 200 Imaging System, Kodak, NY, USA).

A.1.1 50× Tris-acetate-EDTA (TAE) Buffer

Tris base (240 g) was dissolved in 500 ml sterile water. One hundred millilitres of EDTA (0.5 M; pH 8.0) and 57 ml glacial acetic acid were added and the buffer was made up to 1000 millilitres with sterile water. The buffer was stored at room temperature. To prepare 1× TAE buffer, 20 ml of 50× TAE buffer was added to 980 ml sterile water (40 mM Tris-acetate; 1 mM EDTA).

A.2 Extraction of DNA - Qiagen MinElute™ Gel Extraction

The weight of the agarose gel slice was determined and three times the volume of Buffer QG added and the solution incubated in a dry heating block at 42°C for 15 minutes. The microcentrifuge tube was vortexed every two minutes. Once the gel slice was completely dissolved, isoproponal equal to the weight of the gel slice was added and the microcentrifuge tube gently inverted ten times to ensure thorough mixing. The sample

mixture was transferred into a MinElute™ column, which had been placed in a collection tube. The MinElute™ column was centrifuged at 16 000 × g for one minute allowing the DNA to bind to the column. The flow-through was discarded and 500 µl Buffer QG was added to the column. The column was centrifuged for one minute, the flow-through discarded and 750 µl Buffer PE added. The column was centrifuged for one minute and the flow-through discarded. The column was centrifuged again for one minute to ensure any residual ethanol from the Buffer was removed. The MinElute™ column was transferred to a sterile microcentrifuge tube and 20 µl Buffer EB was added to the centre of the column membrane to ensure the maximum yield of DNA was recovered. The MinElute™ column was centrifuged for one minute before being discarded. Working stocks were prepared from the purified DNA and stored at -20°C.

A.3 Preparation of Chemically Competent DH5-α *E.coli* Cells

A culture of bacterial cells was prepared by adding 50 µl of either DH5-α or XL1-blue stock to 10 ml of LB (Appendix A.3.1) before overnight incubation in a shaking incubator at 37°C. A control culture containing ampicillin (Appendix A.3.2) at a final concentration of 100 µg/ml was included. A 1:50 ratio of overnight culture and fresh LB broth was prepared in 50 ml Falcon tubes and incubated for two hours in a shaking incubator at 37°C. The tubes were centrifuged at 1200 × g for 15 minutes. The supernatant was removed and the pellet resuspended in 1 ml transformation buffer (Appendix A.3.3). The resuspension mixture was made up to 20 ml with transformation buffer and incubated on ice for 30 minutes before being centrifuged at 760 × g for 10 minutes at 4°C. The supernatant was removed and the pellet resuspended in 1.5 ml transformation buffer. One hundred microlitre aliquots were prepared and stored at -70°C.

A.3.1 Luria-Bertani Broth (LB Broth)

Bacto-tryptone (10 g), yeast extract (5 g) and NaCl (5 g) were dissolved in 1000 ml sterile water. The broth was autoclaved and stored at room temperature.

A.3.2 1000× Ampicillin

One gram of ampicillin was dissolved in a mixture of 5 ml ethanol and 5 ml sterile water and stored at -20°C.

A.3.3 Transformation Buffer

$CaCl_2.2H_2O$ (1.4702 g), PIPES.HCl (0.3024 g) and 15 ml glycerol were dissolved in 80 ml sterile water. The solution was adjusted to pH7.00 with NaOH. The buffer was made up to 100 ml with sterile water and autoclaved. The buffer was stored at -20°C.

A.4 LB Amp Agar Plates

Ten grams of agar was dissolved in 1000 ml LB broth, autoclaved and cooled to 50°C. Ampicillin was added to the LB agar to a final concentration of 100 µg/ml before being poured into sterile Petri dishes. The plates were stored at 4°C until required

A.5 X-gal (5-bromo-4-chloro-3-indolyl-beta-D-galactopyranoside)

Twenty milligrams of X-gal was dissolved in 1 ml dimethyl formamide and stored at -20°C in foil.

A.6 IPTG (isopropyl thiogalactoside)

One hundred milligrams of IPTG was dissolved in to 1 ml sterile water, filter sterilised and stored at -20°C.

A.7 Blue-white Screening

pTZ57R incorporates the lac operon, which is induced by IPTG to express β-galactosidase. This enzyme metabolises lactose substrates into galactose and glucose products. X-gal is a modified colourless galactose sugar, which releases blue products during enzymatic breakdown. The insertion of DNA into the MCS of pTZ57R causes a disruption in the *lacZ* gene, which results in production of dysfunctional β-galactosidase. The inability of the dysfunctional β-galactosidase to metabolise X-gal causes the colony to remain white, which allows colonies transformed with successfully cloned plasmids to be identified.

A.8 Extraction of pDNA - Roche High Pure Plasmid Isolation

Four milliliters of LB was inoculated with a colony containing the plasmid of interest and incubated overnight at 37°C. The tubes were centrifuged at 1200 × g for 15 minutes to pellet the bacterial cells. The supernatants were discarded and the tubes blotted on paper towel to remove any residual broth. The pellets were gently resuspended in 250 µl Suspension Buffer and transferred to sterile microcentrifuge tubes. The bacterial cells were lysed with 250 µl Lysis Buffer and the microcentrifuge tubes were inverted ten times to ensure thorough mixing. The lysis reaction was neutralised with 350 µl chilled Neutralisation Buffer and the microcentrifuge tubes inverted to ensure thorough mixing. The microcentrifuge tubes were centrifuged at 16 000 × g and the supernatants transferred into a High Pure Filter tube, which had been placed in a collection tube. The filter tubes were centrifuged at 16 000 × g for one minute, allowing the DNA to bind to the columns. The flow-through was discarded and 700 µl Wash Buffer I added to the columns. The columns were centrifuged at 16 000 × g for one minute and the flow-through discarded. The columns were centrifuged at 16 000 × g for one minute to ensure any residual ethanol

from the Wash Buffer I was removed before being transferred to sterile microcentrifuge tubes. One hundred microlitres Elution Buffer was added and the columns centrifuged at 16 000 × g for one minute. DNA working stocks of 100 ng/µl were prepared and stored at -20°C. The concentrations of DNA (ng/µl) were measured at 260 nm.

A.9 Automated Cycle Sequencing

Specific PCR amplicons were sequenced on a SpectruMedix model SCE 2410 automated sequencer (SpectruMedix, State College, PA) using the ABI Big Dye Terminator Cycle Sequencing Kit (Applied Biosystems, CA, USA) according to manufacturers instructions (Appendix A.9.1). Briefly, the PCR products were sequenced using the M13 forward primer, which determined the sequence region preceding the expression cassettes and pri-miRNA shuttle sequences (Inqaba, Pretoria, RSA).

A.9.1 ABI Big Dye Terminator Cycle Sequencing Kit

The amplicons to be sequenced were prepared in a final reaction volume of 10 µl containing 100 ng plasmid DNA, 2 µl 2.5× Ready Reaction Premix, 1 µl 5× BigDye Sequencing Buffer and 10 pmol M13 forward or reverse primers. The PCR was programmed to run with an initial denaturation at 96°C for 1 minute with 25 cycles of ‘sequencing’ PCR (denaturation at 96°C for 10 seconds; annealing at 50°C for 5 seconds and elongation at 60°C for four minutes).

A.10 Isolation of Plasmid DNA by standard Alkaline Lysis

Four millilitres of LB broth was inoculated with a single bacterial colony containing the plasmid of interest and incubated overnight at 37°C. The cultures were centrifuged at 1200 × g for 15 to pellet the bacterial cells. The supernatants were discarded and the tubes

blotted on paper towel to remove any residual broth. The pellets were gently resuspended in 300 µl resuspension buffer (50 mMTris-HCl, pH 8.0; 10 mM EDTA and 100 µg/ml RNase A) and transferred to sterile microcentrifuge tubes. The bacterial cells were lysed with 300 µl of lysis buffer (1% SDS (w/v); 200 mM NaOH) and the microcentrifuge tubes were inverted ten times to ensure thorough mixing. The lysates were neutralised with 300 µl chilled neutralisation buffer (3.0 M potassium acetate, pH 5.5) and the microcentrifuge tubes inverted ten times to ensure thorough mixing before being centrifuged at 16 000 × g for 20 minutes at 4°C. The supernatant was transferred into a sterile microcentrifuge tube and 750 µl isoproponal was added. The microcentrifuge tubes were inverted ten times to ensure complete mixing before being stored overnight at -20°C. The DNA was pelleted by centrifugation at 16 000 × g for 30 minutes at 4°C. The supernatant was removed and 250 µl 70% ethanol was added. The microcentrifuge tubes were centrifuged at 16 000 × g for 5 minutes. The ethanol was removed and the DNA pellet allowed to air dry. The pellet was resuspended in 50 µl nuclease free water and the DNA stored at -20°C. The concentrations of DNA (ng/µl) were measured at 260 nm.

A.11 Promega Dual Luciferase™ Assay

The media was removed from transfected cells and the cells lysed with 100 µl 1 × Passive Lysis Buffer and incubated for 20 minutes at 37°C. The lysed cells were aspirated and 10 µl of each sample was added into a 96 well microplate (Corning, MA, USA). The required amount of Luciferase Assay Reagent II (LAR II), which measures the Firefly luciferase expression, was calculated at 50 µl/well. The required amount of Stop ’n Glo Reagent, which measures the background expression of *Renilla* luciferase, was calculated at 50 µl/well. The ratio of Firefly luciferase to *Renilla* luciferase was measured using the Veritas Microplate Luminometer (Turner Biosystems, CA, USA).

A.12 HBsAg Detection - MONOLISA® Ag HBs PLUS Kit

One hundred microlitres of positive control (R4), 100 µl negative control (R3) and 100 µl of samples were aliquoted into the appropriate microplate wells. Fifty microlitres of conjugate solution (R6 and R7) was dispensed into the sample-containing wells. The plate was covered in adhesive film and incubated at 37°C for one hour followed by washing with a PW40 microplate washer (Sanofi Pasteur Diagnostics, MN, USA) using 1× Wash solution (R2) on the TO2 N5B0.5s 800 cycle. The enzymatic development solution was prepared (R8 and R9) and 100 µl dispensed into each well. The microplate was incubated in the dark, at room temperature for 30 minutes before 100 µl of stopping solution (R10) was dispensed into the wells. The microplate was read at an optical density of 490/655 nm.

A.13 Calcium chloride (2.5 M)

$CaCl_2.2H_2O$ (183.7 g) was dissolved in 500 ml sterile water. The solution was sterilised through a 0.45 µm filter and stored at -20 °C.

A.14 2 × HEPES Buffer

NaCl (16.4 g), HEPES (11.9 g) and Na_2PO_4 (0.21 g) were dissolved in 800 ml sterile water. The solution was adjusted to pH 7.05 with NaOH and the volume made up to 1000 ml with sterile water. The solution was sterilised through a 0.45 µm filter and stored at -20 °C.

A. 15 Cellular Fractionation Method 1

Huh7 cells were prepared as previously described (Section 2.8). The supernatant was removed and the pellet resuspended in 375 µl ice-cold Lysis Buffer (100 mM NaCl; 5 mM $MgCl_2$; 0.5% v/v Nonidet P-40; 50 mM Tris-HCl) and stored on ice for ten minutes. The

samples were centrifuged at 16 000 × g for two minutes at 4°C. The supernatant (cytoplasmic fraction) was aspirated and transferred to a sterile microcentrifuge tube. The pellet (nuclear fraction) was resuspended in 100 µl saline (19). RNA was isolated from the fractionations as previously described (Section 2.7).

A.16 Cellular Fractionation Method 2

Huh7 cells were prepared as previously described (Section 2. 8). The supernatant was removed and resuspended in 450 µl ice-cold Buffer A (10 mM HEPES, pH 7.9; 10 mM KCl; 1 mM DTT; 0.1 M EDTA, pH 8.0) and stored on ice for 25 minutes. The samples were centrifuged at 2300 × g for three minutes at 4°C. The supernatant (cytoplasmic fraction) was aspirated and transferred to a sterile microcentrifuge tube. The pellet (nuclear fraction) was resuspended in 100 µl saline (23). RNA was isolated from the fractions as previously described (Section 2.7).

A.17 Cellular Fractionation Method 3

Huh7 cells were prepared as previously described (Section 2. 8). The supernatant was removed and the pellet resuspended in one millilitre of ice-cold Buffer A (10 mM HEPES, pH 7.9; 1.5 mM $MgCl_2$; 10 mM KCl; 0.5 mM DTT) and stored on ice for five minutes. Resuspended cells were homogenised with 20 strokes of a sterile pre-chilled Dounce homogeniser and transferred to a sterile microcentrifuge tube. The samples were centrifuged at 100 × g for five minutes at 4°C. The supernatant was removed and retained as the cytoplasmic fraction. The pellet containing the nuclear fraction was resuspended in 600 µl Buffer S1 (0.25 M Sucrose; 10 mM $MgCl_2$) and layered over 600 µl Buffer S3 (0.88 mM Sucrose; 0.5 mM $MgCl_2$). The nuclear fraction was centrifuged at 120 × g for ten minutes at 4°C. The cytoplasmic and nuclear fractions were resuspended in 200 µl and 800 µl 1× RIPA Buffer (50 mM Tris, pH 7.5; 150 mM NaCl; 1% Nonidet P-40; 0.5%

Deoxycholate) respectively and centrifuged at 120 × g for ten minutes at 4°C. (Protocol modified from (4)). The purified fractions were transferred into sterile microcentrifuge tubes and RNA isolated as previously described (Section 2.7).

A.18 Extraction of RNA from nuclear and cytoplasmic fractions - PARIS™ Kit

Two hundred and fifty microlitres of the lysate (nuclear or cytoplasmic) was added to 250 µl 2 × Lysis/Binding solution in a sterile microcentrifuge tube and mixed gently by inverting the tubes four times. Two hundred and fifty microlitres of absolute ethanol was added to the mixture and the microcentrifuge tubes were inverted four times to ensure thorough mixing. The sample mixture was added to a Filter Cartridge assembled in a sterile Collection Tube and centrifuged at 500 × g for one minute at 25°C. The flow through was discarded, 700 µl of Wash Solution 1 added to the Filter Cartridge and centrifuged at 500 × g for one minute at 25°C. The procedure was repeated with 500 µl of Wash Solution 2 and then Wash Solution 3. The Filter Cartridge was placed into a sterile Collection Tube. Fifty microlitres of hot Elution Solution (95°C) was added to the Filter Cartridge in sequential aliquots of 40µl and 10 µl and centrifuged at 500 × g for 30 seconds at 25 °C. The extracted RNA fractions were stored at -80°C.

A.19 Preparation of Polyacrylamide Gel

The polyacrylamide gel was prepared in a volume of 60 ml. Bis-acrylamide (0.45 g) and acrylamide (8.55 g) were weighed into a clean 100 ml beaker. Thirty grams of Urea (8 M) was added with 6 ml 10 × Tris-borate-EDTA (TBE) buffer (Appendix A.19.1). The mixture was made up to 60 ml with sterile water. Prior to pouring the gel, 250 µl 1% (w/v)

Ammonium persulphate (APS) and 25 µl TEMED (tetramethylethylenediamine) were added to the mixture.

A.19.1 10 × Tris-borate-EDTA (TBE) Buffer

Boric acid (27.5 g); Tris-base (50 g) and 20 ml EDTA (0.5 M) were dissolved in 400 ml sterile water, and the solution adjusted to pH 8.0 with dilute HCl. The buffer was made up to 500 ml with sterile water, autoclaved and stored at room temperature.

A.20 Radioactive labelling of Oligonucleotide Probes

Oligonucleotide probes were radioactively labelled in a final reaction volume of 20 µl containing 2 µM probe, 2 µl PNK buffer A, 1 µl PNK (Fermentas, MD, USA) and 5 micro Curies (µCi) [γ-^{32}P] ATP (185 kilo becquerel (kBq)) (SepSci, Johannesburg, RSA). The mixture was reconstituted in nuclease free water and incubated at 37°C for 45 minutes.

A.21 20 × Saline-sodium citrate (SSC) Buffer

Sodium chloride (175 g) and sodium citrate (88 g) were dissolved in 800 ml sterile water, and the solution was adjusted to pH 7.0 with HCl. The buffer was made up to 1000 ml with sterile water, autoclaved and stored at room temperature. To prepare 5× SSC buffer, 25 ml of 20× SSC buffer was added to 75 ml sterile water. To prepare a 1× SSC buffer, 5 ml of 20× SSC buffer was added to 95 ml sterile water.

A.22 Quantitative Real Time PCR – LightCycler® FastStart DNA Master^{PLUS} SYBR Green I Kit

Fourteen microlitres of enzyme (1a) was added to the SYBR green Reaction Mix (1b) and gently mixed. The PCR was prepared in a final reaction volume of 20 µl containing 500 ng

DNA, 1 pmol forward primer, 15 pmol reverse primer, and was carried out in a 5× Master Mix. The LightCycler® Carousel-Based System Protocol was programmed as described in Table 6.1 (adapted from Roche LightCycler® FastStart DNA Master^{PLUS} SYBR Green I Kit).

Table 6.1: Quantitative Real Time LightCycler® PCR Protocol

Program	Cycles	Segment	Temperature	Hold Time
Hot Start	1	Denaturation	95°C	00:10:00
Quantification	50	Denaturation	95°C	00:00:10
		Annealing	60°C	00:00:10
		Elongation	72°C	00:00:10
Melting Curve	1	Denaturation	95°C	00:00:00
		Annealing	65°C	00:01:00
		Elongation	95°C	00:00:00
Cool	1	Cooling	40°C	00:00:30

APPENDIX B - ANIMAL ETHICS CLEARANCE

AESC 3

UNIVERSITY OF THE WITWATERSRAND, JOHANNESBURG

STRICTLY CONFIDENTIAL

ANIMAL ETHICS SCREENING COMMITTEE (AESC)

CLEARANCE CERTIFICATE NO. 2007/47/3

APPLICANT: Dr P Arbuthnot

SCHOOL: Molecular medicine and Haematology
DEPARTMENT:
LOCATION: Medical School

PROJECT TITLE: **Assessment of efficacy of anti hepatitis B virus RNA interference expression cassettes using the murine hydrodynamic injection model**

Number and Species

384 male and female mice

Approval was given for to the use of animals for the project described above at an AESC meeting held on 20071127. This approval remains valid until 20091127

The use of these animals is subject to AESC guidelines for the use and care of animals, is limited to the procedures described in the application form and to the following additional conditions:

Report % of animal deaths under this protocol, volume injected must be in proportion to body size with 3ml maximum, retro-orbital bleeds twice only, liaison with CAS vet for injections and retro orbital bleeds, all animals that die other than euthanasia for experimental procedure must be made available to the CAS in line with normal procedure.

Signed: _____ Date: 30/11/2007
(Chairperson, AESC)

I am satisfied that the persons listed in this application are competent to perform the procedures therein, in terms of Section 23 (1) (c) of the Veterinary and Para-Veterinary Professions Act (19 of 1982)

Signed: _____ Date: 30/11/2007
(Registered Veterinarian)

cc: Supervisor:
Director: CAS

Works 2000/Iain0015/AESCCert.wps

APPENDIX C - SUPPLEMENTARY DATA

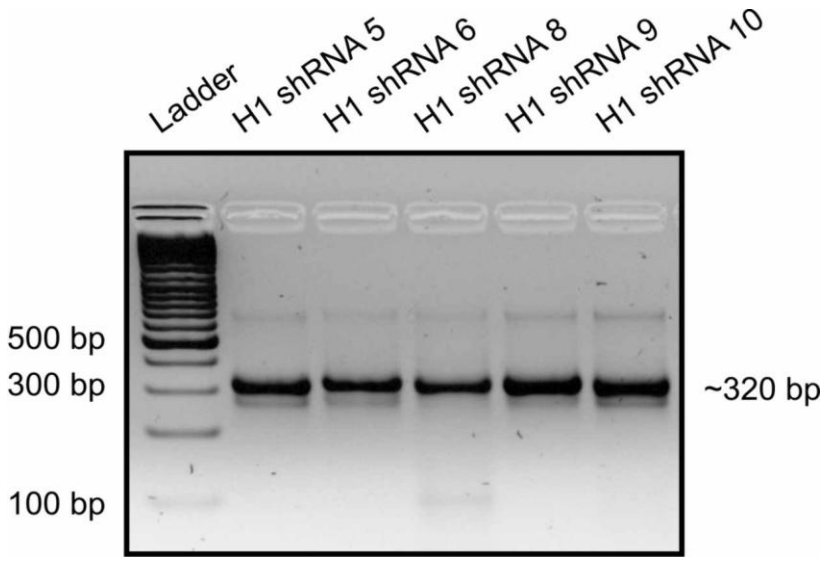


Figure C.1: Verification of the generation of the H1 shRNA expression cassettes.

The size of the completed H1 shRNA expression cassettes were verified to be ~320 bp which correlates to the expected size of 315 bp.

```
H1 shRNA5       GGATCCGATTGATCGAATTCACTAGTGAACGCTGACGTCATCAACCCGCT
H1 Promoter     ----------GATCGAATTCACTAGTGAACGCTGACGTCATCAACCCGCT
H1 shRNA 5 R1   ----------------------------------------------------
shRNA 5 R2      ----------------------------------------------------

H1 shRNA 5      CCAAGGAATCGCGGGCCCAGTGTCACTAGGGCGGGAACACCCAGGCGCGC
H1 Promoter     CCAAGGAATCGCGG-CCCAGTGTCACTAGG-CGGGAACACCCAG-CGCGC
H1 shRNA 5 R1   ----------------------------------------------------
   shRNA 5 R2   ----------------------------------------------------

H1 shRNA 5      GGTGCGCCCTGGCAGGAAGATGGCTGTGAGGGACAGGGGAGTGGCGCCCT
H1 Promoter     G-TGCGCCCTGGCAGGAAGATGGCTGTGAGGGACAGGGGAGTGGCGCCCT
H1 shRNA 5 R1   ----------------------------------------------------
   shRNA 5 R2   ----------------------------------------------------

H1 shRNA 5      GCAATATTTGCATGTCACTATGTGTTCTGGGAAATCACCATAAACGTGAA
H1 Promoter     GCAATATTTGCATGTCGCTATGTGTTCTGGGAAATCACCATAAACGTGAA
H1 shRNA 5 R1   ----------------------------------------------------
   shRNA 5 R2   ----------------------------------------------------

H1 shRNA 5      ATGTCTTTGGATTTGGGAATCTTATAAGTTCTGTATGAGACCACTCGGAT
H1 Promoter     ATGTCTTTGGATTTGGGAATCTTATAAGTTCTGTATGAGACCACTCGGAT
H1 shRNA 5 R1   --------------------------------GTATGAGACCACTCGGAT
   shRNA 5 R2   ----------------------------------------------------

H1 shRNA 5      CCGTCGTGTGCGCTTTGCTTCGCCTCTGeCTTCCTGTCACAGAGGTGAAGC
H1 Promoter     CC--------------------------------------------------
H1 shRNA 5 R1   CCGTCGTGTGCGCTTTGCTTCGCCTCTGCTTCCTGTCACAGA--------
   shRNA 5 R2   ----------------------CTCTGCTTCCTGTCACAGAGGTGAAGC

H1 shRNA 5      GAAGTGCACACGGTTTTTTACGCGTAGATCTGGGAATCTAGATGCATTCG
H1 Promoter     ----------------------------------------------------
H1 shRNA 5 R1   ----------------------------------------------------
   shRNA 5 R2   GAAGTGCACACGGTTTTTTACGCGTAGATCTGGG----------------
```

Figure C.2: DNA sequence of H1 shRNA 5.

The shRNA expression cassette is 100 % homologous to the designed primers. The promoter contains a G153A base change. Four base insertions were identified in the promoter region (red) however, these had no effect on transcription. The shRNA is comprised of the anti-guide sequence (blue), loop (green) and guide sequence with termination site (purple).

```
H1 shRNA 6      GATCCGATTGATCGAATTCACTAGTGAACGCTGACGTCATCAACCCGCTC
H1 Promoter     ---------GATCGAATTCACTAGTGAACGCTGACGTCATCAACCCGCTC
H1 shRNA 6 R1   ----------------------------------------------------
   shRNA 6 R2   ----------------------------------------------------

H1 shRNA 6      CAAGGAATCGGGGGGCCCGGGGTCACTTGGGGGGGAACACCCAGGGGCGC
H1 Promoter     CAAGGAATCGCGG--CCCAGTGTCACTAGGCGGG-AACACCCAGCG-CGC
H1 shRNA 6 R1   ----------------------------------------------------
   shRNA 6 R2   ----------------------------------------------------

H1 shRNA 6      GTGCGCCCTGGCAGGAAGATGGCTGTGAGGGACAGGGGAGTGGCGCCCTG
H1 Promoter     GTGCGCCCTGGCAGGAAGATGGCTGTGAGGGACAGGGGAGTGGCGCCCTG
H1 shRNA 6 R1   ----------------------------------------------------
   shRNA 6 R2   ----------------------------------------------------

H1 shRNA 6      CAATATTTGCATGTCACTATGTGTTCTGGGAAATCACCATAAACGTGAAA
H1 Promoter     CAATATTTGCATGTCGCTATGTGTTCTGGGAAATCACCATAAACGTGAAA
H1 shRNA 6 R1   ----------------------------------------------------
   shRNA 6 R2   ----------------------------------------------------

H1 shRNA 6      TGTCTTTGGATTTGGGAATCTTATAAGTTCTGTATGAGACCACTCGGATC
H1 Promoter     TGTCTTTGGATTTGGGAATCTTATAAGTTCTGTATGAGACCACTCGGATC
H1 shRNA 6 R1   ------------------------------GTATGAGACCACTCGGATC
   shRNA 6 R2   ----------------------------------------------------

H1 shRNA 6      CGTACACCTCGCTTCACCTCTACACATCTTCCTGTCAACGTGCAGAGGTG
H1 Promoter     C-----------------------------------------------------
H1 shRNA 6 R1   CGTACACCTCGCTTCACCTCTACACATCTTCCTGTCAACGT---------
   shRNA 6 R2   --------------------CACATCTTCCTGTCAACGTGCAGAGGTG

H1 shRNA 6      AAGCGAAGTGCATTTTTTACGCGTAGATCTAATCTAGATGCATTCGCGAG
H1 Promoter     -----------------------------------------------------
H1 shRNA 6 R1   -----------------------------------------------------
   shRNA 6 R2   AAGCGAAGTGCATTTTTTACGCGTAGATCTGGG----------------
```

Figure C.3: DNA sequence of H1 shRNA 6.

The shRNA expression cassette is 100 % homologous to the designed primers. There were three alterations observed within the H1 promoter. A double nucleotide insertion (GG) and two nucleotide changes, A65T and G153A. The shRNA is comprised of the anti-guide sequence (blue), loop (green) and guide sequence with termination site (purple).

```
H1 shRNA 8      GATCCGATTGATCGAATTCACTAGTGAACGCTGACGTCATCAACCCGCTC
H1 Promoter     ---------GATCGAATTCACTAGTGAACGCTGACGTCATCAACCCGCTC
H1 shRNA 8 R1   ----------------------------------------------------
   shRNA 8 R    ----------------------------------------------------

H1 shRNA 8      CAAGGAATCGCGGGCCCAGTGTCACTAGGGCGGGAACACCCAGCGCGCGT
H1 Promoter     CAAGGAATCGCGG-CCCAGTGTCACTAGG-CGGGAACACCCAGCGCGCGT
H1 shRNA 8 R1   ----------------------------------------------------
   shRNA 8 R2   ----------------------------------------------------

H1 shRNA 8      GCGCCCTGGCAGGAAGATGGCTGTGAGGGACAGGGGAGTGGCGCCCTGCA
H1 Promoter     GCGCCCTGGCAGGAAGATGGCTGTGAGGGACAGGGGAGTGGCGCCCTGCA
H1 shRNA 8 R1   ----------------------------------------------------
   shRNA 8 R2   ----------------------------------------------------

H1 shRNA 8      ATATTTGCATGTCACTATGTGTTCTGGGAAATCACCATAAACGTGAAATG
H1 Promoter     ATATTTGCATGTCGCTATGTGTTCTGGGAAATCACCATAAACGTGAAATG
H1 shRNA 8 R1   ----------------------------------------------------
   shRNA 8 R2   ----------------------------------------------------

H1 shRNA 8      TCTTTGGATTTGGGAATCTTATAAGTTCTGTATGAGACCACTCGGATCCG
H1 Promoter     TCTTTGGATTTGGGAATCTTATAAGTTCTGTATGAGACCACTCGGATCC-
H1 shRNA 8 R1   ----------------------------GTATGAGACCACTCGGATCCG
   shRNA 8 R2   ----------------------------------------------------

H1 shRNA 8      CAACGTCAACAACCAACCTTGAAGCCTTCCTGTCAGCCTCAAGGTCGGTC
H1 Promoter     ----------------------------------------------------
H1 shRNA 8 R1   CAACGTCAACAACCAACCTTGAAGCCTTCCTGTCAGCCT-----------
   shRNA 8 R2   ------------------GAAGCCTTCCTGTCAGCCTCAAGGTCGGTC

H1 shRNA 8      GTTGACATTGTTTTTTACGCGTAGATCTGGGAATCTAGATGCATTCGCGA
H1 Promoter     ----------------------------------------------------
H1 shRNA 8 R1   ----------------------------------------------------
   shRNA 8 R2   GTTGACATTGTTTTTTACGCGTAGATCTGGG------------------
```

Figure C.4: DNA sequence of H1 shRNA 8.

The shRNA expression cassette is 100 % homologous to the designed primers. There were two single nucleotide insertions (G) at and a G151A base change observed within the H1 promoter. The shRNA is comprised of the anti-guide sequence (blue), loop (green) and guide sequence with termination site (purple).

```
H1 shRNA 9      AATCCGATTGATCGAATTCACTAGTGAACGCTGACGTCATCAACCCGCTC
H1 Promoter     ---------GATCGAATTCACTAGTGAACGCTGACGTCATCAACCCGCTC
H1 shRNA 9 R1   --------------------------------------------------
   shRNA 9 R2   --------------------------------------------------

H1 shRNA 9      CAAGGAATCGCGGGCCCAGTGTCACTAGGCGGGAACACCCAGCGCGCGTG
H1 Promoter     CAAGGAATCGCGG-CCCAGTGTCACTAGGCGGGAACACCCAGCGCGCGTG
H1 shRNA 9 R1   --------------------------------------------------
   shRNA 9 R2   --------------------------------------------------

H1 shRNA 9      CGCCCTGGCAGGAAGATGGCTGTGAGGGACAGGGGAGTGGCGCCCTGCAA
H1 Promoter     CGCCCTGGCAGGAAGATGGCTGTGAGGGACAGGGGAGTGGCGCCCTGCAA
H1 shRNA 9 R1   --------------------------------------------------
   shRNA 9 R2   --------------------------------------------------

H1 shRNA 9      TATTTGCATGTCACTATGTGTTCTGGGAAATCACCATAAACGTGAAATGT
H1 Promoter     TATTTGCATGTCGCTATGTGTTCTGGGAAATCACCATAAACGTGAAATGT
H1 shRNA 9 R1   --------------------------------------------------
   shRNA 9 R2   --------------------------------------------------

H1 shRNA 9      CTTTGGATTTGGGAATCTTATAAGTTCTGTATGAGACCACTCGGATCCGT
H1 Promoter     CTTTGGATTTGGGAATCTTATAAGTTCTGTATGAGACCACTCGGATCC--
H1 shRNA 9 R1   ----------------------------GTATGAGACCACTCGGATCCGT
   shRNA 9 R2   --------------------------------------------------

H1 shRNA 9      AAGAAGCTGTAGGCACAAATTAGTCTTCCTGTCAACCAATTTATGCCTAC
H1 Promoter     --------------------------------------------------
H1 shRNA 9 R1   AAGAAGCTGTAGGCACAAATTAGTCTTCCTGTCAACCA------------
   shRNA 9 R2   ------------------TAGTCTTCCTGTCAACCAATTTATGCCTAC

H1 shRNA 9      AGCCTCCTATTTTTTACGCGTAGATCTGGGAATCTAGATGCATTCGCGAG
H1 Promoter     --------------------------------------------------
H1 shRNA 9 R1   --------------------------------------------------
   shRNA 9 R2   GCCTCCTATTTTTTACGCGTAGATCTGGG--------------------
```

Figure C.5: DNA sequence of H1 shRNA 9.

The shRNA expression cassette is 100 % homologous to the designed primers. There was a single nucleotide insertion (G) and a G149A base change observed within the H1 promoter. The shRNA is comprised of the anti-guide sequence (blue), loop (green) and guide sequence with termination site (purple).

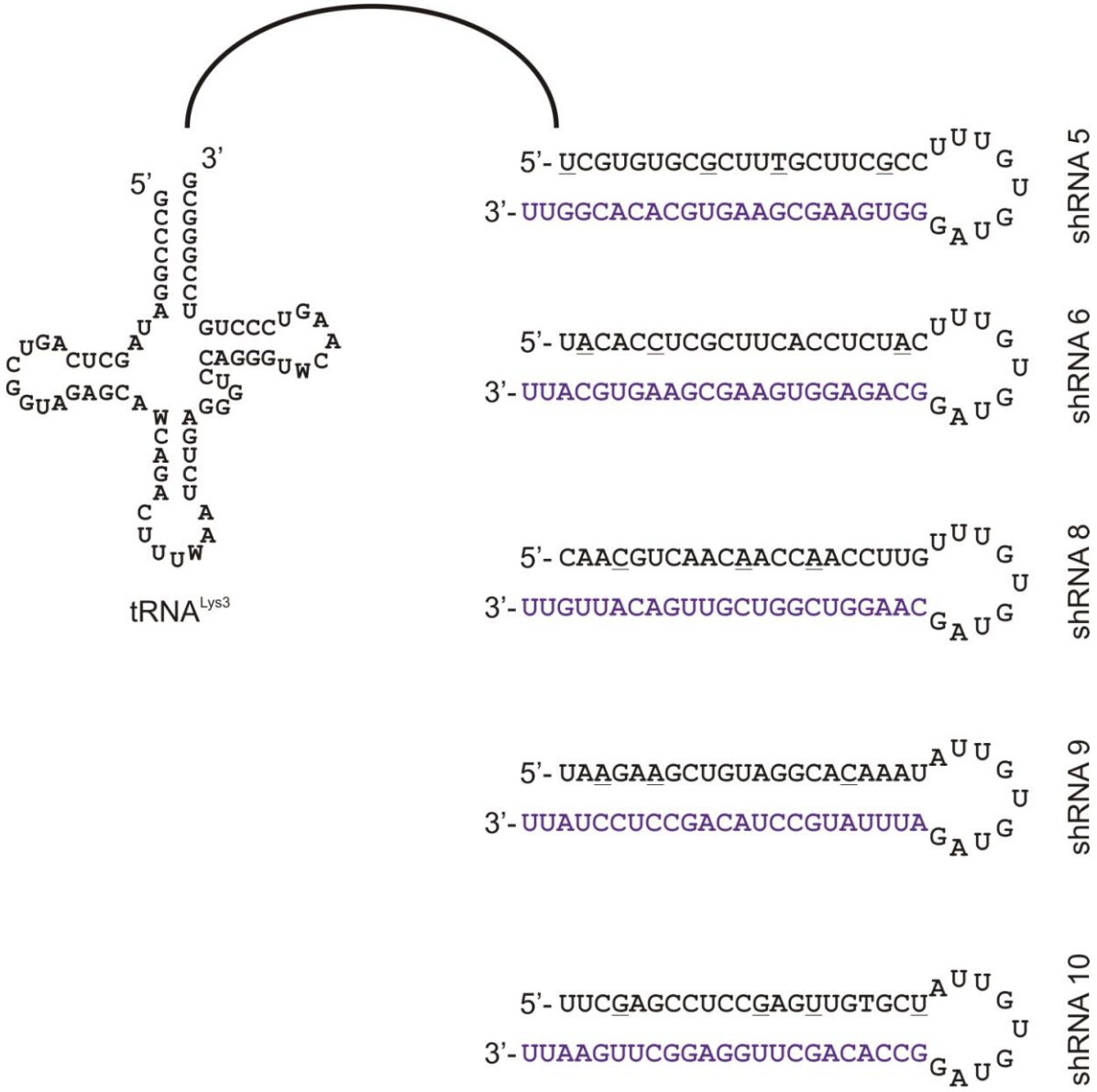


Figure C.6: Predicted structure of tRNA^{Lys3} shRNA expression cassettes.

The tRNA^{Lys3} promoter starts transcription within the structure itself, thus the shRNAs will be transcribed attached to the acceptor arm of the tRNA^{Lys3}. The guide sequence (purple) is four nucleotides shorter than the guide sequences in U6 and H1 shRNA expression cassettes, to counteract for the increased length of the hairpin following transcription (i.e. transcribed tRNA^{Lys3} promoter and hairpin.

```
tRNA^Lys3 shRNA 5  CCCCTCGAGGTCGACGCCCGGATAGCTCAGTCGGTAGAGCATCAGACTTT
tRNA^Lys3 Promoter ---------------GCCCGGATAGCTCAGTCGGTTGAGCATCAGACTTT
shRNA 5 Oligo      ----------------------------------------------------

tRNA^Lys3 shRNA 5  TAATCTGAGGGTCCAGGGTTCAAGTCCCTGTTCGGGCGTCGTGTGCGCTT
tRNA^Lys3 Promoter TAATCTGAGGGTCCAGGGTTCAAGTCCCTGTTCG----------------
shRNA 5 Oligo      ---------------------------------GGCGTCGTGTGCGCTT

tRNA^Lys3 shRNA 5  TGCTTCGCCTTTGTGTAGGGTGAAGCGAAGTGCACACGGTTTTTTGCAGC
tRNA^Lys3 Promoter ----------------------------------------------------
shRNA 5 Oligo      TGCTTCGCCTTTGTGTAGGGTGAAGCGAAGTGCACACGGTTTTTTGCA--
```

Figure C.7: Sequence analysis of tRNA^{Lys3} shRNA 5.

A single base change T21A occurred in the tRNA^{Lys3} promoter (red). The shRNA sequence identified by the anti-guide (blue), loop (green) and guide sequence (purple) is 100% homologous to the hairpin predicted structure (Appendix C.6). The natural accepter arm is highlighted yellow.

```
tRNA^Lys3 shRNA 6  CCCCTCGAGGTCGACGCCCGGATAGCTCAGTCGGTAGAGCATCAGACTTT
tRNA^Lys3 Promoter ---------------GCCCGGATAGCTCAGTCGGTTGAGCATCAGACTTT
shRNA 6 Oligo      ----------------------------------------------------

tRNA^Lys3 shRNA 6  TAATCTGAGGGTCCAGGGTTCAAGTCCCTGTTCGGGCGTACACCTCGCTT
tRNA^Lys3 Promoter TAATCTGAGGGTCCAGGGTTCAAGTCCCTGTTCG----------------
shRNA 6 Oligo      ---------------------------------GGCGTACACCTCGCTT

tRNA^Lys3 shRNA 6  CACCTCTACTTTGTGTAGGCAGAGGTGAAGCGAAGTGCATTTTTTGCAGC
tRNA^Lys3 Promoter ----------------------------------------------------
shRNA 6 Oligo      CACCTCTACTTTGTGTAGGCAGAGGTGAAGCGAAGTGCATTTTTTGCA--
```

Figure C.8: Sequence analysis of tRNA^{Lys3} shRNA 6.

A single base change T21A occurred in the tRNA^{Lys3} promoter (red). The shRNA sequence identified by the anti-guide (blue), loop (green) and guide sequence (purple) is 100% homologous to the hairpin predicted structure (Appendix C.6). The natural accepter arm is highlighted yellow.

```
tRNALys3shRNA 8   CCCCTCGAGGTCGACGCCCGGATAGCTCAGTCGGTAGAGCATCAGACTTT

tRNALys3 Promoter ---------------GCCCGGATAGCTCAGTCGGTTGAGCATCAGACTTT
shRNA 8 Oligo     ----------------------------------------------------

tRNALys3 shRNA 8  TAATCTGAGGGTCCAGGGTTCAAGTCCCTGTTCGGGCGCAACGTCAACAA
tRNALys3 Promoter TAATCTGAGGGTCCAGGGTTCAAGTCCCTGTTCG----------------
shRNA 8 Oligo     --------------------------------GGCGCAACGTCAACAA

tRNALys3 shRNA 8  CCAACCTTGTTTGTGTAGCAAGGTCGGTCGTTGACATTGTTTTTTGCAGC
tRNALys3 Promoter ----------------------------------------------------
shRNA 8 Oligo     CCAACCTTGTTTGTGTAGCAAGGTCGGTCGTTGACATTGTTTTTTGCA--
```

Figure C.9: Sequence analysis of tRNA^{Lys3} shRNA 8.

A single base change T21A occurred in the tRNA^{Lys3} promoter (red). The shRNA sequence identified by the anti-guide (blue), loop (green) and guide sequence (purple) is 100% homologous to the hairpin predicted structure (Appendix C.6). The natural accepter arm is highlighted yellow.

```
tRNALys3 shRNA 9  CCCCTCGAGGTCGACGCCCGGATAGCTCAGTCGGTAGAGCATCAGACTTT
tRNALys3 Promoter ---------------GCCCGGATAGCTCAGTCGGTTGAGCATCAGACTTT
shRNA 9 Oligo     ----------------------------------------------------

tRNALys3 shRNA 9  TAATCTGAGGGTCCAGGGTTCAAGTCCCTGTTCGGGCGTAAGAAGCTGTA
tRNALys3 Promoter TAATCTGAGGGTCCAGGGTTCAAGTCCCTGTTCG----------------
shRNA 9 Oligo     --------------------------------GGCGTAAGAAGCTGTA

tRNALys3 shRNA 9  GGCACAAATATTGTGTAGATTTATGCCTACAGCCTCCTATTTTTTGCAGC
tRNALys3 Promoter ----------------------------------------------------
shRNA 9 Oligo     GGCACAAATATTGTGTAGATTTATGCCTACAGCCTCCTATTTTTTGCA--
```

Figure C.10: Sequence analysis of tRNA^{Lys3} shRNA 9.

A single base change T21A occurred in the tRNA^{Lys3} promoter (red). The shRNA sequence identified by the anti-guide (blue), loop (green) and guide sequence (purple) is 100% homologous to the hairpin predicted structure (Appendix C.6). The natural accepter arm is highlighted yellow.

```
tRNA^Lys3 shRNA 10 CCCCTCGAGGTCGACGCCCGGATAGCTCAGTCGGTAGAGCATCAGACTTT
tRNA^Lys3 Promoter ---------------GCCCGGATAGCTCAGTCGGTTGAGCATCAGACTTT
shRNA 10 Oligo  ----------------------------------------------------

tRNA^Lys3 shRNA 10 TAATCTGAGGGTCCAGGGTTCAAGTCCCTGTTCGGGCGTTCGAGCCTCCG
tRNA^Lys3 Promoter TAATCTGAGGGTCCAGGGTTCAAGTCCCTGTTCG----------------
shRNA 10 Oligo  ----------------------------------GGCGTTCGAGCCTCCG

tRNA^Lys3 shRNA 10 AGTTGTGCTATTGTGTAGGGCACAGCTTGGAGGCTTGAATTTTTTGCAGC
tRNA^Lys3 Promoter ----------------------------------------------------
shRNA 10 Oligo  AGTTGTGCTATTGTGTAGGGCACAGCTTGGAGGCTTGAATTTTTTGCA—
```

Figure C.11: Sequence analysis of tRNA^{Lys3} shRNA 10.

A single base change T21A occurred in the tRNA^{Lys3} promoter (red). The shRNA sequence identified by the anti-guide (blue), loop (green) and guide sequence (purple) is 100% homologous to the hairpin predicted structure (Appendix C.6). The natural accepter arm is highlighted yellow.

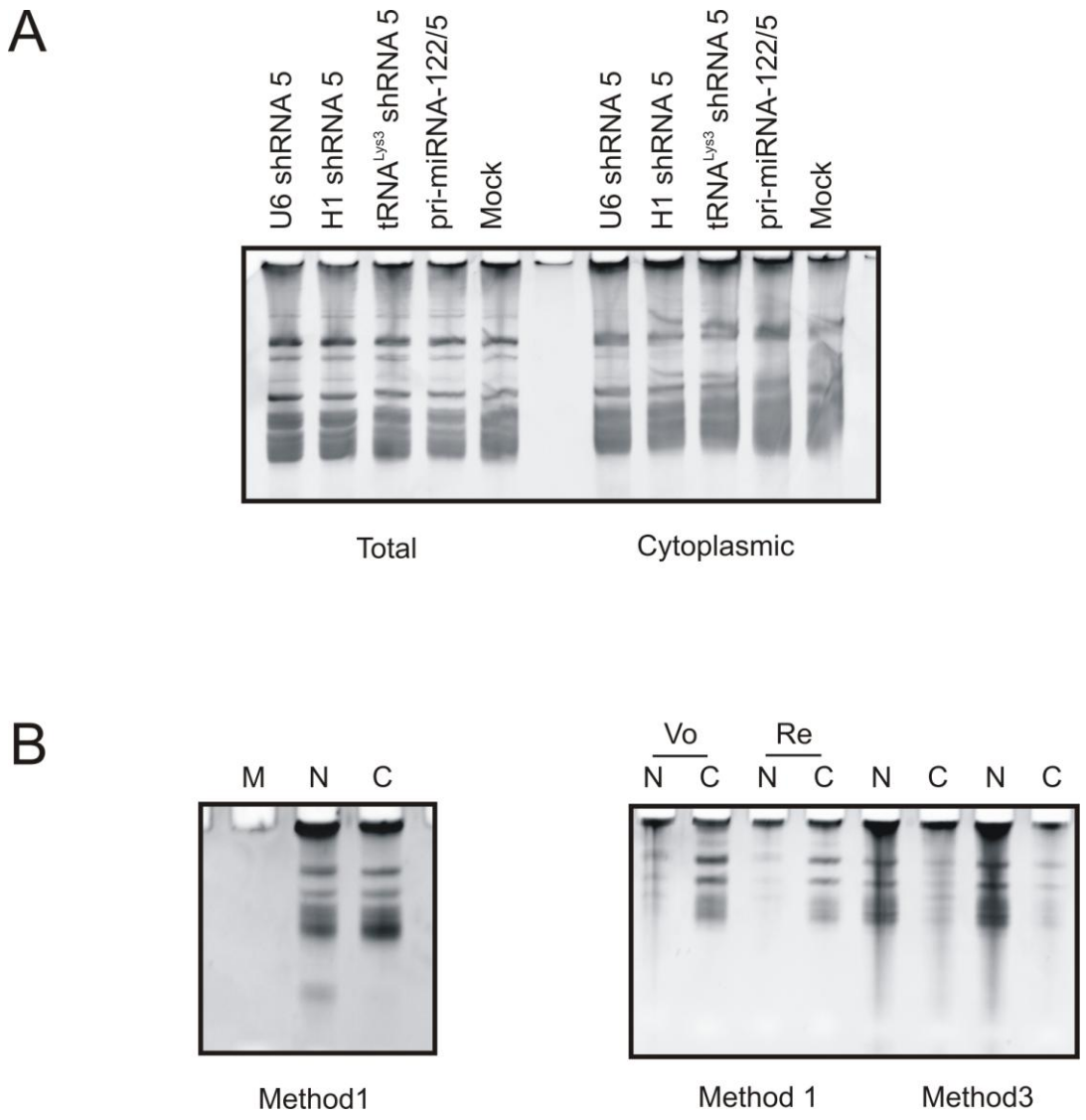


Figure C.12: Analysis of RNA integrity extracted from Total, nuclear and cytoplasmic fractions.

(A) Comparison of total and cytoplasmic RNA. Transfected Huh7 cells were fractionated by Method 1. The cytoplasmic RNA is degraded. **(B)** Comparison of RNA extracted from whole, untransfected Huh7 cellsfrom fractions obtained using Method 1 and Method 2. Method 1 yielded relatively pure RNA (left). Alternative techniques for lysing the cells were tested using Method 1.

Interpretation of Figure C.12: Lysing of the plasma membrane accompanied by vortexing yielded insufficient RNA, however it yielded more cytoplasmic RNA than lysis accompanied by resuspension. Lysis of cells using the dounce homogeniser yielded degraded RNA with insufficient cytoplasmic RNA. Vo – vortex; Re – resuspended by pipette.

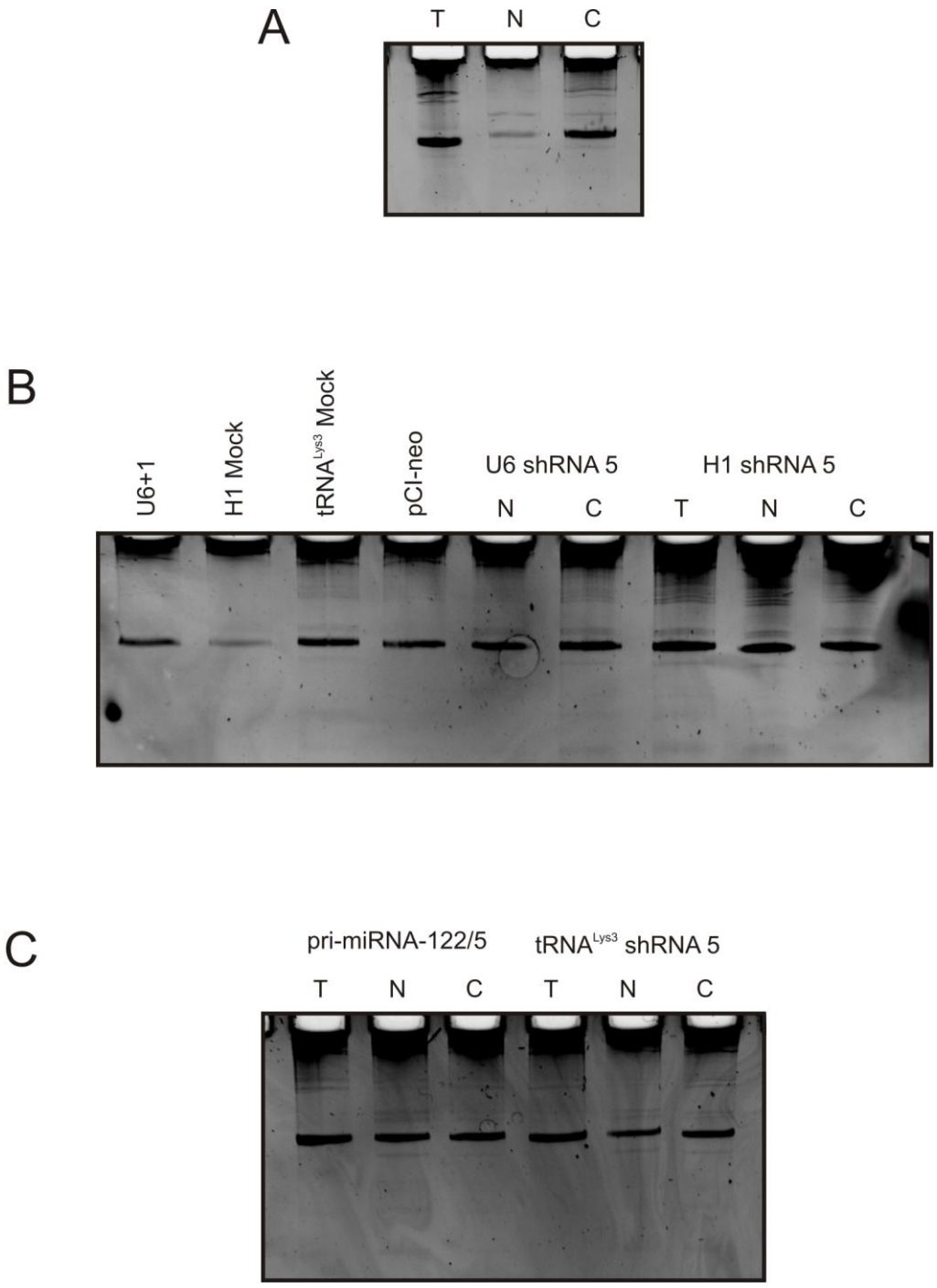


Figure C.13: Analysis of integrity of RNA extracted using the PARIS™ Kit.

(A) Total, nuclear and cytoplasmic RNA extrcted from non-transfected HepG.2.215 cells, yielded insufficient amounts of RNA from all three lysates **(B,C)** RNA was extracted from transfected Huh7 cells. The RNA yield was poor and insufficient, prompting an alternative method of RNA extraction to be implemented.

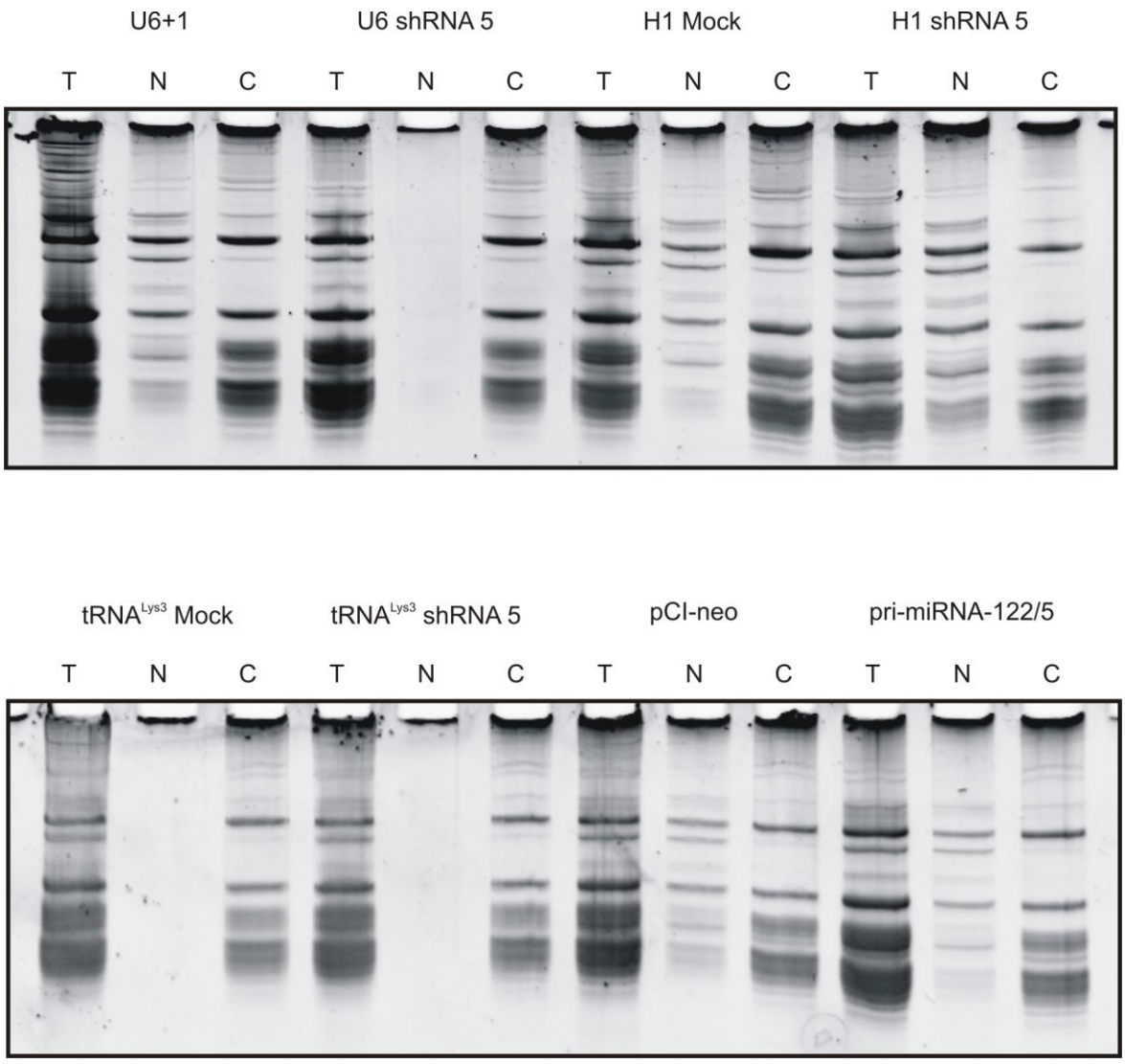


Figure C.14: RNA anaylysis of total, nuclear and cytoplasmic fractions.

The RNA extracted from transfected Huh7 cells yielded sufficient amounts of pure, quality RNA for the majority of the fractions. Nuclear RNA was insuffcient for U6 shRNA 5, tRNA^{Lys3} Mock and tRNA^{Lys3} shRNA 5.

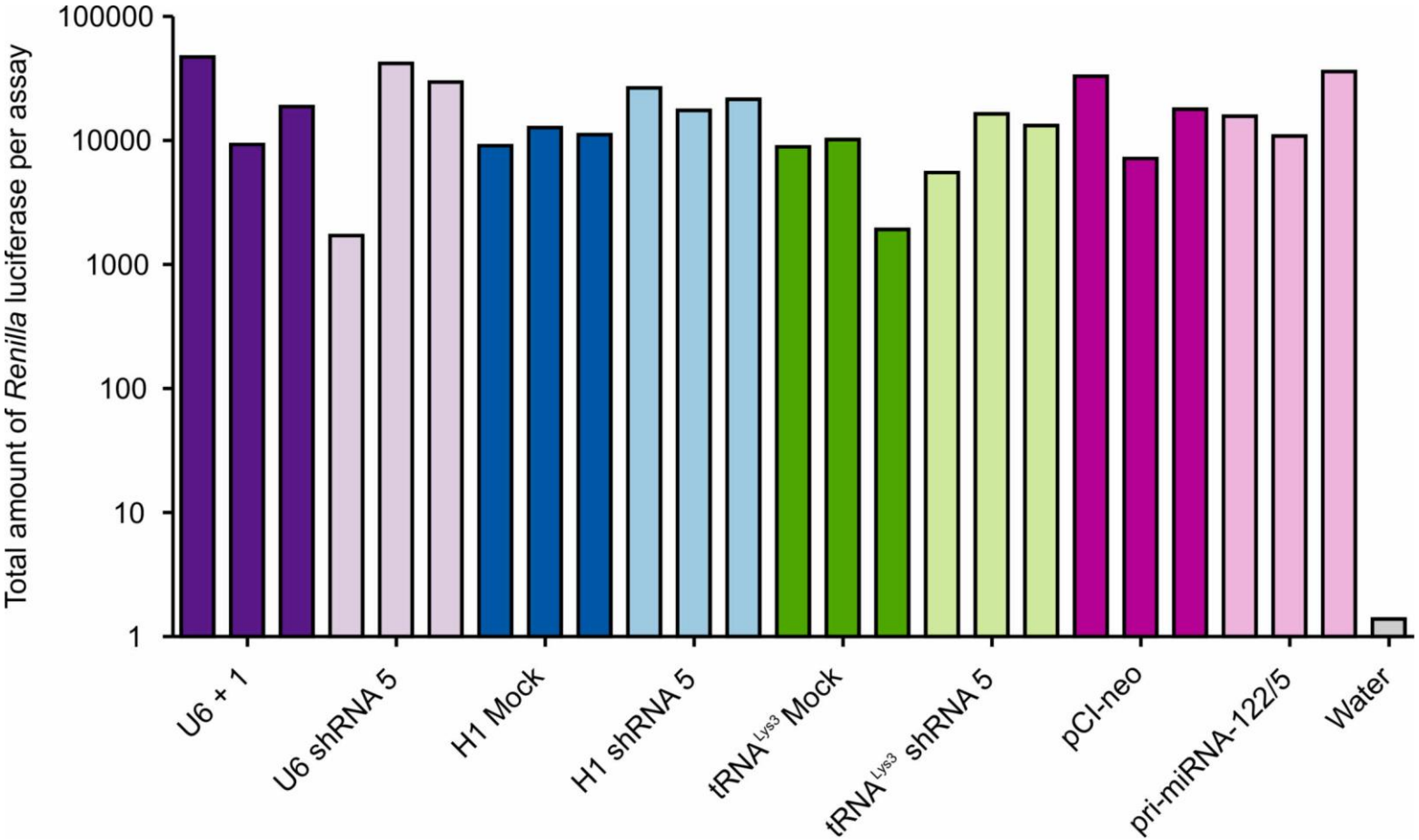


Figure C.15: Delivery efficiency of anti-HBV effecter sequences to the liver.

psi-CHECK 2.2 was co-administered with the indicated plasmids to mice by hydrodynamic tail vein injection. Detection of the amount of *Renilla* luciferase sequence indicates the efficacy at which the DNA expressing plasmids were delivered to the liver.

Table C.1: P values for shRNA 5 and pri-miRNA-122/5 *HBx* Dual Luciferase Assay

Target:Effecter	U6	H1	$tRNA^{Lys3}$	Pri-miRNA-122
1:0.0025	0.0029	0.0455	0.0078	0.1792
1:0.01	0.0004	0.0034	0.0065	0.2224
1:0.05	0.0002	0.0005	0.0006	0.2008
1:0.1	0.0001	0.0001	0.0003	0.0084
1:10	<0.0001	<0.0001	0.0002	0.0022

Table C.2: P values for shRNA 6 and pri-miRNA-122/6 *HBx* Dual Luciferase Assay

Target:Effecter	U6	H1	$tRNA^{Lys3}$	Pri-miRNA-122
1:0.0025	0.0054	0.0753	0.2547	0.0406
1:0.01	0.0027	0.0154	0.0576	0.0341
1:0.05	0.0009	0.0022	0.0085	0.0757
1:0.1	0.0007	0.0009	0.0009	0.0082
1:10	0.0006	0.0006	0.0017	<0.0001

Table C.3: P values for shRNA 8 and pri-miRNA-122/8 *HBx* Dual Luciferase Assay

Target:Effecter	U6	H1	$tRNA^{Lys3}$	Pri-miRNA-122
1:0.0025	0.0528	0.2688	0.4706	0.0150
1:0.01	0.0047	1.0000	0.0455	0.0354
1:0.05	0.0022	0.0132	0.0494	0.0286
1:0.1	0.0001	0.0008	0.1410	0.0066
1:10	<0.0001	0.0001	0.0268	0.0060

Table C.4: P values for shRNA 9 and pri-miRNA-122/9 *HBx* Dual Luciferase Assay

Target:Effecter	U6	H1	$tRNA^{Lys3}$	Pri-miRNA-122
1:0.0025	0.0817	0.0178	0.7525	0.0751
1:0.01	0.0005	0.0039	0.4734	0.0526
1:0.05	0.0001	0.0003	0.0559	0.0539
1:0.1	<0.0001	0.0001	0.0050	0.0131
1:10	<0.0001	<0.0001	<0.0001	0.0001

Table C.5: P values for shRNA 10 and pri-miRNA-122/10 *HBx* Dual Luciferase Assay

Target:Effecter	U6	H1	$tRNA^{Lys3}$	Pri-miRNA-122
1:0.0025	0.0029	0.0455	0.0078	0.1792
1:0.01	0.0004	0.0034	0.0065	0.2224
1:0.05	0.0002	0.0005	0.0006	0.2008
1:0.1	0.0001	0.0001	0.0003	0.0084
1:10	<0.0001	<0.0001	0.0002	0.0022

Table C.6: Statistical analysis of *in vitro* HBsAg (P values)

Effecter Sequence	U6	H1	$tRNA^{Lys3}$	CMV
5	0.0367	0.0198	0.0455	0.0058
6	0.0120	0.0085	0.0205	0.0157
8	0.0174	0.0617	0.1494	0.0688
9	0.0091	0.0928	0.0184	0.0076
10	0.0003	0.0188	0.4367	0.3050

Table C.7: Statistical analysis of *in vitro* Saturation Assay (P values)

Effecter Sequence	U6	H1	$tRNA^{Lys3}$	CMV	Mock
5	<0.0001	<0.0001	<0.0001	<0.0001	<0.0001
6	<0.0001	<0.0001	<0.0001	0.0001	<0.0001